Pathobiological Mechanisms and Treatment of Electrophysiological Dysfunction Following Primary Blast-Induced Traumatic Brain Injury

Edward Weigand Vogel III

Submitted in partial fulfillment of the
requirements for the degree of
Doctor of Philosophy
in the Graduate School of Arts and Science

COLUMBIA UNIVERSITY

2017

ABSTRACT

Pathobiological Mechanisms of Electrophysiological Dysfunction Following Primary Blast-Induced Traumatic Brain Injury

Edward W. Vogel III

Traumatic brain injury (TBI) is the signature injury of the ongoing military conflicts in the Middle East and Afghanistan, largely due to the use of improvised explosive devices (IEDs), which have affected soldiers and civilians alike. Blast-induced TBI (bTBI) biomechanics are complex and multiphasic. While research has clearly demonstrated the negative effects of penetrative (secondary blast) and inertia-driven (tertiary blast) injury, the effect of shock wave loading (primary blast) on the brain remains unclear. Combined primary-tertiary blast exposure *in vivo* has been reported previously to alter brain function, specifically hippocampal function; however, it is extremely difficult to deliver primary blast exposure in isolation with an *in vivo* injury model. The research presented in this thesis utilized a custom-designed *in vitro* blast injury model to deliver military-relevant shock wave exposures, in isolation, to organotypic hippocampal slice cultures (OHSCs). To contextualize blast-induced pathobiology with previous TBI studies, the first goal of this thesis was to characterize the deformation profile induced in OHSCs with our blast injury model experimentally. Using stereoscopic, high-speed cameras and digital image correlation to calculate strain, we found that our blast model induced low strain magnitudes (<9%) but at high strain rates (25-86s^{-1}), which aligned closely with associated computational simulations of our model.

The second aim was to determine if primary blast was capable of altering hippocampal electrophysiological function. We exposed OHSCs to a range of shock intensities and found,

using a micro-electrode array system, that long-term potentiation (LTP), a measure of synaptic plasticity, was very sensitive to primary blast exposure; a threshold for disruption of LTP was found between 9 and 39 kPa•ms impulse. Alternative measures of basal electrophysiology were less sensitive than LTP. Blast exposure significantly reduced LTP between 1 and 24 hours post-injury, and this deficit persisted through 6 days post-injury. Depending on shock intensity, LTP spontaneously recovered 10 days post-injury.

The third aim was to explore the cellular mechanisms for blast-induced LTP deficits. Using a chemical LTP induction protocol, blast exposure altered key proteins necessary for the induction of LTP by 24 hours post-injury including, postsynaptic density protein-95 (PSD-95), a major scaffolding protein that organizes the postsynaptic density (PSD), α-amino-3-hydroxy-5-methyl-4-isoxazolepropionic acid glutamate receptor 1 (AMPA-GluR1), and stargazin, an auxiliary GluR1 protein that binds AMPA-GluR1 to PSD-95. Modulation of the cyclic adenosine monophosphate (cAMP) pathway reversed the observed effects of blast on LTP. We theorized that blast-induced disruption of PSD-95 prevented translocation, and subsequent phosphorylation, of GluR1-containing AMPARs to the postsynaptic membrane, which, in turn, prevented potentiation.

The final aim was to investigate the efficacy of phosphodiesterase-4 (PDE4) inhibitors, which block degradation of cAMP, as a therapeutic strategy. When delivered immediately following primary blast injury, multiple PDE4 inhibitors proved efficacious in restoring LTP measured 24 hours post-injury. Roflumilast, a Food and Drug Administration-approved PDE4 inhibitor, was effective when delivered at a clinically relevant concentration (1nM) and at a delayed time point (up to 6 hours). Roflumilast reversed blast-induced changes in expression/phosphorylation of the key LTP protein targets. We hypothesized that maintenance of

PSD-95 drove the observed therapeutic effect. Greater work is necessary to determine how blast exposure degrades PSD-95 and how roflumilast prevented these detrimental effects.

This thesis has shown that primary blast exposure can negatively alter neurological function, as well as protein expression and phosphorylation. These studies expand the understanding of primary blast injury mechanisms, provide computational models with important tissue-level tolerance criteria, inform protective equipment design, inform clinical care guidelines for bTBI, and present a promising therapeutic candidate for further clinical investigation.

Table of Contents

List of Figures

List of Tables

List of Abbreviations

Abbreviation	Full Name
aCSF	artificial cerebral spinal fluid
AD	Alzheimer's Disease
AKAP	A-kinase anchoring protein
AMPA	α-amino-3-hydroxy-5-methyl-4-isoxazolepropionic acid
ANOVA	analysis of variance
bTBI	blast-induced traumatic brain injury
CA1	Cornu Ammonis 1
CA3	Cornu Ammonis 3
CaMKII	Ca^{2+}/calmodulin-dependent protein kinase II
cAMP	cyclic adenosine monophosphate
CaN	calcineurin
CCI	controlled cortical impact
ConWEP	Conventional Weapons Effect Program
CSF	cerebral spinal fluid
DG	dentate gyrus
DMSO	dimethyl sulfoxide
fEPSP	field excitatory postsynaptic potential
FPI	fluid percussion injury
GABA	γ-aminobutyric acid
GluR1	glutamate receptor 1
GSI	global synchronization index
HEPES	4-(2-hydroxyethyl)-1-piperazineethanesulfonic acid
IED	improvised explosive devices
ISI	inter-stimulus interval
KO	knock-out
LTP	long-term potentiation
MEA	microelectrode array
MF	mossy fiber
MPS	maximum principal strain
mTBI	mild traumatic brain injury
NMDA	N-methyl-D-aspartate
OHSC	organotypic hippocampal slice cultures
PC1	first principal component
PCA	principal component analysis
PDE4	phosphodiesterase-4
PDE10A	phosphodiesterase-10A

PI	propidium iodide
PInd	participation index
PKA	protein kinase A
PKC	protein kinase C
PPF	paired-pulse facilitation
PPR	paired-pulse ratio
PSD	postsynaptic density
PSD-95	postsynaptic density protein-95
PTFE	polytetrafluoroethylene
ROI	region of interest
Ser239/240	serine-239/240
Ser831	serine-831
Ser845	serine-845
SR	stimulus-response
SC	Schaffer collateral
TBI	traumatic brain injury
Thr286	threonine-286
UCH-L1	ubiquitin-c-terminal hydrolase-L1
UPS	ubiquitin-proteasome system

Acknowledgements

I would like to acknowledge the people who contributed to this thesis work during their high school and undergraduate studies: Jessica Villacorta, Charles (CJ) Levin, John Brady, Steve Rwema, Fatima Nathalie Morales, and John Tyson. I would also like to acknowledge the funding sources that made this work possible: National Defense Science and Engineering Graduate (NDSEG) Fellowship and Army Research Laboratories Multi-University Research Initiative (W911NF-10-1-0526). I would like to acknowledge the former and current members of the Neurotrauma & Repair Laboratory at Columbia University for their support, particularly Dr. Barclay Morrison, III whose mentorship, commitment to learning, and high standards of excellence have significantly shaped me as a scientist and a person. I would like to acknowledge Dr. Christopher Hue and Dr. Gwen Effgen for their contributions to my publications and Dr. Cameron R. 'Dale' Bass, and Dr. David F. Meaney for their mentorship and support of my thesis work. Finally, I would like to acknowledge the endless support and patience of my close friends and family throughout this process, in particular my fiancé, Elizabeth Ellis, and my parents, Melanie and Edward Vogel, Jr.

1 Introduction

Traumatic brain injury (TBI) is defined as a disruption of brain function due to mechanical forces acting on the head[1]. These forces can include an impact to the head, inertia-driven deformation of brain tissue due to head acceleration/deceleration, a penetrating injury, or bomb blast exposure, which includes the aforementioned forces in addition to loading from the shock wave[2]. TBI presents a significant problem for US military personnel, with nearly 350,000 TBIs diagnosed in this population since 2000[3]. The majority of military TBI (~83%) is considered mild in severity[3], and most mild TBIs (mTBIs) are attributed to blast exposure[4-6]. Blast-induced TBI is considered the signature injury of the recent military conflicts in Iraq in Afghanistan[4, 7]. The increased incidence of bTBI is due to a number of reasons: rise in the use of improvised explosive devices (IEDs), improved protection against penetrative blast injuries, and general awareness of brain injuries as a whole[5, 6, 8]. Civilians are also victims of bTBI, either as a result of explosive weaponry implemented in terrorist incidents or unexploded military landmines/ordinance[9, 10]. Neuroimaging via computed tomography (CT) or magnetic resonance imaging (MRI) following a mild bTBI is typically normal, and reported symptoms can include, but are not limited to, loss of consciousness (<30 minutes), cognitive dysfunction (memory loss, confusion, reduced attention span, problem-solving difficulties), and changes in personality (depression, anxiety, impulsivity, affected emotional response). While pharmacotherapies exist for treating some chronic symptoms of TBI, no clinically approved therapeutic for treating TBI-related memory loss currently exists. While research into TBI has increased greatly over recent years, further investigation is necessary to improve understanding of the pathophysiology of

bTBI. This thesis will investigate the biomechanics, pathobiological mechanisms, and potential treatment of bTBI.

1.1 Blast-induced traumatic brain injury

An explosive is a chemical substance capable of storing large amounts of energy in a small volume, which is released upon detonation[5]. Blast pressure waves emanate from the source of an explosion following the rapid expansion of gases that occur upon detonation. These waves can propagate through the air at various speeds prior to impinging on surrounding objects (i.e. soldiers, vehicles, buildings, etc.). The fastest, initial front of the pressure pulses, known as the shock wave, is a supersonic, discontinuous disturbance that takes the form of an extreme rise in local pressure over a short period of time[11]. For an open-field explosion, this pressure-time relationship is called a Friedlander curve (Figure 1), characterized by an initial rapid rise (microseconds) in pressure followed by a slow decay (milliseconds), which may drop below the ambient pressure before returning to baseline. Following the shock wave, a forced super-heated airflow, known as the blast wind, can subsequently impinge upon the subject, leading to a rapid acceleration and deceleration of the body[12]. The physics governing the interaction of blast forces and the soldiers' head lead to the initiation of bTBI.

Blast-induced TBI exhibits very complex, multiphasic injury biomechanics[13]. Primary blast injury is caused by the interaction of the shock wave with biological tissue. Secondary blast injury is caused by ejecta (shrapnel) being launched from the blast site and penetrating biological tissue. Tertiary blast injury is caused by inertial forces placed on biological tissue through rapid acceleration/deceleration of the body due to the blast. Finally, quaternary blast

injury encompasses all other forms of injury due to blast (burns, chemical exposure, toxic inhalation, radiation, etc.). Secondary blast injury is well protected against by current military helmet design[14, 15]. Tertiary blast injury is well investigated in the literature, with known potential for cognitive damage, likened to that of civilian TBI (i.e. falls, sports injuries, car accidents, etc.)[2]. It is unclear, however, if primary blast injury has a distinct, injurious effect as compared to other phases of blast. Tertiary and primary blast injury are biomechanically distinct; the former characterized as a high strain (10-50%), low strain rate (<50s^{-1}) exposure and the latter characterized as a low strain (<10%), high strain rate (100-1000s^{-1}) exposure[16, 17]. Identifying a potential pathobiological distinction between the two phases is critical for a complete understanding of bTBI. A major focus of this thesis is to define the injury biomechanics and pathophysiology of primary blast exposure further.

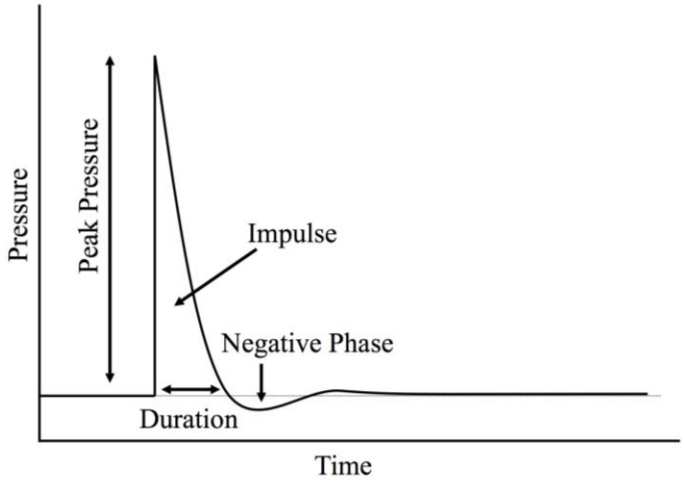

Figure 1 Friedlander wave. Open-field shock exposures are characterized by the Friedlander curve, defined by a peak overpressure, duration, and impulse.

Multiple animal models of blast have been introduced over the past 15 years, including gas-driven shock tubes[18-31], explosive-driven shock tubes[32, 33], open-air explosives[34, 35], and air guns[36, 37]. These models have utilized many different conditions, leading to inconsistencies in outcome measures between and even within models, making comparisons of results difficult. A major factor contributing to the variability is whether the animal's torso was protected from the shock wave, as previous research has shown that the lung is very susceptible to shock exposure[38, 39]. Another major difference across these models is whether motion of the head was controlled. Many studies attempted to restrict head motion in an effort to isolate primary blast[20, 22, 24, 26, 29, 30, 37, 40, 41]; however, even when attempting to restrain head motion, accelerations can be significant (500-1500 G's) and can lead to injurious effects[30, 40]. Eliminating all inertial loading is very difficult, and validation by high-speed video is often unreported[24]. Uncontrolled head acceleration during blast exposure could lead to additional closed-head TBI (tertiary phase) that confounds the delivery of isolated primary blast. The difficulties associated with controlling head kinematics make the study of pure primary blast injury challenging with *in vivo* injury models.

An advantage of studying primary blast injury with *in vitro* models is the ability to isolate specific phases of the injury biomechanics. The delivery of pressure transients to biological tissue was initially achieved through the use of barotrauma and compression chambers[42-45]; however, these injury models delivered pressures at much longer durations (~seconds to minutes) than those representative of a blast event (~milliseconds). Live charges have been used for *in vitro* blast injury models[46, 47]. Researchers also used gas-driven shock tubes to expose *in vitro* biological samples to primary blast[48-51]. One critical design concern with these models is the method of housing the sample during exposure. This factor is important to ensure that

samples do not experience any inertia-driven (tertiary) deformation. We have developed a fluid-filled sample receiver (Figure 2) to house samples during primary blast exposure with a gas-driven shock tube[49, 50, 52-56]. The receiver translates an in-air shock wave into an in-fluid pressure transient, analogous to intracranial pressure waves measured during blast exposures[49]. The advantages of our system are: 1) the delivery of military-relevant exposures, 2) prevention of inertia-driven deformation, 3) the prevention of internal shock wave reflections, and 4) the inclusion of a biofidelic barrier (fluid-filled polyvinyl chloride [PVC] plastic column sealed with a polydimethysiloxane [PDMS] sheet) between the tissue sample and the shock wave.

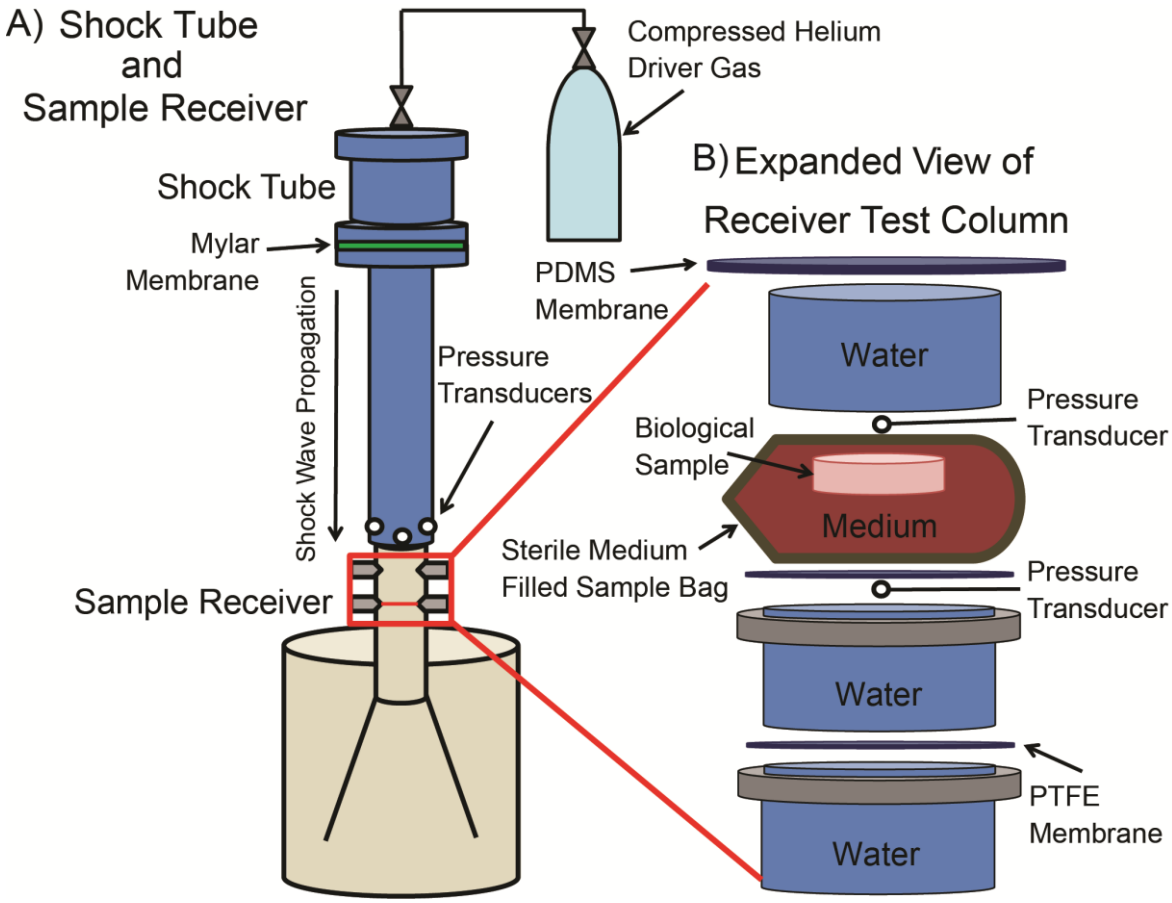

Figure 2 Diagram of *in vitro* primary blast injury model. The shock wave is formed by pressurizing the variable-length driver section of the shock tube (above the Mylar plastic membrane represented in green) with compressed gas (helium or nitrogen) until the membrane bursts, propagates down the length of the driven section, and exits the shock tube. Positioned directly under the shock tube exit, the *in vitro* receiver converts the in-air shock wave an in-fluid pressure transient, houses the sample in a sterile bag that is impedance-matched to water. Piezoresistive pressure transducers record in-air traces at the shock tube exit and in-fluid traces at the sample during blast exposure. Image reproduced with permission[50].

1.2 Blast-induced deficits in behavior and cognition

Symptoms of bTBI are wide-ranging due to a variety of factors (number of exposures, range of blast intensities, surrounding environment, proper use of body-armor, elapsed time since exposure, etc.). Clinical observations report the subtle nature of bTBI effects on motor and cognitive abilities, including both somatic (loss of consciousness, headache, dizziness, balance, hearing problems) and neuropsychiatric (memory loss, irritability, emotional) conditions[57-59]. Memory impairments are the most common and persistent cognitive defect associated with human TBI[60, 61]. The hippocampus has been associated with learning, spatial navigation, and the consolidation of episodic memories to long-term memories[62-65]. The hippocampal anatomy consists of three interconnected regions which make up its trisynaptic circuit: dentate gyrus (DG) filters input to the hippocampus, cornu ammonis 3 (CA3) amplifies neural signal, and cornu ammonis 1 (CA1) transduces signal to the cerebral cortex[66]. Previous research into civilian TBI has identified the hippocampus as an important brain region to study resultant injury effects[67-70]. Common clinical symptoms from patients who have experienced bTBI (memory loss, spatial navigation loss) overlap with the major biological functions of the hippocampus[4].

Motor deficits after *in vivo* bTBI are variable in studies that used the rotarod performance test, which evaluates balance and motor coordination. Some studies measured a significant decline in rotarod performance[71-73] and others measured no change[23-25, 27, 74]. Certain cognitive tests like the Morris Water Maze (MWM), which tests spatial learning and memory, have also produced mixed results[23, 25, 75]; however, others such as the novel object recognition (NOR) test, which tests short-term memory, have consistently measured blast-induced deficits[27, 35, 74, 76, 77].

The reported differences from previous blast animal studies may be linked to the variability in blast injury methodology across experiments.

1.3 Blast-induced deficits in electrophysiological function

Blast injury causes behavioral and neurocognitive deficits; however, it is difficult to directly connect behavioral/cognitive deficits to electrophysiological dysfunction. Studies that explore blast-induced electrophysiological dysfunction are limited, and even less have specifically investigated primary blast. Neurobiologists consider LTP to be the electrophysiological correlate of learning and memory[78-80]. Long-term potentiation is induced by short trains of high-frequency stimulation to excitatory synaptic pathways that cause an sustained increase in the efficiency of synaptic transmission[80]. Two studies have reported deficits in LTP in acute mouse hippocampal slices at 2 and 4 weeks post-blast exposure; however, both implemented a combined primary-tertiary blast model[24, 81]. Other studies observed reductions in hippocampal LTP as early as 1 day and as late as 8 weeks following non-blast TBI[82-86]. Paired-pulse facilitation (PPF) is a measure of short-term synaptic plasticity, governed by presynaptic neurotransmitter release, γ-aminobutyric acid receptor-A ($GABA_A$), $GABA_B$, and NMDA receptor (NMDAR) dynamics. This phenomenon has not been investigated following blast injury; however, conflicting results have been observed after *in vitro* stretch injury[87, 88]. There is a need for greater investigation of neuronal plasticity following blast injury.

Basal electrophysiological function can be evaluated following brain injury as well. Spontaneous activity represents the base level of activity in a quiescent slice. Parameters that define spontaneous function such as event rate, magnitude, or duration, have not been

investigated after blast injury. Studies employing non-blast injury models have reported mixed findings. Outcomes have ranged from decreased event rate to no change to increased event rate[88-90]. Basal evoked function provides insight into the neurons' firing capacity in response to basic electrical stimulus patterns. One study observed a decrease in CA1 excitability when measured 5 days following *in vivo* rodent blast injury[74], while other studies observed no change in basal evoked function in the hippocampus as well as the corpus callosum at 2 weeks following injury[22, 24]. To date, our group is the only one to investigate basal evoked neuronal function with an *in vitro* blast injury model[53]. Non-blast TBI studies found variable changes in basal evoked function across both *in vivo* and *in vitro* injury models[83, 88, 90-93]. The effect of blast injury on basal electrophysiological function remains unclear and warrants further research.

1.4 Cellular mechanisms of blast-induced electrophysiological dysfunction

In primary blast injury models, many studies have observed minimal amounts of overt neuronal death or tissue damage after exposure [21, 24, 30, 48, 53]; however, some have reported contradictory findings of significant cell loss or tissue damage after blast[51, 94]. The variability in findings most likely stems from the variability in blast injury models, as described above. Large amounts of cell death have been observed in non-blast injury models and can contribute to subsequent deficits in function[69, 89, 90, 95-98]. Neuronal death can clearly influence functional deficits after injury. Although less common, functional deficits in the absence of cell death were observed in non-blast TBI models, as well[61, 99, 100].

Investigations into cellular mechanisms of primary blast-induced functional deficits are minimal. One study associated changes to the cytoskeleton, specifically neurofilament-200 and

αII-spectrin, and voltage-gated sodium channel anchoring and expression with increased anxiety and reduced compound action potential amplitudes and durations measured in unmyelinated fibers at 48 hours following a low-level shockwave exposure in rats[101]. This data suggested that disrupted postsynaptic receptor anchoring to cytoskeletal proteins might be one cause for the observed injury effect. It is important to note that the animals' heads were not restrained nor were kinematics verified with high-speed video. Another study observed deficits in memory and cognition concurrent with hippocampal LTP deficits without changes in basal synaptic transmission after combined primary-tertiary blast exposure in mice[24], suggesting that dendritic protein synthesis or changes in gene transcription may interrupt cellular signaling transduction downstream of synaptic glutamate release, thus preventing LTP[80, 102-104]. It is important to note that blast exposure did not induce behavioral deficits when head motion was limited in this study[24]. These two studies suggest that blast exposure disrupts postsynaptic receptor integrity.

Non-blast TBI induced mixed alterations to postsynaptic membrane receptors. Reduced subunit expression and electrophysiological function of the excitatory NMDAR have been observed following controlled cortical impact (CCI) and fluid percussion injury (FPI), respectively[85, 105]; however, other studies have observed increased NMDA channel activity and protein expression after weight drop injury *in vivo* and *in vitro* stretch injury[90, 106, 107]. NMDARs, specifically the NR2B subunit, have been identified as the mechanosensitive synaptic membrane protein in stretch injury[108]. *In vitro* stretch injury to cortical cultures potentiated currents for the postsynaptic excitatory α-amino-3-hydroxy-5-methyl-4-isoxazolepropionic acid receptor (AMPAR)[109, 110]. Other studies have observed a decrease in AMPAR gene and protein expression after CCI[111, 112]. Some studies observed an increase in GABA receptor (GABAR) inhibition after FPI, CCI, and *in vitro* stretch injury, while others observed decreased GABAR

inhibition following *in vitro* stretch[87, 113-115]. Significant changes in GABAR subunit expression were observed from 3 hours out to 7 days following FPI and CCI[112, 116, 117]. Changes to these excitatory and inhibitory receptors and others cause alterations to the synaptic excitatory-inhibitory tone, neurotransmitter concentrations, free radical concentration, and ionic content within the neuron, all of which can affect neuronal function and survival[74, 115, 118-122]. Secondary effects on synaptic cytoskeletal proteins, protein kinases, protein phosphatases, and transcription factors can cause further electrophysiological dysfunction and neuronal death[85, 123-136].

1.5 Neuroprotection through phosphodiesterase-4 inhibition

One electrophysiological process that has been shown to be affected by both blast and non-blast TBI is LTP[24, 83-85]. High-frequency stimulation triggers activation of NMDARs which lead to an influx of Ca^{2+} ions into the postsynaptic space and subsequent activation of protein kinases[80]. At a cellular level, the potentiated signal is represented by an increase of phosphorylated AMPA-GluR1 in the postsynaptic density (PSD), which is modulated by activation of Ca^{2+}/calmodulin-dependent protein kinase II (CaMKII), cyclic adenosine monophosphate (cAMP)-dependent PKA, and protein kinase C (PKC)[137-140]. PKA is activated by cAMP, which is synthesized from adenosine triphosphate (ATP) by adenylate cyclase (AC)[141]. An important step in the regulation of cAMP is its hydrolysis into adenosine monophosphate (AMP) by phosphodiesterase-4 (PDE4)[142, 143].

Investigation of blast-induced alterations to cAMP signaling has been limited. One study observed that 3',5'-cAMP did not significantly change in prefrontal cortex (PFC) following mild blast injury in rats[29]. Conversely, studies have reported that TBI can affect the cAMP

pathway[130, 144, 145]; and that subsequent modulation of the cAMP pathway with PDE4 inhibitors reversed the negative impact of injury on cAMP[146-148], improved neurocognitive function, and restored LTP[147]. PDE4 inhibition enhanced cognition for neurological conditions such as Alzheimer's disease (AD), schizophrenia, and aging[149-152]. All of these studies utilized the highly-selective PDE4 inhibitor rolipram, which has previously failed clinical trials to treat depression due to the high incidence of adverse side-effects, which included myocardial and liver degeneration, nausea, and altered behavior[153, 154]. Another selective PDE4 inhibitor, roflumilast, improved memory and has been Food and Drug Administration (FDA)-approved for the treatment of chronic obstructive pulmonary disorder[155-157]. The only concern with roflumilast is that permeability across the blood-brain barrier (BBB) is poor[158]. This motivates the development of potential therapeutic strategies to help protect against primary blast-induced electrophysiological deficits. Modulation of the cAMP pathway through PDE4 inhibition, specifically with roflumilast, could provide a potential treatment for observed deficits.

1.6 Significance

TBI is a serious public health issue. The CDC has estimated that 1.7 million persons sustain a TBI each year[159]. Of those diagnosed, approximately 1.36 million were treated and released from the emergency department, 275,000 were hospitalized, and 52,000 patients died[159]. These estimates do not include the countless people who sustain a mild TBI but fail to seek medical attention. An estimated 5.3 million U.S. residents are living with TBI-related disabilities, which include long-term motor, cognitive, and psychological impairments[160]. Among civilians, the leading causes of TBI are motor vehicle accidents, physical violence, and

falls[159]. The estimated socioeconomic cost of TBI in the U.S. in 2010 was $76.5 billion, including $11.5 billion in medical costs and $64.8 billion in indirect costs (loss of productivity, lost wages, and non-medical expenditures)[161, 162].

In 2014, over 25,000 U.S. military service members worldwide were diagnosed with a TBI[3]. Annual medical costs for veterans with a TBI were about 4-times greater than veterans without a TBI[163]. The cost of care for TBI within the U.S. military population rose from $21 million in 2003 to approximately $646 million in 2010[164]. For U.S. military personnel, there is a large concern regarding the possible long-term effects of mild TBI as a result of deployment-related head injuries, particularly those due to proximity to explosive blasts[14]. Although it is difficult to quantify how often blast events result in brain injuries, the rate is estimated to be approximately 60%[165, 166]. IEDs have been implicated as the primary cause of battlefield injuries to the head and neck to soldiers in Iraq[167]. Blast-induced TBI accounts for a significant portion of injuries that military personnel sustained in training and combat. Mild bTBI presents both acute and chronic health problems. Registry data of 1129 post-deployment military personnel showed that those with mild bTBI were five times more likely to report negative health changes 6 months after diagnosis than were those exposed to mild blast without TBI[168]. Researchers concluded these results diverged from non-blast mTBI, which suggested that recovery from shock exposure might be different. A better understanding of the pathobiological mechanisms of primary bTBI is necessary to provide better combat equipment and emergency care for active duty soldiers, as well as treatment protocols for injured veterans.

The proposed studies will elucidate the biomechanics, functional deficits, injury mechanisms, and potential therapeutics for primary blast exposure. These studies will be the

first to measure the mechanical response (i.e. tissue strain and strain rate) of OHSCs to primary blast exposure. Currently, it is difficult to compare findings from bTBI studies and non-blast TBI studies due to the difference in strains and strain rates applied to the brain tissue in each injury model. An understanding of the induced deformation in our *in vitro* primary blast model would inform comparisons of functional outcomes (cell death, electrophysiology, etc.) to *in vitro* non-blast injury models. These studies will be the first to determine operational thresholds for primary blast-induced electrophysiological dysfunction to be used in computational models, identifying peak overpressure, duration, and impulse levels that induce functional changes. This thesis, in combination with FE models and greater preclinical research, will advance the understanding of operational thresholds for blast injury, improving military helmet designs and military guidelines for rest. These studies will investigate the time course of functional deficits after primary blast injury and begin to determine the specific cellular mechanisms responsible for dysfunction. Understanding the cellular mechanisms and time course of primary bTBI will assist researchers in the development of therapeutics and assist military emergency care personnel in the management of blast-injured soldiers. Finally, this study will be the first to investigate the therapeutic potential of PDE4 inhibitors, specifically FDA-approved roflumilast, in bTBI. To date, there are no pharmacological agents approved to treat TBI-induced memory deficits, as all Phase III clinical trials in TBI have failed[169], hence there is a compelling need for the development of an effective TBI therapeutic.

The broader impact of this work will be to improve the overall understanding of bTBI and the treatment of military personnel, as well as civilians, who have suffered bTBI[4, 10, 170]. Current military emergency practice requires that any war fighter within 50 meters of an explosive blast must be screened by a first responder for TBI[170]. The discovery of an operational

blast threshold for neurological dysfunction could provide military healthcare professionals with a more informed evaluation of the potential incidence of TBI. TBI-induced neuronal dysfunction on the cellular level can lead to altered macroscopic cognitive function[69, 171]. Therefore, a thorough understanding of bTBI-induced electrophysiological dysfunction is critical to characterize the effect of bTBI on neurocognitive function. Current treatment protocols for bTBI include mandatory removal from activity, rest, and potentially non-narcotic analgesics and/or anti-migraine medication[5, 170]. There is a dire need for an effective pharmacological intervention to assist in the recovery from bTBI. The proposed studies will help elucidate the contribution of primary blast exposure to the overall epidemiology of bTBI and attempt to identify a potential therapeutic.

2 *In vitro* primary blast exposure induced low-strain, high-strain rate deformation in hippocampal slice cultures[1]

2.1 Introduction

Blast-induced traumatic brain injury (bTBI) is a serious health concern for military personnel and civilians in areas of conflict around the world. Between April 2007 and December 2015, the Veterans Health Administration determined that nearly 138,000 US service personnel were diagnosed with combat TBI, mainly mild TBI (mTBI) caused by blast[172]. The increased use of improvised explosive devices (IEDs) coupled with greater surveillance by medical professionals for brain injuries have raised the incidence of bTBI. The injury biomechanics of blast-induced TBI are complex and multi-phasic[13]. Primary blast injury is initiated by the interaction of the shock wave with the skull and the brain as the shock wave transits the head[5]. Secondary blast injury is defined as a penetrating injury, caused by ejecta launched from the blast origin. Tertiary blast injury is driven by inertial forces loading the biological tissue through rapid acceleration/deceleration of the body due to blast. Although secondary and tertiary blast exposures are known to be injurious, the effect of primary blast in isolation is still debated.

Research into bTBI has increased over the last 20 years with studies using a variety of methods to model blast exposure including gas-driven shock tubes[18-31, 51, 74, 173], explosive-driven shock tubes[32, 33], open-air explosions[34, 35, 47, 174], and air guns[36, 37]. Previous bTBI studies using *in vivo* animal models have reported altered memory and cognition following injury[23, 24, 27, 30, 35, 37,

[1] A modified version of this chapter is currently in preparation: **Vogel III, E.W.**, Panzer, M.B., Morales, F.N., Varghese, N., Meaney, D.F., Bass, C.R.D., Morrison III, B. Direct observation of low strain, high rate deformation of cultured brain tissue during primary blast and validation of finite element simulations, In preparation. (2017).

[71, 74, 75, 81, 173, 175]. Some of these studies assert that motion of the head, and hence inertial loading, was eliminated, thereby providing a model of pure primary blast loading, i.e. the shock wave only[24, 37, 74, 173, 175]; however, it is extremely difficult to completely fix the head during blast exposure. Even when extra steps were taken to secure the head, significant head accelerations remained as revealed by analysis of high-speed video[24, 30, 74]. Therefore, it remains a considerable challenge to investigate pure primary blast in animal models. We expressly designed our *in vitro* injury model to eliminate inertia-driven acceleration, thus isolating primary blast exposure[49, 50]. Through high-speed video analysis, we observed no bulk motion of the tissue within the receiver, confirming an absence of inertia-driven forces on the tissue sample[50]. We have previously reported that primary blast *in vitro* has negative effects on hippocampal electrophysiological function, protein expression, and blood-brain barrier integrity[52-56, 176].

Contemporary *in vitro* models of non-blast TBI injure cultures with deformations in the range of 20-50% strain applied at strain rates <50s^{-1} [16, 177, 178]. Computational models of inertia-driven TBI have predicted deformations of similar strain magnitudes and rates[179-182]. Conversely, computational simulations of the head under shock wave loading have predicted that brain tissue deformation is ≤10%, but applied at higher rates from 12-960s^{-1} [17, 183]. Modeling of our *in vitro* receiver under shock tube loading predicted tissue strains of ≤8% at high strain rates (80s^{-1}); however, these biomechanics have not been confirmed experimentally[49]. The purpose of this study was to characterize the tissue biomechanics within organotypic hippocampal slice cultures (OHSCs) during shock wave loading in our *in vitro* blast injury model experimentally. We utilized a stereoscopic high-speed camera system, in combination with digital image correlation to quantify strain histories for a range of shock exposures. We found that primary blast exposure induced low strains (<9%) and high strain rates (25-85s^{-1}) in OHSCs *in vitro*, with

peak tissue strain and rate occurring after the pressure wave had passed the sample in the fluid filled receiver. Blast-induced strains and rates were highly correlated with in-air blast impulse and in-fluid peak pressure parameters. We observed thresholds for electrophysiological dysfunction, defined by deficits in long-term potentiation (LTP), between 3.7-6.7% strain and 25-33s^{-1} rate. This study experimentally confirmed computationally predicted strain magnitudes and rates using our *in vitro* blast model. The findings within this study provide biomechanical injury thresholds for future computational models of primary bTBI that will contribute to the design of protective equipment and diagnostic capabilities.

2.2 Materials and Methods

2.2.1 Organotypic hippocampal slice cultures

All animal procedures were approved by the Columbia University Institutional Animal Care and Use Committee (IACUC). OHSCs were generated from P8-P10 Sprague Dawley rats as previously described[50, 53, 55, 184]. In brief, the hippocampus was excised, cut into 400μm thick sections on a McIlwain tissue chopper (Ted Pella Inc, Redding, CA), and plated onto Millicell inserts (EMD Millipore, Billerica, MA) in Neurobasal medium supplemented with 2mM GlutaMAX™, 1X B27 supplement, 10mM 4-(2-hydroxyethyl)-1-piperazineethanesulfonic acid (HEPES), and 25mM D-glucose (Life Technologies, Grand Island, NY). Cultures were fed every 2-3 days after plating with full serum medium, containing 50% Minimum Essential Medium, 25% Hank's Balanced Salt Solution, 25% heat inactivated horse serum, 2mM GlutaMAX, 25mM D-glucose, and 10mM HEPES (Sigma). Cultures were maintained for 10-14 days prior to blast exposure.

2.2.2 Cell death measurement

Propidium iodide (PI) fluorescence was used to assess tissue health prior to blast exposure, applying 2.5 μM PI (Life Technologies) in serum-free medium to tissue samples immediately before injury. Cell death was determined using MetaMorph (Molecular Devices, Downingtown, PA) according to published methods[50, 53, 55, 95]. Cultures that exhibited greater than 5% cell death before exposure were eliminated. Previous studies with this injury model have reported that blast injury at the levels used in this study caused minimal cell death[53, 55].

2.2.3 Primary blast exposure

Blast injury methods have been described previously in detail[49, 50, 52-56]. For this study, a square box was attached around the receiver column and filled with water to minimize image distortion caused by the cylindrical column. Cultures were first spray painted to create a stochastic fiducial pattern for strain analysis and then placed into sterile bags filled with serum-free medium that was pre-equilibrated with 5% CO_2 at 37°C. Any air bubbles were fastidiously removed from the bag, which was sealed and placed into the receiver column. The receiver column was filled with pre-warmed water (37°C), sealed with a silicone membrane, and the shock tube was fired. Blast exposure levels (Table 1) were chosen so that in-fluid peak pressure and duration parameters were minimally correlated ($r^2 = 0.04$).

	In-air			*In-fluid*		
Exposure Level	***Pressure (kPa)***	***Duration (ms)***	***Impulse (kPa•ms)***	***Pressure (kPa)***	***Duration (ms)***	***Impulse (kPa•ms)***
Level 1	106 ± 2	0.25 ± 0.01	9 ± 2	134 ± 2	1.5 ± 0.01	89 ± 1
Level 2	93 ± 3	1.4 ± 0.01	39 ± 1	270 ± 15	2.6 ± 0.02	295 ± 56
Level 3	190 ± 2	1.2 ± 0.01	73 ± 1	516 ± 31	1.30 ± 0.03	254 ± 35
Level 4	336 ± 8	0.84 ± 0.01	87 ± 2	598 ± 15	1.85 ± 0.30	440 ± 13

Table 1 Blast exposure levels tested in Chapter 2. Blast exposures were characterized by three different parameters of the shock wave: peak overpressure (kPa), duration (ms), and impulse (kPa•ms). Four different exposure levels (in addition to sham exposure) were utilized as previously reported by Effgen et al. (2014)[53]. Parameters are reported for the in-air shock wave and the in-fluid pressure transient. These blast pressure histories are similar to those experienced in-theater[53].

Piezoresistive pressure transducers (Endevco 8530B-500, San Juan Capistrano, CA, USA) recorded incident pressure at the shock tube exit. Peak overpressure, duration, and impulse were recorded, processed, and quantified as previously described[50, 52, 53, 55]. Representative in-fluid pressure traces for each blast exposure level are presented in Figure 3.

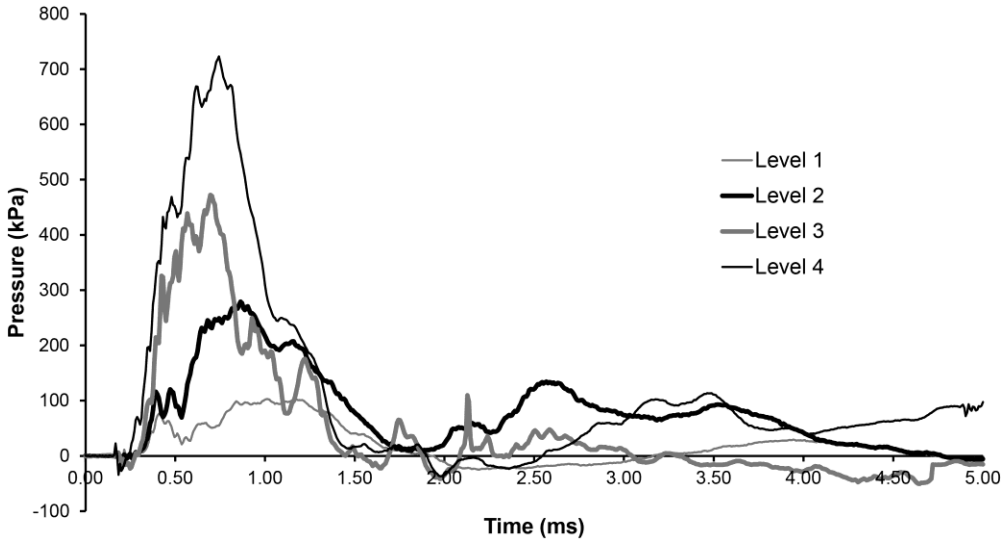

Figure 3 Representative in-fluid pressure profiles for blast exposures used in this study. The traces represent the in-fluid pressure profiles at the level of the sample for each of the blast levels tested in this study (Levels 1-4). Note that the duration of the pressure pulse is less than 5ms.

2.2.4 High-speed videography and digital image correlation (DIC)

A pair of Fastcam SA-X2 charge-coupled device (CCD) cameras (Photron USA, San Diego, CA) captured stereophotogrammetric videos of OHSCs during blast exposure. A calibration cube (15mm x 12mm) established a global coordinate system to orient the cameras in 3D space. The two cameras simultaneously recorded the culture during blast exposure at 5,000 frames per second (FPS) with a resolution of 896 x 896 (20μm pixel size).

Digital image correlation (DIC) was used to map unique correlation areas, or facets, of the spray pattern on the hippocampal slices to identify the same location in the images from the left and right cameras (Aramis, GOM, Brunswick, Germany). At each time step, the algorithm successively identified the location of the center of each facet in the left and right image. Knowing the global positions of the cameras relative to the sample, the facet's location within both images was converted into a single set of 3D coordinates in real space. To calculate facet deformations, the 3D coordinates were transformed onto the surface of the culture using the assumption that the local neighborhood of a point can be well approximated by a tangential plane. The tangential plane was calculated separately for both the undeformed and deformed states, and then the points in the local neighborhood were projected perpendicularly onto the tangential plane. This transformation resulted in two sets of points on the tangential plane for the undeformed and deformed state.

Facet coordinates were tracked between the reference frame and the deformed frame to calculate the deformation gradient (F) for each facet at each time step. Each deformation gradient was decomposed into the product of two tensors using the polar decomposition theorem (Equation 1): a pure stretch tensor (U) and a pure rotation matrix (R).

$$\boldsymbol{F} = \boldsymbol{R} \cdot \boldsymbol{U} \tag{1}$$

The stretch tensor was computed from the Cauchy-Strain tensor (C) and the orthogonal rotation matrix (Equations 2-4).

$$\boldsymbol{C} = \boldsymbol{F}^{\boldsymbol{T}} \cdot \boldsymbol{F} = \boldsymbol{U}^{\boldsymbol{T}} \cdot \boldsymbol{R}^{\boldsymbol{T}} \cdot \boldsymbol{R} \cdot \boldsymbol{U} \tag{2}$$

$$\boldsymbol{R}^{\boldsymbol{T}} \cdot \boldsymbol{R} = \boldsymbol{I} \tag{3}$$

$$\boldsymbol{U} = \sqrt{\boldsymbol{C}} \tag{4}$$

The first eigenvalue of the stretch tensor yielded the maximum principal strain (MPS) within each facet plane at each time step. For all facets across the sample at each time, the MPS was averaged. Strain rate was calculated from the average MPS history. Both strain and strain rate induced strains across the range of blast intensities were analyzed by ANOVA, followed by Bonferroni *post hoc* tests with statistical significance set as $p < 0.05$. The Pearson correlation coefficient was calculated to determine with which blast parameters strain and rate were most highly correlated (duration, peak overpressure, and impulse measured in-air and in-fluid).

2.3 Results

2.3.1 Primary blast exposure induced low strains

The initial rise in strain occurred over the first 2ms of pressure loading; however, strain did not reach maximum magnitudes until the pressure pulse had transited the sample (>3ms). After this point, strains were induced by deformation of the Millipore membrane with limited bulk motion of the sample. We provided a time history of induced strains (Figure 4) following Level 4 blast exposure to visualize slice deformation during blast.

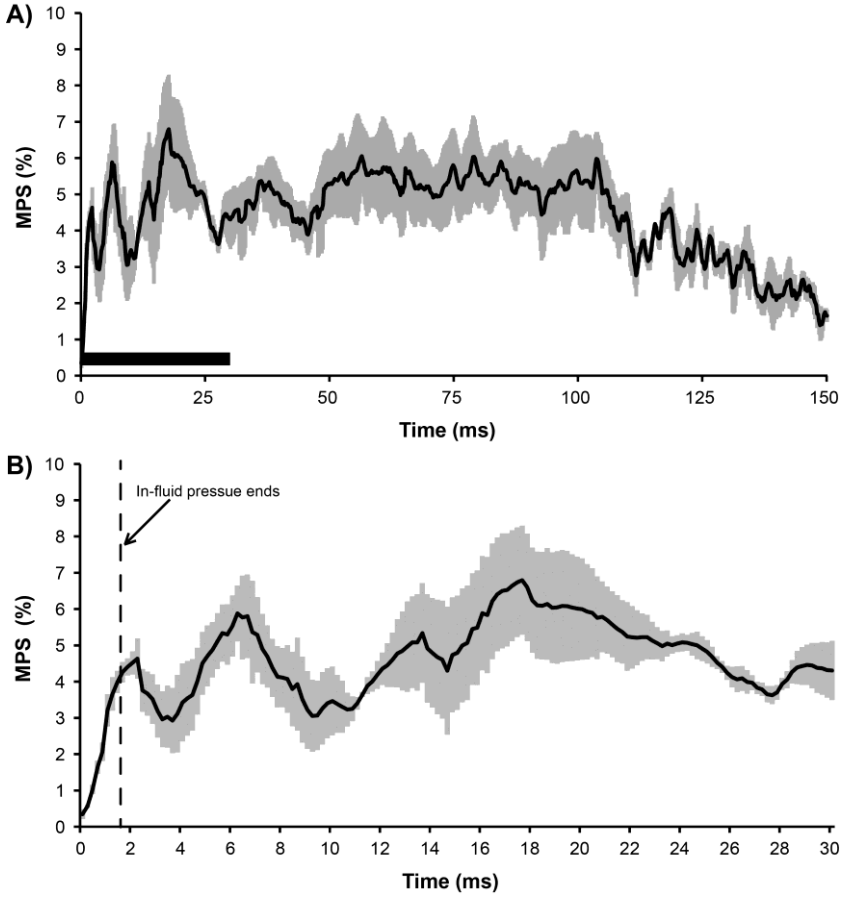

Figure 4 Time history of tissue strains induced by Level 4 blast exposure. (A) The trace represents the average maximum principal strain (MPS) on the tissue sample surface (± SEM, N=3) over the first 150ms following Level 4 blast exposure. The black bar marks 30ms after blast, which is expanded in B. (B) The trace represents the MPS on the tissue sample surface (± SEM, N=3) over the first 30ms following Level 4 blast exposure. The dotted vertical line indicates the time point when the in-fluid pressure transient passes the sample.

We observed that blast exposure induced strains of low magnitude (< 10%) (Figure 5A). Level 1 blast exposure induced average maximum principal strains of 3.7 ± 0.4%. Level 2 blast exposure significantly (p = 0.046) increased strains (6.7 ± 0.6%), as compared to Level 1 blast. Level 3 (8.2 ± 0.8%) and Level 4 (8.2 ± 0.6%) blast exposures induced significantly (p = 0.005) higher strains than Level 1 blast, but not Level 2 blast.

When compared to blast input parameters (Figure 5B: duration, Figure 5C: peak pressure, and Figure 5D: impulse), strain best correlated with in-air impulse (R^2 = 0.9105) and in-fluid peak pressure (R^2 = 0.8579). Strain was somewhat correlated to in-fluid impulse (R^2 = 0.7118), but only weakly correlated to in-air pressure (R^2 = 0.4363), in-air duration (R^2 = 0.5209), and in-fluid duration (R^2 = 0.0044).

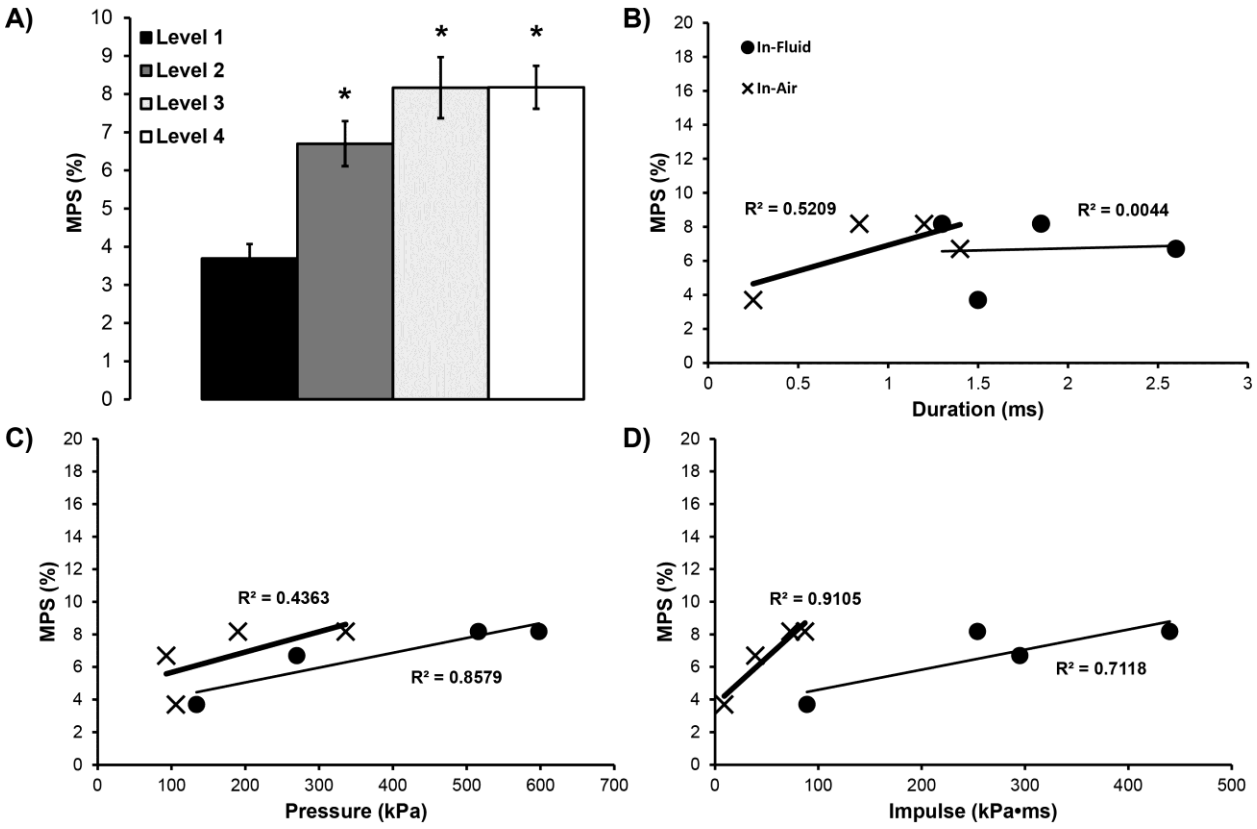

Figure 5 Primary blast exposure induced strains of low magnitudes. (A) Increasing blast exposure increased the average maximum principal strain (MPS) in OHSCs, but remained below 9% (mean ± S.E.M.; n=3, * $p<0.05$, as compared to Level 1 blast). (B) Linear correlation between MPS and blast duration in-air and in-fluid, indicating a weak association with R2 = 0.0044 and R2 = 0.5209, respectively. (C) Linear correlation between MPS and blast peak pressure, indicating a strong association with in-fluid (R2 = 0.8579) and a weak association with in-air (R2 = 0.4363) peak pressure. (D) Linear correlation between MPS and blast impulse indicating a strong association with in-air (R2 = 0.9105) and a moderate association with in-fluid (R2 = 0.7118) impulse.

2.3.2 Primary blast exposure induced high strain rates

Blast exposure above Level 2 significantly elevated maximum strain rate (Figure 6A). Level 1 and Level 2 blast exposure induced average maximum strain rates of 25.2 ± 6.6 and 32.9 ± 2.4s^{-1}, respectively. Level 3 blast exposure significantly increased strain rate (76.5 ± 4.6s^{-1}), as compared to Level 1 (p = 0.02) and Level 2 (p = 0.047) blast. Level 4 (85.6 ± 15.3s^{-1}) blast

exposure induced significantly (p = 0.005) higher strains than Level 1 (p = 0.007) and Level 2 (p = 0.017) blast.

When compared to blast input parameters (Figure 6B: duration, Figure 6C: peak pressure, and Figure 6D: impulse), blast-induced strain rates best correlated with in-fluid pressure (R^2 = 0.9739) and in-air impulse (R^2 = 0.9346). Strain rate was somewhat correlated to in-air pressure (R^2 = 0.7995) but only weakly correlated with in-fluid impulse (R^2 = 0.5422), in-air duration (R^2 = 0.0787), and in-fluid duration (R^2 = 0.1184).

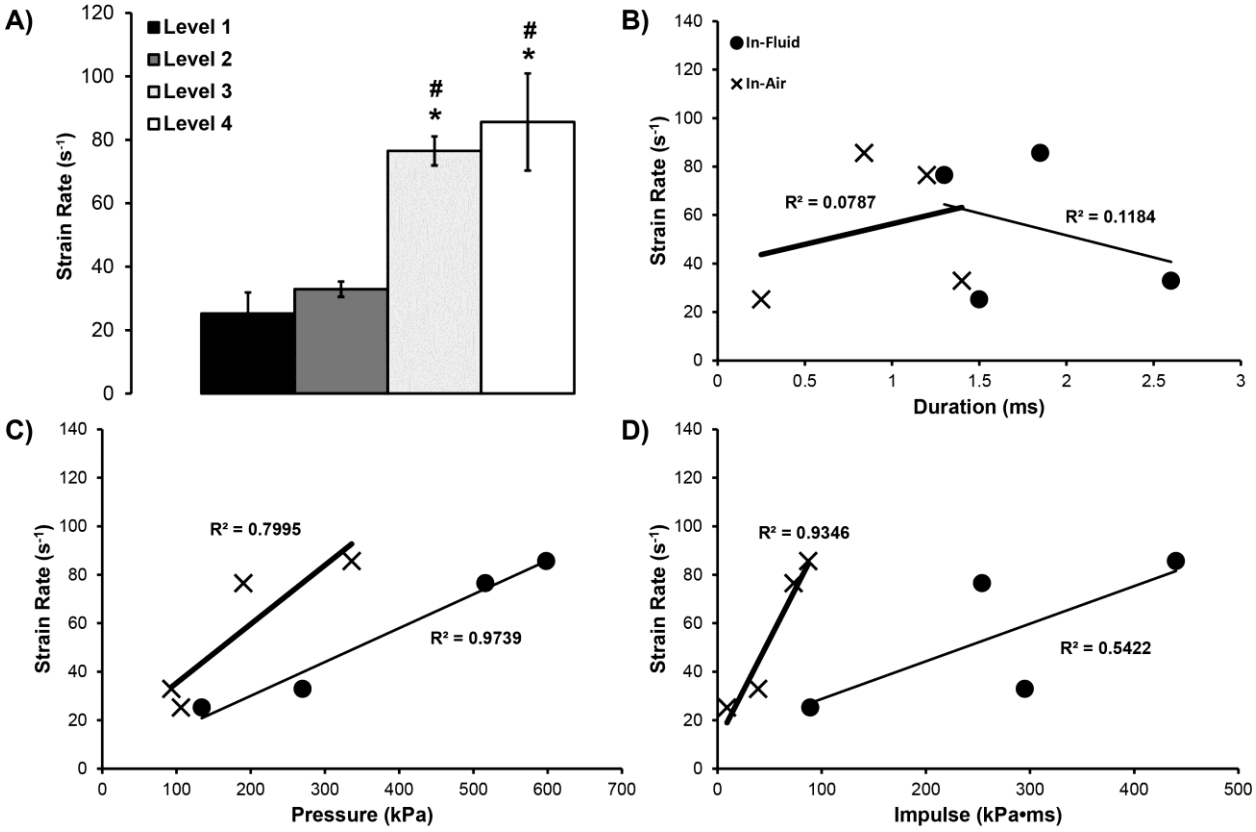

Figure 6 Primary blast exposure induced deformations with strain rates in excess of 80 s^{-1}. (A) Increasing blast exposure increased the average peak strain rate in OHSCs. Both Level 3 and Level 4 blast exposures induced significantly greater strain rates over both Level 1 and Level 2 blast. (mean ± S.E.M.; n=3, * p<0.05, as compared to Level 1 blast, # p < 0.05 as compared to Level 2 blast). (B) Linear correlation between strain rate and blast duration in-air and in-fluid, indicating a weak association with R^2 = 0.0787 and R^2 = 0.1184, respectively. (C) Linear correlation between strain rate and blast peak pressure

indicating a strong association with in-fluid (R^2 = 0.9739) and a moderate association with in-air (R^2 = 0.7995) pressure. (D) Linear correlation between strain rate and blast impulse indicating a strong association with in-air (R^2 = 0.9346) and a weak association with in-fluid (R^2 = 0.5422) impulse.

2.3.3 Strain and rate thresholds for blast-induced LTP deficits

We then compared the measured strain and strain rates at these blast levels to potentiation at the same blast intensities measured previously [55]. After an applied strain of 3.7%, LTP (Figure 7A) was not different from sham cultures; however, after an applied strain of 6.7% or greater, LTP was significantly reduced. Potentiation exhibited a strong negative correlation with strain (R^2 = 0.8688). After an applied strain rate of 25s^{-1}, LTP (Figure 7B) was not different from sham cultures; however, after an applied strain of 33s^{-1} or greater, LTP was significantly reduced. Potentiation exhibited a moderate negative correlation with strain rate (R^2 = 0.7967).

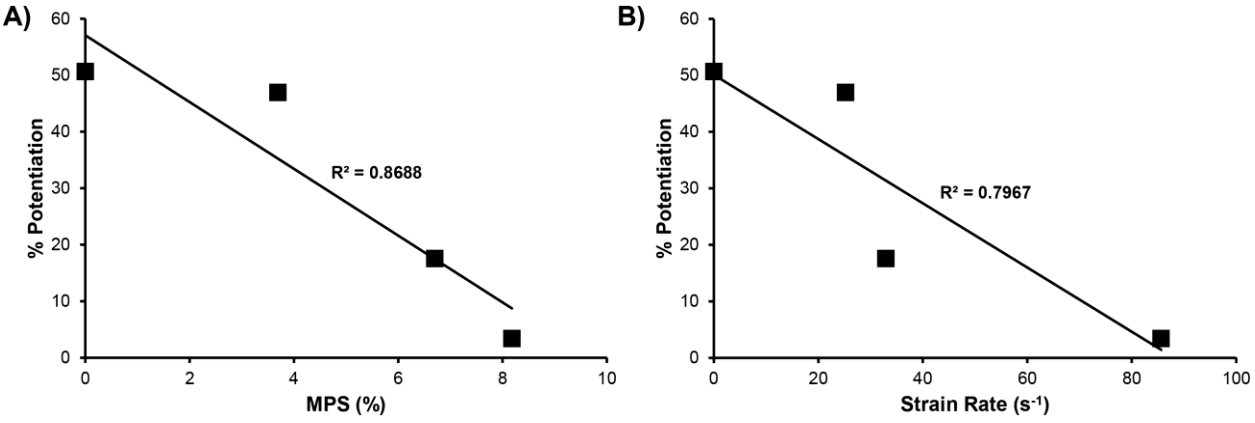

Figure 7 Increased strain magnitude and rate reduced long-term potentiation (LTP). (A) We observed a threshold for significant LTP deficits between 3.7% and 6.7% MPS. LTP deficits were strongly correlated with MPS with an R^2 = 0.8688. (B) We observed a threshold for LTP deficits for strain rates between 25 and 33s^{-1}. LTP deficits were moderately correlated with strain rate with an R^2 = 0.7967.

2.4 Discussion

This is the first study to experimentally measure primary blast-induced strain and strain rates in hippocampal tissue. We exposed OHSCs to a range of blast exposures (Levels 1-4) and observed that primary blast induced low strains (3-9%) and high strain rates (25-86s^{-1}). A strain threshold for LTP deficits ranged between 3.7-6.7% and a strain rate threshold ranged between 25-33s^{-1}. Both induced tissue strain and strain rate were highly correlated with in-air impulse and in-fluid peak pressure. The observed tissue strain and rate were well predicted computationally for this injury model by Panzer and colleagues (<8%, ~80s^{-1}), similarly observing maximum strains after the pressure wave had passed the sample.

Although no other study has experimentally quantified strain fields in brain tissue following blast exposure, one study found that shock loading of a poly-(methyl methacrylate)/Perma-Gel model of a human skull/brain induced 4.5% strain or less within the Perma-Gel[185]. Although strain rates were not explicitly reported, the study reported that loading occurred at high-strain rates. Peak pressures in the gel were 350kPa, which is slightly greater than our Level 2 blast that induced 6% strain. Another study employed a Split-Hopkinson Bar to induce strain rates of over 8000s^{-1}, across a range of strains (3-42%), in acute coronal brain slices embedded in gelatin blocks[186]. Although the pressure transient at the tissue level exhibited a similar rise-time (~300μs) and duration (~1ms) applied in our study, the peak pressures within the aCSF greatly exceeded those within the receiver from our study (11MPa vs. 0.6MPa). Average maximum principal strains in that study were 28%, which subsequently induced degenerating neurons in CA1 at 6 hours post-injury. Although that study corroborates our finding that increased fluid pressures caused elevated strains and strain rates, the strain and rates greatly exceeded those in our study, which could explain the differences in observed cell death between the models[53].

Multiple studies have computationally modeled blast exposure for both *in vitro* and *in vivo* loading scenarios[8, 13, 17, 49, 180, 187-189]. As previously mentioned, Panzer and colleagues predicted that shock loading of tissues in our *in vitro* receiver would induce MPS less than 8% and maximum strain rates of $80s^{-1}$ or less, which aligns closely with our findings[49]. Computational models of the human head under shock loading corroborated the biomechanical loading observed with our injury model[17, 183, 189]. Those studies predicted maximum strains below 10% and maximum strain rates to reach between 10-$570s^{-1}$, depending on loading conditions. Panzer and colleagues reported that strain was mainly dependent on the impulse of the blast, which we corroborated with our findings (Figure 5D)[17]. We have previously reported that biological outcomes such as LTP and blood-brain barrier disruption were also depended on the impulse of the blast wave[52, 53]. Another computational study predicted higher strains (7-47%) within the brain after shock loading; however, this discrepancy from our results could have been due to the coarseness of the finite element mesh (> 1mm) in that study[190]. In the aforementioned computational studies, maximum strains were observed after the pressure pulse had passed through the *in vitro* sample or the skull/brain model. While our study corroborated this result, video analysis suggested that primary blast-induced deformation was driven by vibration of the Millipore membrane, on which the culture was adhered, within the test apparatus. This result may have been driven by bulk fluid motion within the column, which was observed in computational models of the receiver[49].

Comparing the strain field induced by primary blast versus tertiary blast, *in vitro* and *in vivo* studies have reported that inertial-driven TBI leads to higher strain magnitudes, but lower strain rates than what we report for primary blast. One common methodology for inducing inertial-driven strains is stretching of cultured cells or tissue by deformation of the culture

substrate. In these studies, applied strains range from 1-140% whereas strain rates remained below $50s^{-1}$ [191-196]. Alternatively, shearing devices have been developed for 3D cell cultures, capable of inducing up to 50% shear strain at rates from $1\text{-}30s^{-1}$ [197]. Another study utilized magnetic resonance imaging (MRI) to quantify the strain field applied using an *in vivo* brain impact device[198]. In this study, MPS ranged from 20-40% in certain regions, applied at rates between $10\text{-}40s^{-1}$. Most computational simulations predicted that impact or accelerative forces on human head models induced high strain magnitudes (6-96%) and low strain rates ($<80s^{-1}$)[180, 181, 199-202]. Interestingly, computational models of controlled cortical impact (CCI), a commonly used blunt-impact injury model, predicted high strain magnitudes (5-60%) and strain rates ($> 400s^{-1}$)[181, 203]. Since the strain rate differs greatly from other experimental and computational models of inertial TBI, precautions must be taken when comparing CCI-induced pathobiology to other TBI models. It is clear that the injury biomechanics of primary and tertiary bTBI are distinct and should be considered when interpreting pathobiological or behavioral outcomes following blast exposure.

In this study, we correlated our previously reported levels of potentiation following *in vitro* blast to the induced strain magnitudes and strain rates at the same levels[55]. From the correlations, blast-induced LTP deficits were dependent on both strain and strain rate, with strains above 3.7% and strain rates above $25s^{-1}$ inducing significant LTP deficits. Although no other study has investigated LTP deficits at high-strain rates, our group has previously observed that a single mild stretch injury (12%, $5\text{-}6s^{-1}$) did not affect LTP; however, a subsequent mild stretch delivered 24 hours after the first significantly reduced LTP without altering other evoked response measures[204]. It is possible that the observed strain threshold for LTP deficits in our study is lower since the primary blast injury model deforms tissue at higher rates than the stretch

injury model. Although LTP was not investigated, another stretch injury study found that the strain threshold for electrophysiological dysfunction was potentially as low as 5% when stretched at 5 s^{-1} [97]. Upon mathematically fitting functional changes to applied strain/rate injury parameters, Kang and colleagues found that most changes to basal hippocampal and cortical electrophysiological dysfunction were dependent on both strain magnitude and rate, even at low strain magnitudes[88, 205]. Another study observed that changing the rate of stretching hippocampal cultures, increasing from 1 to 5 to 50s^{-1}, while maintaining low strain magnitudes (<6%) increased cytosolic [Ca^{2+}], an important parameter for LTP induction[194, 206]. Previous studies hypothesized that macro- and micro-interfaces between cellular structures with disparate properties, e.g. the dendritic spines and transmembrane structures critical to LTP induction, could be particularly vulnerable to damage from high strain rate loading[197, 207-209].

It has been shown that electrophysiological dysfunction can occur even in the absence of cell death; however, multiple experimental studies have similarly investigated strain thresholds for cell death[53, 95, 203, 210, 211]. Biomechanical thresholds for electrophysiological dysfunction and cellular death are critical to the advancement of computational TBI models. Current finite element models of the human head can incorporate a neural tract structure, identified by diffuse tensor imaging, to predict the effect of injury on neural connections[201, 212]. For example, Kraft and colleagues found that 20% of the neural connectome links between brain regions were fully degraded by 96 hours post-frontal TBI, when using an axonal strain threshold (18%) for functional deficits identified *in vitro*[210, 212]. Our study connects blast parameters (peak pressure, duration, impulse) to biomechanical deformation (strain magnitude, rate) and provides computational studies with additional threshold information to better inform their models.

While our study provided insights into the biomechanics of primary blast injury, several limitations should be considered. The Aramis software required that a fiducial pattern be applied to the OHSCs so that facets can be assigned for subsequent deformation tracking. It is possible that the spray paint used to make that pattern altered the physical properties of the OHSC and, thus, the strain response. The use of spray paint prevented subsequent electrophysiological recording from patterned slices. In the future, different biological dyes or staining could be implemented to determine whether the induced strains were altered by the paint. To prevent image distortion that accompanies recording a sample through a cylindrical PVC receiver, a square box was built to surround the receiver and filled with water. This structure served to better match the refractive indices of the intervening media, PVC (n = 1.5390) and water (n = 1.33) and present a flat surface through which to image, minimizing image-distortion and allowing for proper calibration of the system. An ideal setup would be to redesign the receiver with a square column. An inherent limitation of any stereophotogrammetric technique is that only strains on visible surfaces were measured, although, this may not be a significant limitation because the OHSCs are a few hundred microns thick [51, 213]. Recording speed was limited by lighting conditions, which were somewhat limited by space constraints around the receiver. The onset time of the in-fluid pressure transient at the level of the sample was approximately 500µs, which allows capture of this onset in only two frames. Although the maximum strain magnitudes and rates were observed after pressure loading had subsided, a higher frame rate would be desirable in future studies.

In summary, we report that *in vitro* primary blast exposure induced low strain magnitudes and high strain rates in OHSCs with strain magnitudes between 3-9% and rates between 25-86s^{-1} for Level 1-4 blasts. Both strain magnitude and rate were highly correlated with in-air blast

impulse and in-fluid peak pressure. Peak strains and rates were observed after the pressure wave had passed the sample, suggesting that this mode of strain was driven by either bulk fluid motion or vibration of culture substrates like a drumhead. Our results aligned closely with computational simulations of our blast injury device under shock loading[49]. When comparing biomechanical parameters to blast-induced LTP deficits, we observed that a strain magnitude and rate threshold for LTP-loss was found between 3.7-6.7% and 25-33s^{-1}, respectively. The reported findings will advance computational modeling of the brain under shock loading by providing tissue-level tolerance criteria for neuronal dysfunction.

3 Isolated primary blast injury to *in vitro* organotypic hippocampal slice cultures inhibits long-term potentiation[2]

3.1 Introduction

Traumatic brain injury has been considered the signature injury of the US military operations in Iraq and Afghanistan for more than a decade[7]. In 2015 alone, there were 22,672 identified cases of TBI within the four branches of the US military, with 82.4% of these cases being mild in severity[3]. The biomechanics of blast-induced injury are complex but classified into four mechanisms: primary blast due to the interaction of the supersonic shock wave with biological tissues; secondary blast due to ejecta causing penetrating injuries; tertiary blast due to blunt impact or rapid acceleration / deceleration leading to injurious deformation within the brain; and quaternary blast due to remaining mechanisms including burning, poisoning, infection, and electromagnetic waves[53, 214]. Although the mechanisms and consequences of brain deformation, the mechanism of tertiary injury, are well-studied[2, 215], the existence and pathobiology of TBI due to primary blast injury remain controversial.

Animal studies investigating the effects of primary blast injury have produced conflicting results. Some studies report reduced motor function in the rotarod test following primary blast [71-73]; however, others have reported no decline in motor skills from primary blast[23-25]. Similar discrepancies appear for cognition, as well. Following blast exposure, cognitive performance in

[2] A modified version of this chapter previously appeared in print: **Vogel III, E.W.**, Effgen, G.B., Patel, T.P., Meaney, D.F., Bass C.R.D., Morrison III, B. Isolated primary blast inhibits long-term potentiation in organotypic hippocampal slice cultures, J Neurotrauma. 2016, 33, p 652-661. Reproduced with permission (doi:10.1089/neu.2015.4045).

the MWM significantly decreased in some studies[23, 75], but not in others[24, 25]. These mixed results may be due to the large range of bTBI models in use today in which many critical factors are not standardized, including injury biomechanics (e.g. the head acceleration during blast exposure is often not measured[30]), thorax protection, scaling of the blast magnitude and duration, and orientation of the subject to the blast wave[19, 23, 24, 216].

It remains unclear whether isolated primary blast affects neurological function. Our *in vitro* approach allows for the precise control of injury biomechanics and removes the potentially confounding influence of systemic pathophysiology (e.g. lung damage, ischemia, etc.) and brain deformation due to blast-induced head acceleration[53]. The goal of our study was to determine the minimum primary blast exposure to produce a significant deficit in neuronal network function in the absence of cell death, i.e. a tissue-level tolerance criterion for functional deficits. We have previously characterized our blast-injury model (Figure 2), which is comprised of a shock tube and a fluid-filled sample receiver for exposing OHSC to primary blast[53, 216, 217]. The system converts the in-air shock wave into an in-fluid pressure transient to simulate the blast-induced intracranial pressure wave for interaction with the brain culture[216]. Previously, in-fluid pressure transients to injure cultures have been implemented in *in vitro* TBI models to simulate non-blast loading and to replicate the loading associated with fluid percussion injury. Those loading conditions with much longer rise times (~5ms) and durations (~20ms) differed substantially from the loading conditions of the current study[42, 44]. Loading conditions employed in the current study were designed specifically to replicate blast-loading with much faster rise-times (~ 0.2ms) and shorter durations (~ 3ms). We measured changes in electrophysiological function in OHSCs with 60-channel microelectrode arrays (MEAs). Although we have previously reported that electrophysiological deficits occur at lower primary

blast levels than cell death[53], a threshold for functional deficits has not been reported. In this study, we report that a shock wave produced subtle changes in neuronal network function. However, long-term potentiation was significantly impaired or eliminated following primary blast exposure of 9 and 39 kPa•ms impulse, respectively. Determining a tolerance threshold could be used to increase safety during military training, as well as improve helmet technology to protect military personnel better.

3.2 Materials and Methods

3.2.1 Organotypic hippocampal slice culture

All animal procedures were approved by the Columbia University Institutional Animal Care and Use Committee (IACUC). OHSC were generated as previously described from approximately 25 dams and 100 pups. In brief, P8-11 Sprague-Dawley rat pups were decapitated and the brains removed[218-220]. Hippocampi were excised, sectioned into 400 μm thick slices and separated aseptically in ice-cold Gey's salt solution supplemented with 25 mM D-glucose (Sigma, St. Louis, MO). Next, 2-3 slices were plated onto each porous Millipore Millicell cell culture inserts (Millipore, Billerica, MA) in Neurobasal medium supplemented with 1 mM L-GlutaMAX, 1X B27 supplement, 10 mM 4-(2-hydroxyethyl)-1-piperazineethanesulfonic acid (HEPES), and 25 mM D-glucose (Life Technologies, Grand Island, NY). Every 2-3 days, half of the medium was replaced with full-serum medium containing 50% Minimum Essential Medium, 25% Hank's Balanced Salt Solution, 25% heat inactivated horse serum, 2 μM L-GlutaMAX, 25 mM D-glucose, 10 mM HEPES (Sigma, St. Louis, MO). Cultures were grown for 10-14 days prior to testing.

3.2.2 Primary blast exposure

Blast injury methods have been previously described in detail[216, 217]. In brief, a shock wave was generated with a 76 mm diameter aluminum shock tube with an adjustable-length driver section (25 mm, 50 mm, and 190 mm used for the current studies) pressurized with helium or nitrogen and a 1240 mm long driven section[216, 217]. Individual culture wells were sealed inside sterile, 57 µm-thick, low-density polyethylene bags (Whirl-Pak, Fort Atkins, WI) filled with 10 mL of pre-warmed, serum-free culture medium (containing 75% Minimum Essential Medium, 25% Hank's Balanced Salt Solution, 2 mM Glutamax, 25 mM D-glucose, 10 mM HEPES) that had been equilibrated with 5% CO_2 / 95% O_2 (37°C) before being placed in the fluid-filled blast receiver, maintained at 37°C. These bags were selected because their acoustic impedance matched that of water, thus preventing attenuation of the pressure transient, as previously reported[217]. The culture and the bag were submerged 85 mm into the receiver column, oriented perpendicular to the pressure wave propagation. The receiver was sealed (without air bubbles) with a polydimethylsiloxane (PDMS) sheet and positioned directly at the shock tube exit (5 mm gap).

Piezoresistive pressure transducers (Endevco 8530B-500, San Juan Capistrano, CA, USA) were flush-mounted at the exit of the shock tube and in the fluid-filled blast receiver at the location of the culture and were oriented perpendicular to the direction of propagation to record side-on (incident) pressure. Analog outputs from the transducers were conditioned using amplifiers (gain of 50) and low-pass filters (corner frequency of 40 kHz, Alligator Technologies, Costa Mesa, CA, USA). Signals were digitized with an X-series data acquisition card at 125 kHz and LabVIEW™2010 (National Instruments, Austin, TX, USA). Peak overpressure,

overpressure duration, and impulse were calculated with custom MATLAB (Mathworks, Natick, MA) code[217].

For injured cultures, the shock tube was then fired; sham cultures were treated identically except the shock tube was not fired. Four blast exposure levels were utilized (Table 2, levels referenced to Effgen et al., 2014[53]), characterized by the peak pressure (kPa), duration (ms), and impulse (kPa•ms) of the in-air shock wave and the in-fluid pressure transient. Blast levels (specific parameters given below in the results) simulated real-world exposures and were chosen both below and above the threshold for causing cell death based on previous studies[53]. Following blast- or sham exposure, the culture was immediately removed from the receiver and returned to the incubator in fresh, full serum medium.

	In-air			***In-fluid***		
Exposure Level	***Pressure (kPa)***	***Duration (ms)***	***Impulse (kPa•ms)***	***Pressure (kPa)***	***Duration (ms)***	***Impulse (kPa•ms)***
Level 1	106 ± 2	0.25 ± 0.01	9 ± 2	134 ± 2	1.50 ± 0.01	89 ± 1
Level 2	93 ± 3	1.40 ± 0.01	39 ± 1	270 ± 15	2.60 ± 0.20	295 ± 56
Level 4	336 ± 8	0.84 ± 0.01	87 ± 2	598 ± 15	1.85 ± 0.30	440 ± 13
Level 9	424 ± 6	2.31 ± 0.03	248 ± 3	1510 ± 91	2.80 ± 0.10	1420 ± 87

Table 2 Blast exposure levels tested in Chapter 3. Blast exposures were characterized by three different parameters of the shock wave: peak overpressure (kPa), duration (ms), and impulse (kPa•ms). Four different exposure levels (in addition to sham exposure) were utilized as previously reported by Effgen et al. (2014)[53]. Parameters are reported for the in-air shock wave and the in-fluid pressure transient. These blast pressure histories are similar to those experienced in-theater[53].

3.2.3 Cell death measurement

Propidium iodide (PI) fluorescence was used to measure cell death immediately prior to and four days following injury. Previous studies with this injury model have demonstrated that significant cell death does not occur until four days post-injury[53]. OHSCs were incubated in 2.5 μM PI (Life Technologies) in serum-free medium for 1 hour before imaging. Images were acquired at the indicated time points using an Olympus IX81 microscope with 568/24 nm (peak/width) excitation and 610/40 nm emission filters. Following imaging, cultures were returned to fresh, full serum medium.

Cell death was determined for specific OHSC regions (DG, CA1, CA3), as previously described, using MetaMorph (Molecular Devices, Downingtown, PA)[221]. In brief, the same threshold for fluorescence was used to analyze all images at both pre- and post-injury time points for a given culture. Cell death was quantified as the percentage area of a specific region exhibiting fluorescence above the threshold. To confirm OHSC viability after blast, a subset of cultures were exposed to the highest blast level (Level 9) and subsequently subjected to an excitotoxic injury (10mM of glutamate for 3 hours) 4 days following blast exposure. Slice cultures were returned to fresh serum-free medium following excitotoxic exposure, and cultures were imaged for cell death 24h later. Cell death was analyzed by analysis of variance (ANOVA), followed by Dunnett post hoc tests with statistical significance set at $p < 0.05$ (SPSS v22, IBM, Armonk, NY).

3.2.4 Electrophysiology

Electrophysiological activity within the OHSC was recorded using 60-channel MEAs (8×8 electrode grid without the corners, 30μm electrode diameter, 200μm electrode spacing) 4-6

days following blast injury (60MEA200/30iR-Ti-gr, Multi-Channel Systems, Reutlingen, Germany). This time point coincided with the observed delay for increased cell death previously measured in this injury model[53]. Before transferring OHSCs to MEAs, the MEAs were plasma cleaned (Harrick Plasma, Ithaca, NY) and coated with 5 µL of 0.01% nitrocellulose (GE Healthcare Life Sciences, Piscataway, NJ) in methanol (Pharmco-AAPER, Brookfield, CT) to adhere the tissue to the electrodes. Individual OHSCs were excised from the Millipore membranes and inverted onto the MEA. A nylon mesh, harp slice grid (ALA Scientific Instruments, Farmingdale, NY) held the OHSC stationary and helped ensure contact with the electrodes.

OHSCs were perfused with artificial cerebral spinal fluid (aCSF) containing 125 mM NaCl, 3.5 mM KCl, 26 mM $NaHCO_3$, 1.2 mM KH_2PO_4, 2.4 mM $CaCl_2$, 1.3 $MgCl_2$, 10mM HEPES, and 10 mM glucose (pH = 7.40), which was bubbled with 5% CO_2/95% O_2 and warmed to 37°C, as previously described [97]. Recordings were acquired with an MEA1060-BC amplifier and data acquisition system (Multi-Channel Systems). The system recorded neural signals at 20 kHz with a 6 kHz analog, anti-aliasing filter. Recordings were further filtered in MATLAB using an 8^{th} order, digital, low-pass (1000Hz) and a 4^{th} order, digital, high-pass (0.2Hz) Butterworth filter. The sample numbers for each injury group for a given recording protocol are listed in the results section.

3.2.5 Spontaneous activity

Spontaneous neural activity was measured by recording continuously for 3 minutes from all electrodes within the hippocampus. The raw data was passed through a 60 Hz comb filter

using a custom MATLAB script, before neural event activity was detected based on the multi-resolution Teager energy operator[88, 115, 205, 222, 223]. Events were characterized by their start time, magnitude, and duration.

Spontaneous network synchronization was also quantified using previously published methods[115, 121, 224, 225]. Correlation, c^{τ}, between neural events was calculated for each electrode pair (*x* and *y*) given neural event-timing t_i^x and t_j^y (i = 1, …, m_x; j = 1, …, m_y) according to[224]:

$$\boldsymbol{c^{\tau}(x|y) = \sum_{i=1}^{m_x}\sum_{j=1}^{m_y} J_{ij}^{\tau}} \begin{cases} \boldsymbol{J_{ij}^{\tau} = 1 \; if \; 0 < t_i^x - t_j^y \leq \tau} \\ \boldsymbol{J_{ij}^{\tau} = \frac{1}{2} \; if \; t_i^x = t_j^y} \\ \boldsymbol{J_{ij}^{\tau} = 0 \; otherwise} \end{cases} \quad (5)$$

in which τ was the duration in which two events were considered synchronous (1.5 ms) and m_x & m_y were the total number of events to be compared on each electrode.

An activity correlation matrix, Q_{xy}, was calculated as:

$$\boldsymbol{Q_{xy} = \frac{c^{\tau}(x|y) + c^{\tau}(y|x)}{\sqrt{m_x m_y}}} \quad (6)$$

with individual entries ranging from 0 (completely uncorrelated) to 1 (perfectly correlated). The eigenvalues, λ_b, and associated eigenvectors, v_{ab}, of the correlation matrix provided insight to the structure of the neuronal activity. To identify clusters of simultaneously active electrodes, the participation index (PInd) was calculated for each electrode *a* that contributed to a cluster *b* as:

$$\boldsymbol{PInd_{ab} = \lambda_b v_{ab}^2} \quad (7)$$

where v_{ab} represented the a^{th} element of eigenvector b. Electrodes contributing to cluster *b* were those with PInd ≥ 0.01[225].

To determine statistical significance, randomized surrogate time-series data without correlated activity was generated with an event-rate equal to the measured event-rate of the experimental recordings[225]. The surrogate process was repeated 50 times, and the mean ($\bar{\lambda}'_k$) and standard deviation (SD_k) of surrogate eigenvalues were calculated (k = 1,…, M, where M represented the number of electrodes in the experiment). We identified the number of synchronized clusters that were significantly different from the randomized, asynchronous surrogate clusters as:

$$\boldsymbol{Number\ of\ Clusters} = \sum_{\boldsymbol{k}} \boldsymbol{sgn}\left[\boldsymbol{\lambda_k} > \left(\boldsymbol{\bar{\lambda}'_k} + \boldsymbol{K} \times \boldsymbol{SD_k}\right)\right] \quad (\mathbf{8})$$

where *sgn* was the sign function, λ_k was the eigenvalue of each electrode of the experimental data, and *K* was a constant (*K* = 3 was chosen to provide a 99% confidence level, i.e. $p < 0.01$).

Finally, a global synchronization index (GSI), ranging from 0 (random, uncorrelated activity) to 1 (perfectly synchronous, correlated activity on all electrodes), was calculated for the cluster with the highest degree of synchronization:

$$\boldsymbol{GSI} = \begin{cases} \frac{\boldsymbol{\lambda_M} - \boldsymbol{\bar{\lambda}'}}{\boldsymbol{M} - \boldsymbol{\bar{\lambda}'}} & \boldsymbol{if\ \lambda_M > \bar{\lambda}'} \\ \mathbf{0} & \boldsymbol{otherwise} \end{cases} \quad (\mathbf{9})$$

where $\bar{\lambda}'$ was the mean of the largest surrogate eigenvalues, λ_M was the maximal eigenvalue of the correlation matrix from the experimental data, and *M* was the number of electrodes in the experiment. Active regional percentage in the most synchronized cluster (i.e.

the cluster corresponding to λ_M) was quantified as the ratio of regional electrodes involved in the cluster to the total number of electrodes in the respective region.

Spontaneous and synchronization parameters were averaged for a given recording and analyzed by ANOVA, followed by Dunnett *post hoc* tests with statistical significance set as $p < 0.05$ (SPSS v22, IBM). In addition, principal component analysis (PCA) was performed with the built-in MATLAB function *pca.m* on the parameters together to identify significant changes (ANOVA) in the first principal component score (PC1), followed by Dunnett *post hoc* tests. Observed power was calculated for the effect of injury severity (impulse) with $\alpha = 0.05$.

3.2.6 Stimulus-response curves

Stimulus-response (SR) curves were generated by applying a constant current, biphasic, bi-polar stimulus (100 μs positive phase followed by 100 μs negative phase) of increasing magnitude (0-200 μA in 10 μA increments) to electrodes located in either the Schaffer collateral (SC) or mossy fiber (MF) pathways, and the data was analyzed with respect to stimulation site. Evoked responses were recorded from each electrode throughout the hippocampal tri-synaptic circuit. As in previous studies, each electrode's response was fit to a sigmoidal curve[97] as:

$$\boldsymbol{R(S) = \frac{R_{max}}{1 + e^{m(I_{50} - S)}}} \qquad (\mathbf{10})$$

R_{max} represented the maximum amplitude of the evoked response and I_{50} represented the current necessary to generate a half-maximal response. The term *m*, which is proportional to the slope of the sigmoidal fit, represented the spread in the firing threshold for the population of neurons[88, 97, 205]. Data from each electrode was segregated by anatomical region of interest (ROI:

CA1, CA3, DG). Each parameter (I_{50}, m, R_{max}) for an electrode was averaged within a region to determine that regional response for any given slice. Data reported for each region is the average across slices within a given experimental group.

A PCA was also performed to identify significant multivariate changes in the SR parameters. Individual parameters as well as PC1 were analyzed by ANOVA followed by Dunnett *post hoc* tests with statistical significance set as $p < 0.05$ (SPSS v22, IBM). Observed power was calculated for the effect of impulse with $\alpha = 0.05$.

3.2.7 Paired-pulse ratios

Short-term plasticity was investigated by delivering two successive stimuli of the same intensity (I_{50}) at interstimulus intervals (ISI) of 20, 35, 50, 70, 100, 140, 200, 300, 500, 1000, and 2000 ms. Paired-pulse ratios (PPR) were calculated as the ratio of the peak-to-peak amplitude of the second response to the peak-to-peak amplitude of the first response. A PPR greater than 1 indicated paired-pulse facilitation, whereas a PPR less than 1 indicated paired-pulse depression [226]. ISIs were assigned to one of four bins that are biologically relevant to short-term synaptic plasticity. Short-term ISI (20 ms) produce paired pulse depression thought to be mediated by the neurotransmitter GABA, specifically via the $GABA_A$ class of GABA receptors[227, 228]. Early-mid ISIs (35 – 100 ms) elicit a rebound in excitation thought to be caused by $GABA_A$ mediated disinhibition and activation of NMDARs[227, 229]. Late-mid ISIs (140 – 500 ms) produce late phase paired pulse depression thought to be mediated by $GABA_B$ receptors[227, 230]. Lastly, Long-term ISIs (> 500 ms) are not expected to elicit a response resulting from the interaction of the paired pulse stimulation and instead results in two independent and equal responses[231, 232]. PPRs

for each bin were averaged across a given recording and analyzed by ANOVA, followed by Dunnett *post hoc* tests with statistical significance set at $p < 0.05$ (SPSS v22, IBM). Additionally, PC1 was analyzed to identify significant multivariate changes in PPR. Observed power was calculated for the effect of impulse with $\alpha = 0.05$.

3.2.8 Long-term potentiation

In a separate cohort of cultures, the ability to induce LTP was quantified after blast. Baseline behavior was evoked by stimulating at I_{50} once every minute for 30 minutes. LTP was then induced by stimulating across the SC pathway with a high frequency stimulus, which consisted of three trains of 100 Hz pulses applied for 1 second at I_{50}, with each train separated by 10 seconds[233, 234]. Immediately following LTP induction, post-LTP responses were evoked by stimulating at I_{50} once every minute for 60 minutes. LTP induction was calculated as percent potentiation above baseline based on the last 10 minutes of recording in each recording window. To ensure only stable responses were included for analysis, electrodes were discounted if the coefficient of variance (pre or post-induction) was greater than 20%[235]. LTP induction was averaged among electrodes within the CA1 and analyzed by ANOVA followed by Dunnett post hoc tests with statistical significance set as $p < 0.05$ (SPSS v22, IBM).

3.3 Results

3.3.1 Primary blast-induced cell death in the hippocampus was minimal

We observed a region-specific threshold for blast-induced cell death, but the relative amount of cell death was significantly less than excitotoxic insult. Four days following sham injury or blast exposure and prior to electrophysiology recording, cell death was evaluated within the OHSC (Table 2). In all three regions, cell death (Figure 8) was minimal, but significantly increased following a Level 9 blast exposure, as compared to sham. Level 4 blast exposure induced minimal, but significant cell death in only the DG but not the CA3 or CA1. Cell death was not significantly increased after Level 2 or Level 1 blast exposure. Although Level 9 blast exposure induced significant cell death in all ROI, it remained minimal (< 5%). In comparison, glutamate exposure 4 days after Level 9 blast exposure significantly increased cell death in all ROIs as compared to a Level 9 blast exposure alone. These data are consistent with a previous study from our group which reported significant but minimal cell death after a Level 9 exposure[53].

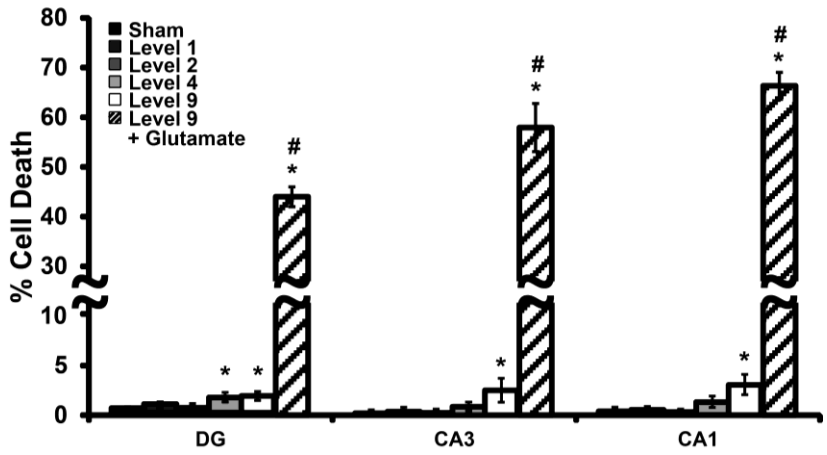

Figure 8 Cell death measured for each ROI of the hippocampus 4 days after injury. Groups are in order of increasing impulse from left to right. Minimal cell death was significantly induced after Level 9 blast exposure in all ROI. Minimal cell death was significantly induced after Level 4 blast exposure in DG only. Level 2 and Level 1 blast exposure did not significantly increase cell death. Glutamate exposure 4 days following Level 9 blast induced significant cell death in all ROI. (mean ± S.E.M.; n≥7; * $p<0.05$ as compared to sham, # $p<0.05$ as compared to Level 9)

3.3.2 Primary blast exposure impaired long-term potentiation

Four to six days following blast exposure, LTP (Figure 9) was significantly reduced following Level 9, Level 4, and Level 2 blast exposures as compared to sham. Following Level 1 blast exposure, potentiation closely resembled that of sham-injured cultures.

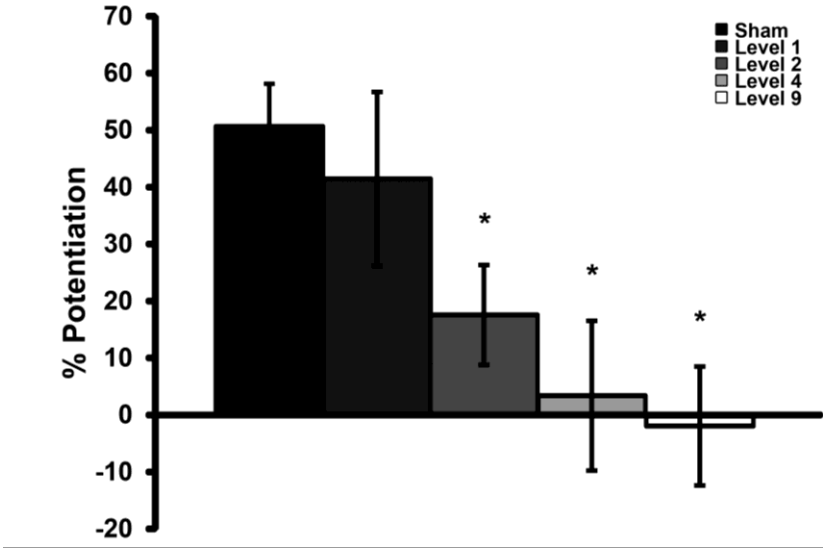

Figure 9 Long-term potentiation measured in CA1 4-6 days after injury. Groups are in order of increasing impulse from left to right. LTP was significantly reduced after Level 2 and eliminated after Level 4 or Level 9 blast exposures. (mean ± S.E.M.; $n \geq 5$; * $p < 0.05$, as compared to sham)

3.3.3 Primary blast exposure reduced hippocampal synchronization

One feature that is often critical for transmitting information through neural circuitry is the synchronization of activity across distinct regions, an aspect that may underlie the process of memory consolidation [236]. To this end, GSI (Figure 10A) across recording regions was significantly reduced following Level 9 and Level 4 blast exposures as compared to sham. Blast did not alter the number of synchronized clusters identified (Figure 10B). Level 9 and Level 4 blast exposure significantly reduced the active regional percentage in the most synchronized cluster (Figure 10C) in CA3, as compared to sham.

3.3.4 Primary blast exposure minimally affected spontaneous activity

An additional measure to reflect the general excitability of the circuitry is the spontaneous activity recorded within different regions. There was a decreasing trend in spontaneous event rate (Figure 11A) as the impulse increased from Level 1 to 9 primary blast exposures for all three ROIs; however, the deficits did not reach significance. Level 9 blast exposure significantly decreased spontaneous event magnitude (Figure 11B) in DG. There was no significant change in event duration (Figure 11C) after blast exposure for any ROI. Lastly, Level 9 blast exposure significantly reduced PC1 (Figure 11D) in DG, but the change did not reach statistical significance in CA3 or CA1. PC1 captured over 95% of the variance in the overall data set. The statistical power was ≥ 0.18 for all non-significant comparisons.

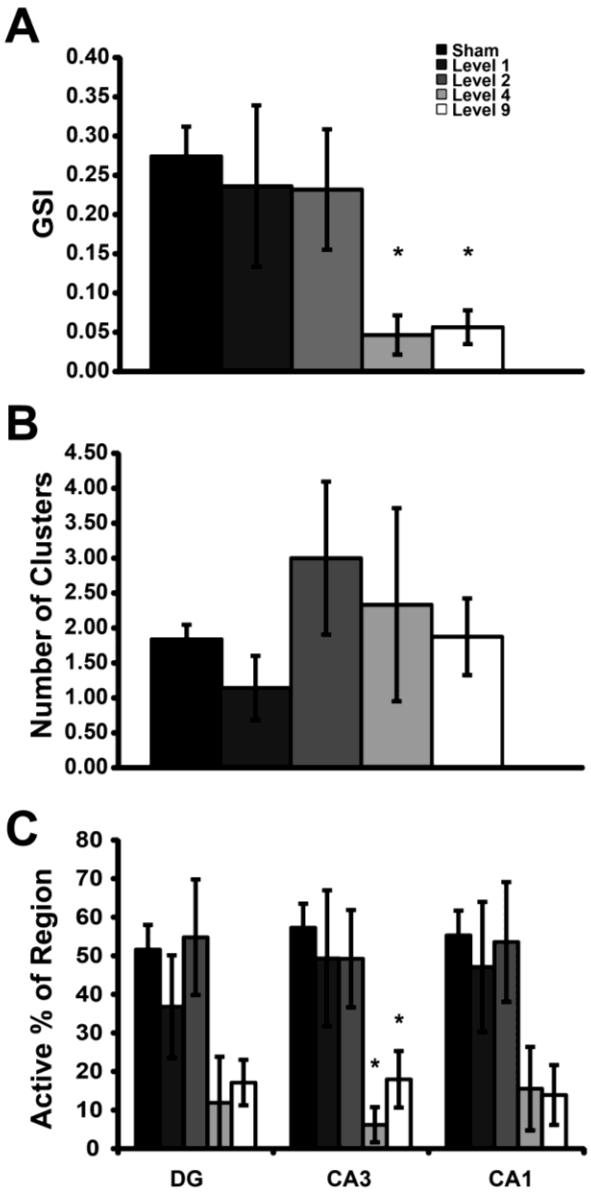

Figure 10 Synchronization of spontaneous activity 4-6 days after injury. Groups are in order of increasing impulse from left to right. The global synchronization index (GSI, [A]) was significantly decreased following Level 9 and Level 4 blast exposures compared to sham exposure. The number of synchronized clusters (B) per slice was not significantly affected by primary blast exposure ($p \geq 0.43$ with a calculated power of 0.29). Following Level 9 and Level 4 blast exposure, active regional percentage in the most synchronized cluster (C) significantly decreased in CA3, as compared to sham exposure. (mean ± S.E.M.; $n \geq 6$; *$p < 0.05$, as compared to sham)

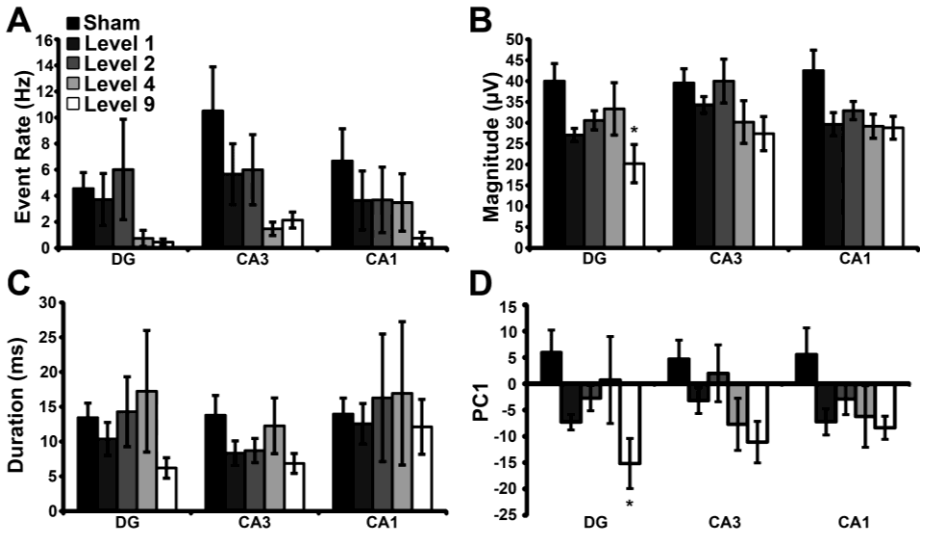

Figure 11 Blast injury altered spontaneous event properties. There was a decreasing trend in spontaneous event rate (A) as impulse increased. Level 9 blast exposure significantly decreased event magnitude (B) in DG, as compared to sham. There was no significant change in event duration (C) after blast exposure for any ROI ($p>0.40$ with a calculated power < 0.28). Level 9 blast exposure significantly altered PC1 (D) in DG, but there was no significant change in CA3 ($p>0.08$ with a calculated power of 0.54) or CA1 ($p>0.35$ with a calculated power of 0.33). (mean ± S.E.M.; $n\geq7$, * $p<0.05$, as compared to sham)

3.3.5 Primary blast exposure minimally altered basal evoked responses

Spontaneous activity only reveals the state of the circuitry with existing inputs. Alternatively, a full stimulus/response characterization in response to external stimulation would reveal any alterations in the ability to stimulate local circuitry in the OHSC or the progressive stimulation of downstream circuits due to synaptic transmission. When stimulating across the MF pathway, there was no effect on R_{max} (Figure 12A) or I_{50} (Figure 12B) following blast exposure, as compared to sham. Level 4 blast exposure significantly decreased the slope of excitation (m) (Figure 12C) for DG and CA3, as compared to sham. There was no significant change in PC1 (Figure 12D) for any ROI following blast exposure. PC1 captured over 99% of the variance in the overall data set. The statistical power was greater than or equal to 0.20 for all non-significant comparisons.

For stimulation across the SC pathway, Level 9 blast exposure significantly reduced R_{max} (Figure 13A) in DG, as compared to sham. Level 9 blast exposure significantly increased I_{50} (Figure 13B) in CA3. Level 9 and Level 4 blast exposure reduced the parameter m (Figure 13C) in all ROI; however, no change reached significance. Level 9 blast significantly reduced PC1 (Figure 13D) in DG, as compared to sham. The statistical power was greater than or equal to 0.31 for all non-significant comparisons.

One explanation for changes in circuit activation would be impairments in presynaptic release, as identified by paired-pulse stimulation paradigms. For stimulation across the MF or SC pathway, primary blast exposure did not change paired pulse responses (data not shown) in any ROI for any temporal bin of ISIs.

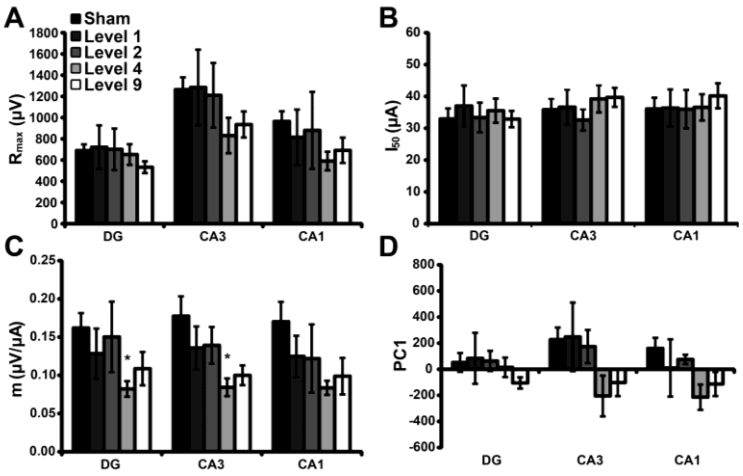

Figure 12 Blast injury minimally affected stimulus-response parameters when stimulated across the mossy fiber (MF) pathway. There was no significant effect on Rmax (A, $p>0.14$ with a calculated power < 0.12) or I50 (B, $p>0.88$ with a calculated power < 0.44) following blast exposure, as compared to sham. Level 4 blast exposure significantly reduced m (C) in DG and CA3; however, the change did not reach significance in CA1 ($p>0.09$ with a calculated power of 0.53), as compared to sham exposure. Level 9 exposure reduced m for all ROI, but the changes did not reach significance ($p>0.07$). There was no significant change ($p>0.15$ with a calculated power < 0.44) in PC1 (D) following blast exposure for any ROI. (mean ± S.E.M.; $n\geq6$, * $p<0.05$, as compared to sham)

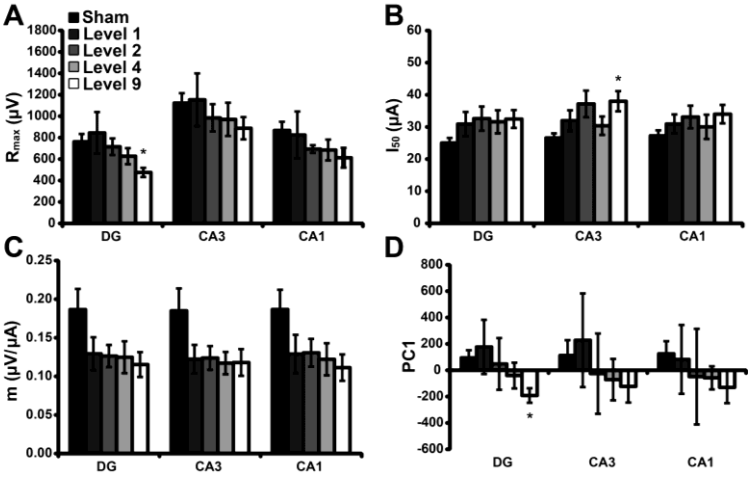

Figure 13 Blast injury minimally affected stimulus-response parameters when stimulated across the Schaffer collateral (SC) pathway. Level 9 blast exposure significantly decreased Rmax (A) in DG. Level 9 blast exposure significantly increased I50 (B) in CA3. Level 9 and Level 4 blast exposure levels reduced the parameter m (C) for all ROI; however, no change reached significance ($p>0.09$ with a calculated power < 0.56). Level 9 blast exposure significantly reduced PC1 (D) in DG. (mean ± S.E.M.; $n\geq5$, * $p<0.05$, as compared to sham)

3.4 Discussion

The current study reports that 1) primary blast exposure in isolation can disrupt LTP; 2) a threshold for significantly impairing LTP lies between 9 kPa•ms (Level 1) and 39 kPa•ms (Level 2) impulse; 3) primary blast exposure significantly reduced hippocampal synchrony with a threshold lying between 39 kPa•ms (Level 2) and 87 kPa•ms (Level 4) suggesting that synchrony is less sensitive to blast than LTP; and 4) other measures of spontaneous and evoked activity were less sensitive to blast. These functional alterations occurred in the absence of cell death, demonstrating that cell death is not necessary for a change in neuronal function. Functional and cognitive deficits in the absence of cell death have been observed with earlier non-blast models of TBI, as well[61, 99]. Although the highest blast level tested (248 kPa•ms; Level 9) altered electrophysiological function as well as caused significant cell death, average cell death was never above 5% in any ROI, which agreed with previous literature[53]. In comparison, glutamate exposure 4 days following Level 9 blast exposure caused over 40% cell death in all ROI, confirming the presence of viable cells following blast, which were not killed by primary blast alone.

Although not investigated in previous *in vitro* blast models, LTP has been investigated in acute hippocampal slices following *in vivo* blast exposure. LTP, induced either chemically or by theta-burst stimulation in acute mouse hippocampal slices was significantly reduced 2 and 4 weeks post-blast injury *in vivo* (167 kPa•ms)[24]. In this previous work, the injury was a combination of the blast pressure wave through the brain and induced head-acceleration. In general, head acceleration (tertiary blast loading) is a well-known causal factor for brain injury, and therefore it is not possible to prove conclusively that blast pressure alone can cause circuit

impairment. Although mild fluid pressure loading to the brain can also cause LTP impairments one day[83], one week[85, 86], and 8 weeks[84] post-injury, this injury model is also a mix of pressure and deformation throughout the brain[237, 238]. To our knowledge, our data is the first to show that primary blast (shock wave alone) is also capable of disrupting LTP.

Alterations in the function of the hippocampal circuitry after blast was not restricted to only LTP impairments. We found that primary blast exposure reduced global synchronization of hippocampal activity, correlating to observations in humans and other experimental models (Figure 10A). For example, electroencephalographic synchronization was significantly reduced in the frontal brain regions of US personnel one month after blast-exposure without impact[239]. Likewise, non-blast TBI reduced cortical synchronization during learning and recognition tasks [240]. Network synchronization was decreased after *in vitro* stretch injury in both hippocampal slices[115] and cultured cortical neurons[121]. Proposed mechanisms behind these deficits include intracellular chloride imbalance[115], calpain activation[121], and loss of white matter tract structural integrity[239]. TBI-induced deficits in network synchronization could explain some short-term learning and memory impairments as previous studies have shown that the basis for working memory is persistent, synchronized neural activity[241, 242]. While previous studies have demonstrated the potential for reduced neural synchrony after various types of injury, our study supports that primary blast exposure, in isolation, is capable of causing deficits in synchronization.

Although spontaneous function (event rate, magnitude, duration) has not been previously investigated after blast injury, the non-blast TBI literature is divided. In our study, our highest blast level (Level 9) was capable of subtly reducing event rate, magnitude, and duration in

certain regions of the hippocampus. The decreasing trend for PC1 suggested that clustering the three spontaneous parameters uncovered an underlying deficit in the spontaneous signaling that was not obvious by observing just a single parameter in isolation. After mild controlled cortical impact (CCI) injury in rats, spontaneous event rate was increased in CA1, but not CA3, starting 2 hours and out to 24 hours post-injury[89]. Alternatively, severe *in vitro* stretch injury decreased spontaneous event rate[90]; however, mild stretch injury did not alter spontaneous event rate at 24 hours after injury[115]. These discrepancies may be related to injury severity and the associated cell death in that spontaneous rates did not change in the absence of cell death[115]. The injury biomechanics between our blast model, the CCI model, and the stretch injury model may contribute to the varying changes following injury. It is possible that the deficits in post-injury synchronization observed in our study could be linked to the slight alterations in the spontaneous functional behavior, but will need further testing to confirm.

In our study, stimulus-response curves (i.e. input/output curves) were only minimally affected by primary blast exposure, with the largest effects due to a Level 9 blast capable of causing (minimal) cell death. In an *in vivo* rat study, no changes in corpus callosum compound action potentials were measured three days post-blast despite cell death in the corpus callosum[22]. However, the duration of the blast was only 200 μs, which is not operationally realistic unless scaled. Applying previously published scaling relationships[243], this duration would scale to about 2ms. Non-blast FPI increased I_{50} out to seven days post-injury in rodent CA1[83, 92] and decreased R_{max} out to two days post-injury in rat CA1[83], in response to SC stimulation. However, similar injury studies reported decreased I_{50} and increased R_{max} between three and seven days post-injury in rodent CA1 in response to SC stimulation[91, 93]. Results from *in vitro* mechanical TBI were similar to the complex *in vivo* results. Cell-death-inducing stretch injury

(10% strain, 20 s^{-1} rate) decreased field excitatory postsynaptic potential (fEPSP) and population spike R_{max} in the hippocampus at 4 days post-injury[90]. Hippocampal R_{max} peaked as strain rate increased at high strain 4-6 days post-stretch injury, but reached a minimum as strain rate increased at low strain[88]. The same study also observed that I_{50} was increased after injury[88]. Although conflicting, previous investigations have demonstrated that normal neuronal transmission can be affected by injury, which our study confirms. The minimal changes we observed at lower impulse blast exposures (i.e. Level 2 and Level 4) suggests that normal neuronal transmission is less sensitive to primary blast exposure than LTP and GSI.

Paired-pulse facilitation (PPF) is one form of short-term synaptic plasticity[244], governed at different ISI (40-2000 ms) by presynaptic neurotransmitter release[245, 246] along with $GABA_A$, $GABA_B$, and NMDA receptor dynamics[227-231]. In our study, primary blast exposure did not affect PPR. The lack of changes in short-term plasticity observed in this study suggests that damage to presynaptic cellular machinery may not be responsible for the LTP deficits we observed[85, 247]. Previous FPI studies have shown reduced paired-pulse inhibition (PPI) at short-term (<100ms) ISIs and at mid-length (~500 ms) ISIs in rat CA1[87]. PPI was similarly reduced in rat hippocampal slices after mild stretch *in vitro* at shorter ISIs (< 100ms) in response to MF stimulation; however, PPI increased when exposed to low strain, high-strain rates at late-mid length ISIs (~500 ms), in response to SC stimulation[88]. In these time windows, paired-pulse depression is driven by $GABA_A$ and $GABA_B$ receptors, respectively[227, 228]. The lack of effect of blast on PPR in our study suggests that GABA-mediated depression was not appreciably altered, but would require further testing to confirm. The difference in outcomes at the short-term and late-mid ISIs may be related to differences between the injury-models employed in each study, suggesting that changes in paired-pulse facilitation may not be a blast-related phenomenon.

The blast levels tested in our study are similar to those commonly experienced in-theater[53]. Our Level 1 exposure is similar to the blast from an M49A4 60mm mortar round at a standoff distance of 0.25-2 m and the Level 9 exposure represents an explosion from an M118 bomb at a standoff distance of 10-32 m, according to the Conventional Weapons Effect Program (ConWEP). Our experimental conditions, whether unscaled or scaled for different species[243], are consistent with the range of real world blast exposures encountered by service members.

Although we report that primary blast exposure disrupted LTP and neuronal synchronization, there are limitations associated with this study. Translating the electrophysiological alterations measured *in vitro* to behavioral or cognitive changes *in vivo* is difficult[24, 73, 81]; however, our model provided the benefit of precise control over injury biomechanics, which remains a challenge for *in vivo* systems. Another limitation of this model is the inherent difficulty into translating tissue-level results to macroscopic loading scenarios. However, one of this study's strengths is the extensive characterization of pressure histories from the shock tube and the sample receiver. Measured fluid pressure histories applied to the tissue in the receiver could be extended to macroscopic loading conditions via realistic finite element models, which provide an intermediate step in the clinical understanding of tissue-level results. In the current study, neuronal activity was recorded at only one time frame (4-6 days) post-injury, which was chosen to allow for secondary injury cascades to develop but before regeneration mechanisms could repaired damaged circuits[53, 97, 221]. One potentially important injury mechanism that is not reproduced with our *in vitro* model is the breakdown of the BBB following blast exposure, which is increasingly a common observation in both *in vivo* and *in vitro* models[20, 21, 52, 248-250]. Therefore, future studies will examine the time course of electrophysiological changes after blast. In our study, cell viability was a major outcome

measure; however, other more subtle structural or protein alterations could be responsible for the observed electrophysiological deficits.

In summary, we report that primary blast disrupted LTP and decreased the synchronization of spontaneous activity in the hippocampus, while minimally affecting other functional measures. Disruption of LTP was dose-dependent with respect to blast impulse in the absence of cell death. Future studies will examine the molecular mechanisms underlying disruption of LTP.

4 Primary blast injury depressed hippocampal long-term potentiation through disruption of synaptic proteins[3]

4.1 Introduction

Blast-induced TBI poses a substantial problem for both training and active duty members of the military. Nearly 83% of military TBIs are considered mild TBI [3]. Although TBI can occur from blunt impact and penetrating injury, blast forces are considered the cause of the majority of mTBIs[4, 166]. Although the physiological consequences of brain deformation, i.e. tertiary injury, are well studied[215, 251], the pathobiology of TBI due to primary blast, or shock wave exposure, remains debated[13].

Animal studies that investigated the effects of primary blast injury have produced conflicting results for motor[24, 25, 71-73, 252] and cognitive deficits[23-25, 75]. One potential reason for these discrepancies is the lack of standardization in several critical factors in the bTBI injury models, such as verification of head immobilization, thoracic protection, blast exposure magnitude and duration, and subject orientation. In comparison, appropriately developed *in vitro* models of blast injury allow one to overcome these complications of *in vivo* models and focus on the precise effect of blast loading to brain tissue[12]. A major feature of our *in vitro* injury model is that it isolates the shock wave component of blast from the other, confounding phases of injury including secondary (transection due to shrapnel), tertiary (large deformations due to inertial

[3] A modified version of this chapter previously appeared in print: **Vogel III E.W.**, Rwema S.H., Meaney D.F., Bass C.R.D., Morrison III, B. Primary blast injury depressed hippocampal long-term potentiation through disruption of synaptic proteins, J Neurotrauma. 2016, Available online. Reproduced with permission (doi: 10.1089/neu.2016.4578).

loading), and quaternary blast loading[50]. By using a system with controlled biomechanics, we can determine whether primary blast in isolation affects neuronal function of the hippocampus.

Common symptoms of bTBI include memory deficits and loss of spatial navigation which implicate damage to the hippocampus[18]. Many studies showed bTBI impairs memory processing in animal models through cognitive tests[23-25, 73, 75, 252], but fewer reveal their underlying electrophysiological basis[22, 24, 53, 55]. Long-term potentiation is thought to functionally represent experience-driven neural circuitry changes[253, 254] and numerous TBI studies have reported deficits in LTP *in vitro* following non-blast injury[83-85, 255, 256]; however, there is a dearth of studies showing LTP deficits following bTBI[24, 55]. Our group was the first to observe that LTP was disrupted after pure primary blast exposure[55], and this report examines the molecular mechanisms behind primary blast-induced LTP deficits.

We observed that primary blast reduced LTP in a delayed manner, requiring more than 1 hour to develop. LTP spontaneously recovered 10 days after exposure to an 87 kPa•ms impulse blast, but not after a 248 kPa•ms blast. With LTP induction, blast significantly reduced phosphorylation of AMPA-GluR1 subunits at the serine-831 (Ser831) site and reduced phosphorylation of stargazin at the serine-239/240 (Ser239/240) site. Primary blast exposure significantly decreased expression of GluR1 subunits, with LTP induction, and PSD-95, regardless of LTP. Post-exposure treatment with the FDA-approved PDE4 inhibitor roflumilast prevented blast-induced LTP deficits. The observed improvement in LTP with roflumilast treatment warrants further investigation as a potential therapeutic for blast-induced LTP-loss.

4.2 Materials and Methods

4.2.1 Organotypic hippocampal slice culture

All animal procedures were approved by the Columbia University IACUC. OHSCs were generated from P8-P10 Sprague Dawley rat pups as previously described[50, 53, 55, 184]. In brief, the hippocampus was isolated, cut into thin sections (400μm) with a McIlwain tissue chopper (Ted Pella, CA), and plated onto Millicell inserts (EMD Millipore, Billerica, MA) in Neurobasal medium supplemented with 2mM GlutaMAX^{TM}, 1X B27 supplement, 10mM HEPES, and 25mM D-glucose (Life Technologies, Grand Island, NY). Thereafter, cultures were fed every 2-3 days with full serum medium, containing 50% Minimum Essential Medium, 25% Hank's Balanced Salt Solution, 25% heat inactivated horse serum, 2mM GlutaMAX, 25mM D-glucose, and 10mM HEPES (Sigma). Prior to blast injury, cultures were maintained for 10-14 days.

4.2.2 Primary blast exposure

Blast injury methods have been previously described in detail[49, 50, 52-55]. Piezoresistive pressure transducers (Endevco 8530B-500, San Juan Capistrano, CA, USA) recorded side-on (incident) pressure at the shock tube exit and inside the fluid-filled receiver. Peak overpressure, overpressure duration, and impulse were recorded, processed, and quantified as previously described[50, 52, 53, 55].

For injured cultures, the shock tube was fired; sham cultures were treated identically except the shock tube was not fired. Two blast exposure levels were utilized (Table 2, Level 4 and Level 9, referenced to Vogel et al., 2016[55]), characterized by the peak pressure (kPa),

duration (ms), and impulse (kPa•ms) of the in-air shock wave and the in-fluid pressure transient. Blast levels (specific parameters given in the table) simulated real-world exposures and were chosen both below and above the threshold for causing cell death based on previous studies[53, 55]. Following blast- or sham exposure, the culture was immediately removed from the receiver and returned to the incubator in fresh, full serum medium. Cultures were maintained in full serum medium for up to 10 days post exposure.

4.2.3 Cell death measurement

Propidium iodide (PI) fluorescence was used to measure cell death immediately prior to injury, and at one hour and 10 days following injury using 2.5 µM PI (Life Technologies) in serum-free medium; previous studies with this injury model have reported that cell death remains minimal between 1 and 4 days after blast[53, 55]. Cell death was determined for specific ROI (DG, CA3, CA1), as previously described, using MetaMorph (Molecular Devices, Downingtown, PA), and reported as percentage area[50, 53, 55, 95]. To confirm OHSC viability after blast, a subset of cultures were exposed to the highest blast level tested (Level 9) and subsequently subjected to an excitotoxic injury (10mM of glutamate for 3 hours) 10 days following blast exposure. OHSC were returned to fresh serum-free medium following excitotoxic exposure, and cultures were imaged for cell death 24h later. Cell death was analyzed by ANOVA, followed by Dunnett *post hoc* tests with statistical significance set at $p < 0.05$ (SPSS v22, IBM, Armonk, NY).

4.2.4 Electrophysiology

In a separate set of cultures, electrophysiological activity within the OHSC was recorded using 60-channel MEAs (8×8 electrode grid without the corners, 30μm electrode diameter, 200 μm electrode spacing) at either 1 hour, 1 day, 2 days, 4 days, 6 days, or 10 days following blast injury (60MEA200/30iR-Ti-gr, Multi-Channel Systems, Reutlingen, Germany). In our previous studies, electrophysiological deficits were measured at only 4-6 days after blast[53, 55]. The MEAs were prepared and slices were placed onto the arrays as previously described[53, 55]. OHSCs were perfused with aCSF containing 125 mM NaCl, 3.5 mM KCl, 26 mM NaHCO3, 1.2 mM KH2PO4, 2.4 mM CaCl2, 1.3 mM MgCl2, 10mM HEPES, and 10 mM glucose (pH = 7.40), which was bubbled with 5% CO2/95% O2 and warmed to 37°C, as previously described[97]. Recordings were acquired with an MEA1060-BC amplifier and data acquisition system (Multi-Channel Systems).

4.2.5 Stimulus-response curves

Stimulus-response (SR) curves were generated by applying a constant current, biphasic, bi-polar stimulus (100 μs positive phase followed by 100 μs negative phase) of increasing magnitude (0-200 μA in 10 μA increments) to electrodes located in the SC pathway. Evoked responses were recorded from each electrode throughout the hippocampal tri-synaptic circuit. As in previous studies, each electrode's response was fit to a sigmoidal curve and three parameters were quantified: R_{max}, represented the maximum amplitude of the evoked response, I_{50} represented the current necessary to generate a half-maximal response, and the term *m*, represented the slope of the sigmoidal fit[97]. Each parameter (I_{50}, m, R_{max}) for an electrode was averaged within a region to determine that regional response for any given slice. Data reported

for each region is the average across slices within a given experimental group. Individual parameters were analyzed by ANOVA followed by Dunnett *post hoc* tests with statistical significance set as $p < 0.05$ (SPSS v22, IBM).

4.2.6 Long-term potentiation

Following SR evaluation, the ability to induce LTP was measured. Baseline response was evoked by stimulating at I_{50} once every minute for 30 minutes. LTP was then induced by stimulating across the SC pathway with a high frequency stimulus, which consisted of three trains of 100 Hz pulses applied for 1 second at I_{50}, with each train separated by 10 seconds[233, 234]. Immediately following LTP induction, post-LTP responses were evoked by stimulating at I_{50} once every minute for 60 minutes. LTP induction was calculated as percent potentiation above baseline based on the last 10 minutes of recording in each recording window. To ensure only stable responses were included for analysis, electrodes were discounted if the coefficient of variance (pre or post-induction) was greater than 20%[235]. LTP induction was averaged among electrodes within the CA1 and analyzed by ANOVA followed by Dunnett *post hoc* tests with statistical significance set as $p < 0.05$, as compared to time-matched shams (SPSS v22, IBM).

4.2.7 Chemical LTP

In separate sets of cultures, LTP was chemically induced with two distinct protocols. Baseline electrical activity was recorded for 30 minutes as above. The first chemLTP protocol replaced electrical LTP induction with a 3 minute perfusion with a modified aCSF solution (gly-aCSF) [257]: aCSF containing 200 µM glycine and 0 mM MgCl (reduced from 1.3mM). The

perfusate was then switched back to aCSF and washed out for 20 minutes prior to post-induction electrical stimulation. Percent potentiation was calculated by comparing the average of the final 10 minutes of post-induction responses to the average of the final 10 minutes of pre-induction responses, as above. The gly-aCSF solution activates synaptic NMDARs, allowing Ca^{2+} ions to enter the dendritic spine, similar to electrically-induced LTP [257].

The second chemLTP protocol replaced electrical LTP induction with a 20 minute perfusion with a modified aCSF solution (cAMP-aCSF) [258]: aCSF containing 1 mM MgCl (reduced from 1.3mM), 50µM forskolin, 50µM picrotoxin, and 100nM rolipram. Forskolin, rolipram, and picrotoxin stocks were dissolved in dimethyl sulfoxide (DMSO) with a final DMSO concentration in cAMP-aCSF of 0.07%. The perfusate was then switched back to aCSF and washed out for 20 minutes prior to post-induction stimulation for 60 minutes. Percent potentiation was calculated as above. The cAMP-aCSF solution acts to upregulate the cAMP-PKA pathway through inhibition of PDE4 (rolipram) and activation of adenylate cyclase (forskolin), which results in elevated cAMP levels and consequently PKA activation[258]. Picrotoxin, a $GABA_A$ inhibitor, reduced inhibition and enhanced stability of the potentiated signal, while not inducing LTP on its own[258].

Chemically-induced LTP was averaged among electrodes within the CA1 and analyzed by ANOVA followed by Dunnett *post hoc* tests with statistical significance set as $p < 0.05$, as compared to time-matched shams (SPSS v22, IBM).

4.2.8 Western blotting

For each condition tested by western blotting, 8 slices from 2 different animals were collected for protein extraction. Groups receiving chemLTP induction (gly-aCSF or cAMP-aCSF) were treated, switched back to normal aCSF after respective treatment times, incubated for appropriate induction times, and then lysed. Slices were rinsed twice with ice-cold PBS and immediately placed in chilled lysis buffer A (40mM HEPES, 120mM NaCl, 1 mM EDTA, 1% Triton X-100, 10mM sodium pyrophosphate, 50mM sodium fluoride, 0.5mM sodium orthovanadate, 10mM β-glycerophosphate, Sigma). Samples were sonicated (Sonicator 3000, Misonix, NY, USA), incubated on ice and then centrifuged to remove cellular debris. Protein concentrations were determined by the bicinchoninic acid assay (BCA) according to the manufacturer's instructions (Thermo Fisher Scientific, Waltham, MA, USA), and 50 µg of protein per sample were loaded in a 4-12% Bis-Tris gel (Life Technologies). Proteins were separated by electrophoresis (150V, 1.5h) and transferred (100mA, 40mins) to a nitrocellulose membrane (Life Technologies) using a semi-dry apparatus (Fisher Scientific, NY, USA). The membrane was blocked in Tris-buffered saline (TBS, pH 7.4) with 1% bovine serum albumin (BSA) for 1 hour. Membranes were incubated overnight at 4°C with primary antibodies (total GluR1 [Millipore, #04-855], phosphorylated GluR1-Ser^{831} [Millipore, #04-823], phosphorylated GluR1-Ser^{845} [Millipore, #04-1073], total CaMKII [Sigma, #SAB4503250], phosphorylated CaMKII-Thr^{286} [Abcam, #ab5683], total NMDA NR2B [Millipore, MAB5778], total PSD-95 [Thermo Fisher, MA1-046], phosphorylated stargazin-Ser239/240 [Millipore, AB3713], β-actin [Sigma, #A1978]) in TBS with Tween (TBS-T, 0.1% Tween-20, pH 7.4) and 0.25% BSA. Following the primary antibody incubation, membranes were washed 3 x 10 min in TBS-T. To detect protein bands, the membranes were labeled with a corresponding secondary antibody (Donkey anti-Rabbit Alexa Fluor 488 or Goat anti-Mouse Alexa Fluor 647, Life Technologies).

Fluorescence was detected using a CRi Maestro 2 Imaging System (Perkin Elmer). The bands were quantified using ImageJ software. Average fluorescence was quantified from, at minimum, 4 lysates per exposure group (8 slices per lane, 32 slices in total) and analyzed by ANOVA with statistical significance set as $p < 0.05$, as compared to treatment-matched shams (SPSS v22, IBM). A post-hoc Bonferroni analysis revealed statistical significant differences between injury-matched treatments for each antibody, with significance set as $p < 0.05$.

4.2.9 Roflumilast treatment

To test the ability of a PDE4 inhibitor to rescue LTP after blast exposure, 1 μM roflumilast (SML1099, Sigma-Aldrich; dissolved in 0.07% DMSO) in full serum media was delivered to sham and Level 4-exposed cultures immediately after blast exposure. For comparison, DMSO vehicle was also delivered to a second set of cultures that had received either sham or Level 4 blast exposure. The cultures' ability to generate LTP through high frequency electrical stimulation was evaluated at 24 hours post-exposure. Potentiation was averaged in CA1 region of the hippocampus and analyzed by ANOVA with statistical significance set as $p < 0.05$, as compared to similarly treated shams.

4.3 Results

4.3.1 Primary blast exposure inhibited LTP in a delayed manner

Potentiation (Figure 14) was not reduced when measured 1 hour (Day 0) after Level 4 or Level 9 blast exposures, as compared to sham. When measured at 24 hours (Day 1) post-blast

exposure, potentiation was significantly reduced in cultures exposed to either a Level 4 or Level 9 exposure. This deficit was maintained at Day 2, Day 4, and Day 6 post-Level 4 and Level 9 blast exposure. At 10 days after Level 4 blast, potentiation had partially recovered and was no longer significantly different from time-matched sham-exposed cultures; however, potentiation remained significantly depressed in the Level 9 exposed cultures at the same time point.

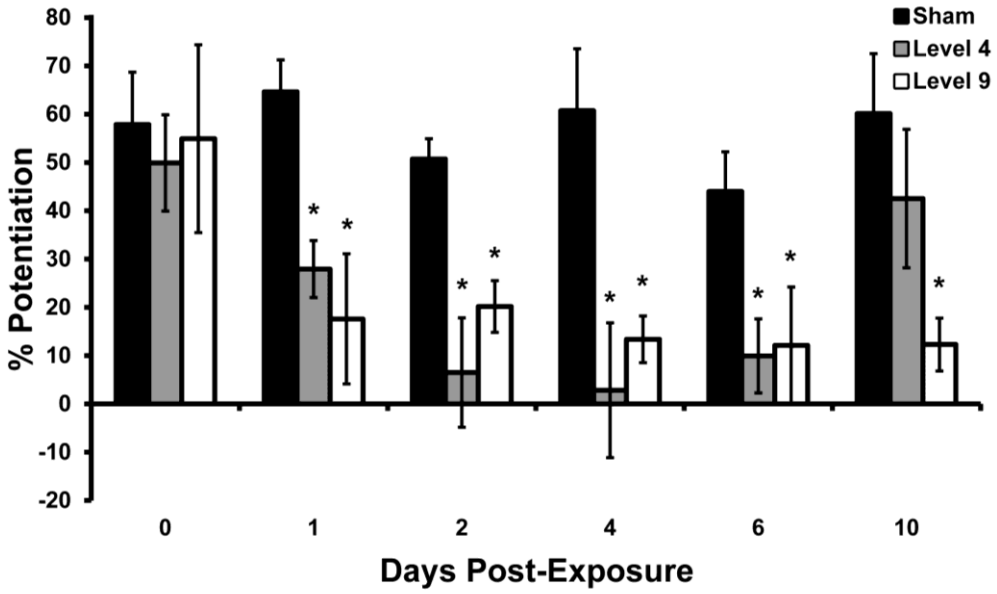

Figure 14 LTP measured in CA1 at multiple time points after primary blast injury. Groups are organized by increasing time after exposure [Day 0, Day 1, Day 2, Day 4, Day 6, Day 10] and then by increasing impulse from left to right [Sham, Level 4, Level 9]. LTP was significantly reduced 1 day following Level 4 or Level 9 blast exposures. This deficit persisted out to 6 days following either injury exposure. LTP spontaneously recovered 10 days after Level 4 blast exposure, but not Level 9 blast exposure. (mean ± S.E.M.; $n \geq 5$; * $p < 0.05$, as compared to time-matched sham)

4.3.2 Primary blast exposure did not induce neuronal death

One possible explanation for changes in potentiation is neuronal degeneration and loss after blast exposure. Previous work has reported that this injury model does not induce substantial cell death at the time points previously examined, i.e. between days 1 and 4 following

blast exposure [53, 55]. We evaluated cell viability (Figure 15) at a longer time point (Day 10) to confirm that cells remained alive at extended periods following Level 9 blast exposure, the most severe blast condition used in the study. We found that cell death was not significantly increased for any ROI at 10 days following Level 9 exposure compared to sham cultures. Although cell death was slightly higher in the DG (~ 10%) than other regions following blast, this pattern was also present in sham cultures. To confirm the presence of living neurons, exposure to toxic levels of glutamate 10 days following Level 9 primary blast caused significant cell death (> 80%) across all ROI, confirming the presence of cells not killed by primary blast exposure alone.

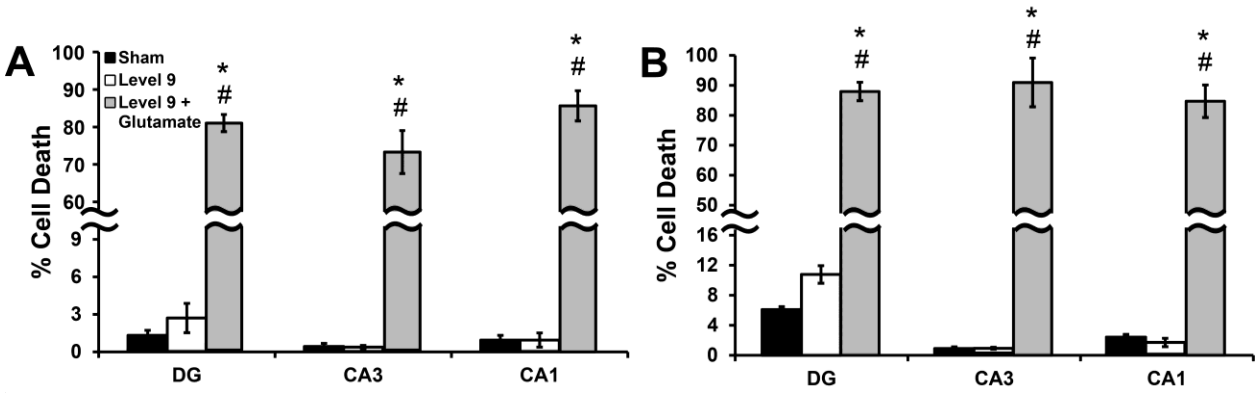

Figure 15 Cell death measured for each ROI of the hippocampus at 1 hour and 10 days after Level 9 blast. Cell death was not significantly induced after Level 9 blast exposure in any ROI compared to sham-injured cultures. Glutamate exposure at (A) 1 hour and (B) 10 days following Level 9 blast induced significant cell death in all ROI. (mean ± S.E.M.; n=12; * $p<0.05$ as compared to sham, # $p<0.05$ as compared to Level 9)

4.3.3 Primary blast exposure did not induce deficits in basal evoked function

Alterations in basal evoked function, the ability to stimulate local circuitry or transmit stimulation to downstream networks, could potentially explain the observed change in LTP following blast injury. We have previously reported that our injury model induced minimal changes in basal evoked function, when stimulating across the SC pathway, at 4-6 days post-primary blast exposure [55]. In the current study, we observed that neither blast level significantly altered the maximum voltage response (Figure 16A, R_{max}), the current necessary to generate a half-maximal response (Figure 16B, I_{50}), or the spread in the firing threshold for the population of neurons (Figure 16C, m) for any ROI at any time point following injury. These results confirmed the previous findings from this system and revealed that basal evoked function was not disrupted at acute or longer time points following blast exposure.

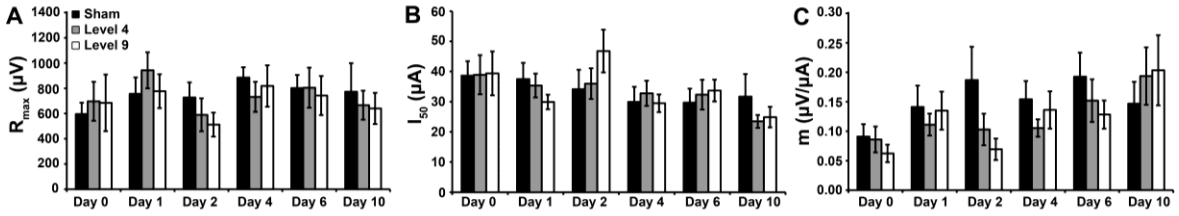

Figure 16 Blast injury minimally affected stimulus-response parameters in CA1 when stimulated across the Schaffer collateral (SC) pathway. There was no significant effect on R_{max} (**A,** p>0.35), I_{50} (**B,** p>0.42), m (**C,** p>0.10) at any time point following blast exposure, as compared to sham. (Data not shown for CA3 and DG, mean ± S.E.M.; n≥5)

4.3.4 Primary blast exposure reduced potentiation when induced with gly-aCSF

To explore blast-induced deficits in LTP further, we investigated the effect of blast injury on chemical induction of LTP using gly-aCSF. We observed that potentiation (Figure 17A) was significantly reduced in Level 4 blast-exposed cultures measured at 1 day after injury when induced with gly-aCSF. When measured at 10 days following Level 4 blast exposure, gly-aCSF-induced potentiation (Figure 17A) recovered and was not significantly different from time-matched, sham-exposed cultures. These findings matched the time course of blast-induced LTP deficits when induced electrically. To verify that the shorter treatment duration with gly-aCSF did not confound results, we extended gly-aCSF treatment from 3 to 20 minutes and observed that Level 4 blast exposure significantly decreased potentiation (27 ± 13%) as compared to sham (78 ± 15%) exposure (data not shown).

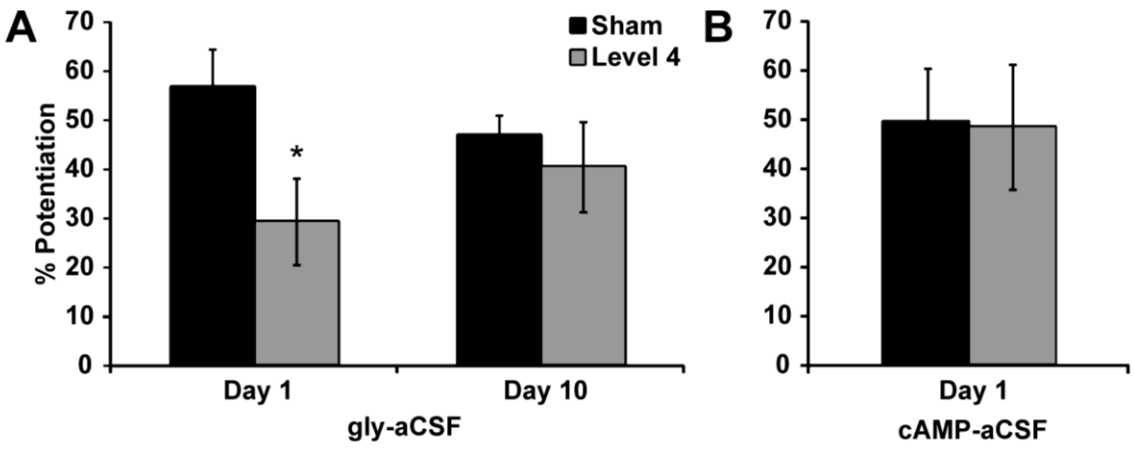

Figure 17 Blast injury significantly reduced glycine-induced LTP, but not rolipram/forskolin-induced LTP. (**A**) LTP was significantly reduced when induced by gly-aCSF at 1 day following Level 4 blast exposure. There was no significant change in glycine-induced LTP at 10 days following Level 4 blast exposure. (**B**) LTP was not reduced when induced by cAMP-aCSF at 1 day following Level 4 blast exposure. (mean ± S.E.M.; n≥8, * $p<0.05$, as compared to sham)

4.3.5 Primary blast exposure did not reduce potentiation when induced with cAMP-aCSF

In contrast, potentiation (Figure 17B) was not significantly reduced at 1 day following a Level 4 blast exposure using a chemLTP induction protocol that upregulated the cAMP/PKA pathway (cAMP-aCSF). To verify the extended treatment duration with cAMP-aCSF did not confound results, we shortened cAMP-aCSF treatment from 20 to 3 minutes and observed that blast exposure did not significantly reduce potentiation (48 ± 11%) as compared to sham (42 ± 17%) exposure (data not shown). These results suggested that modulation of the cAMP/PKA pathway might act therapeutically against primary blast-induced LTP loss.

4.3.6 Phosphorylated GluR1-Ser831 and total GluR1 expression was significantly reduced by primary blast injury

Blast prevented a significant increase in phosphorylation of AMPAR-GluR1 subunits at the Serine-831 site at 24 hours post-injury as compared to shams, when LTP was induced with gly-aCSF (Figure 18A). There was no observed effect of blast with vehicle-treated cultures or with the cAMP-aCSF treatment. Treatment with either gly-aCSF or cAMP-aCSF significantly increased GluR1-Ser831 phosphorylation over vehicle-treated sham cultures, i.e. no induction of LTP; however, only cAMP-aCSF significantly increased GluR1-Ser831 phosphorylation over vehicle-treated blast-cultures.

Blast also significantly decreased the expression of total GluR1 subunits (Figure 18B) as compared to shams, when LTP was induced with gly-ACSF. Although this deficit was not observed with vehicle-treated cultures or with the cAMP-aCSF treatment, it is important to note

that there was an increase in total GluR1 expression for both sham and blast-exposed cultures receiving cAMP-aCSF treatment, as compared to the vehicle-treated cultures.

We observed no significant change in the phosphorylation state of AMPAR-GluR1 subunits at the Serine-845 site (Figure 18C) between blast and sham cultures for any chemical treatment; however, both chemical treatments significantly increased GluR1-Ser845 phosphorylation over vehicle treated cultures.

There also was no significant change to NMDAR-NR2B subunits (Figure 18D) because of either injury exposure or chemical treatment.

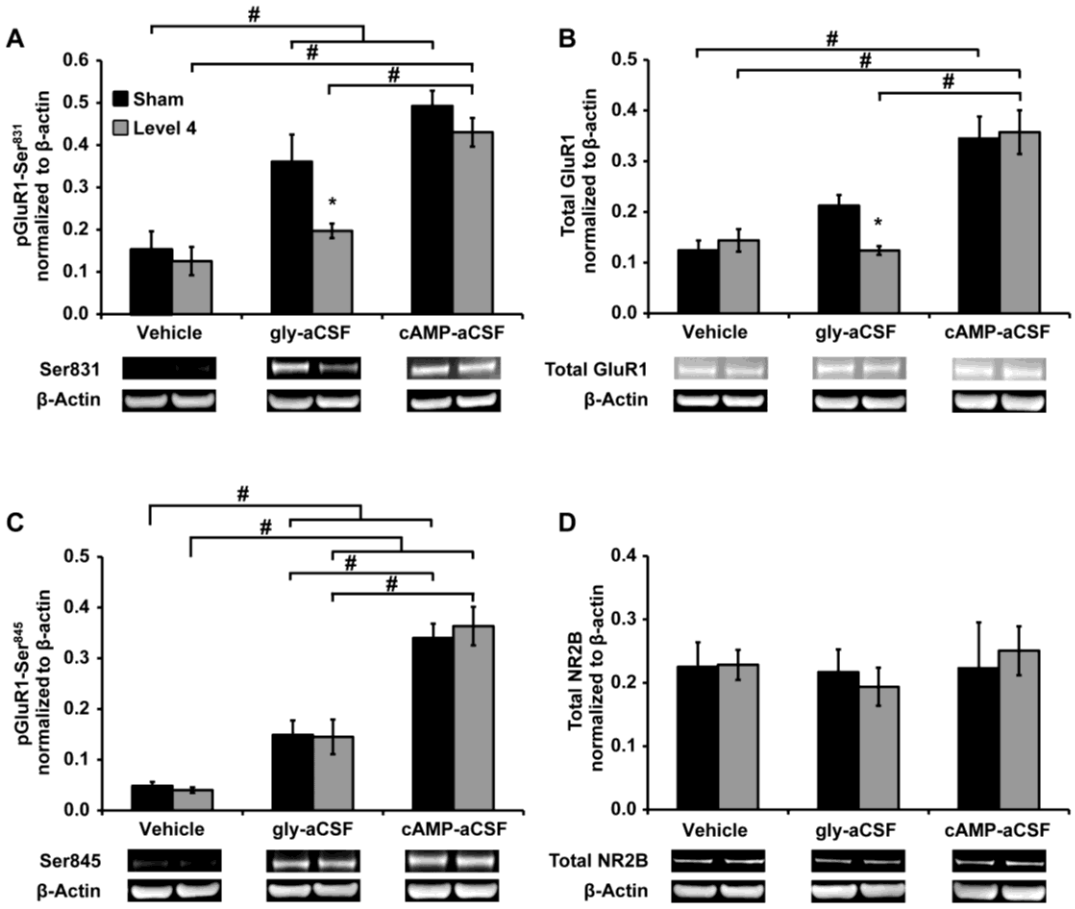

Figure 18 Phosphorylation of GluR1-Ser831 and total GluR1 expression was reduced at 24 hours following Level 4 blast injury. Protein expression (normalized to loading control β-actin) was evaluated at 24 hours following Level 4 blast injury for four different synaptic membrane protein targets: pGluR1-Ser831 (**A**), total GluR1 (**B**), pGluR1-Ser845 (**C**), and total NMDA-NR2B (**D**). Cultures were either untreated (vehicle) or LTP was induced by either gly-aCSF or cAMP-aCSF prior to cell lysis. Phosphorylation of GluR1-Ser831 and total GluR1 expression were significantly reduced when LTP was induced by gly-aCSF, but not by cAMP-aCSF, at 1 day following Level 4 blast exposure. Representative bands from each group are shown below the graphs. (mean ± S.E.M.; n≥4, * $p<0.05$, as compared to treatment-matched sham, # $p<0.05$ as compared to injury-matched treatment)

4.3.7 Primary blast injury did not affect total CaMKII nor phosphorylated CaMKII-Thr286

Another important target in the LTP pathway is CaMKII as CaMKII phosphorylation is necessary for the induction of some forms of LTP [80, 138, 259]. We observed that phosphorylation of CaMKII at the Threonine-286 (Thr-286) site was not affected by injury (Figure 19A). There was an expected increase in phosphorylation with both chemLTP treatments. We also observed that total expression of CaMKII (Figure 19B) was not altered because of injury ($p > 0.33$) or chemical treatment ($p = 1.0$).

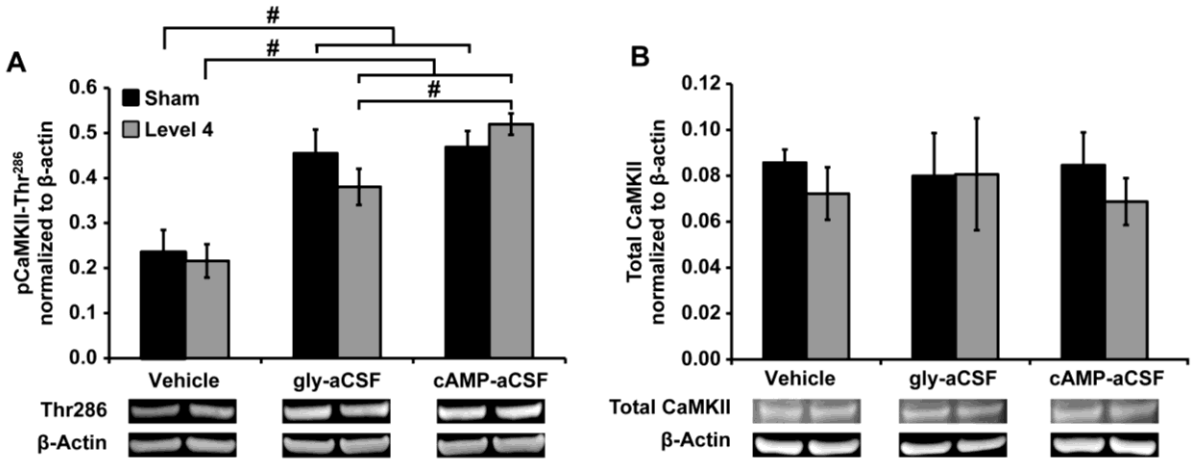

Figure 19 Primary blast exposure did not affect (A) phosphorylation of CaMKII-Thr286 or expression of (B) total CaMKII at 24 hours post-injury with or without induction of LTP. Representative bands from each group are shown below the graphs. (mean ± S.E.M.; n≥4, # $p<0.05$ as compared to injury-matched treatment)

4.3.8 Primary blast injury significantly reduced PSD-95 and pStargazin-Ser239/240

We also examined two key proteins responsible for receptor integration at the synapse: PSD-95 and stargazin. We found that blast decreased expression of total PSD-95 for both vehicle and gly-aCSF treated cultures as compared to shams, but not for cAMP-aCSF treated cultures (Figure 20A). We observed that blast exposure reduced the phosphorylation of stargazin (Ser239/240) after gly-aCSF treatment, but not for vehicle or cAMP-aCSF treated cultures (Figure 20B).

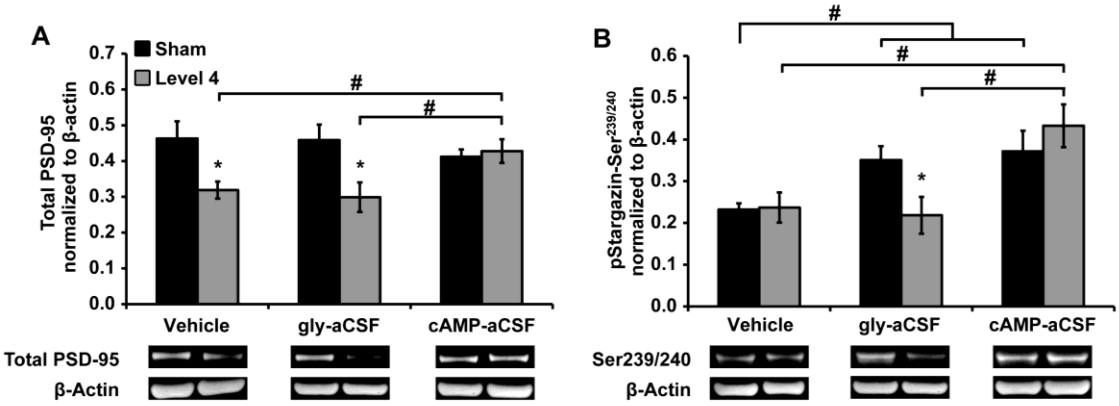

Figure 20 Blast exposure reduced total PSD-95 expression and phosphorylation of stargazin at the Ser239/240 site. Total PSD-95 expression (A) was significantly reduced at 24 hours following Level 4 blast exposure in vehicle treated and gly-aCSF-treated cultures, but not in cAMP-aCSF-treated cultures. Phosphorylation of stargazin-Ser239/240 (B) was significantly reduced at 24 hours following Level 4 blast exposure in gly-aCSF-treated cultures, but not in cAMP-aCSF-treated cultures. Representative bands from each group are shown below the graphs. (mean ± S.E.M.; $n \geq 4$, * $p<0.05$, as compared to treatment-matched sham, # $p<0.05$ as compared to injury-matched treatment)

4.3.9 Roflumilast treatment immediately following exposure prevented blast-induced LTP deficits

Roflumilast treatment immediately following blast exposure prevented a deficit in electrically-induced LTP at 24 hours post-injury (Figure 21). Level 4 blasted cultures that were treated with vehicle (0.07% DMSO in aCSF) immediately following injury were unable to potentiate at 24 hours post-exposure, as compared to sham-vehicle treated cultures. This indicated that PDE4 inhibitors have the potential to prevent primary blast-induced LTP loss.

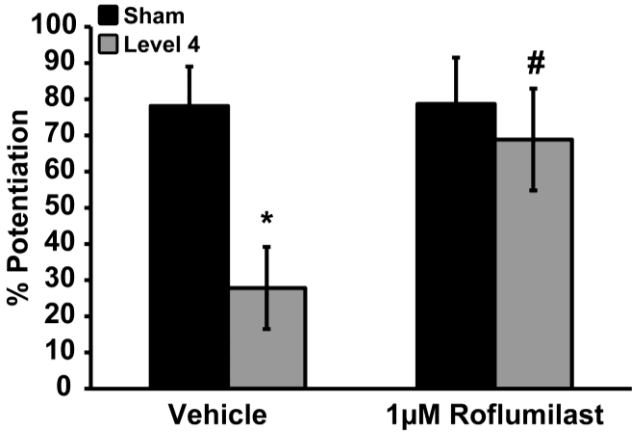

Figure 21 Roflumilast treatment prevented blast-induced LTP deficits at 24 hours post-injury. Cultures were exposed to Level 4 blast and immediately treated with either 1μM roflumilast or vehicle (0.07% DMSO in medium). LTP was electrically-induced and evaluated 24 hours post-injury. (mean ± S.E.M.; n≥5, * $p<0.05$, as compared to treatment-matched sham, # $p<0.05$ as compared to injury-matched vehicle)

4.4 Discussion

This study elucidates important details regarding the mechanisms behind LTP-deficits following primary blast exposure. The onset of blast-induced LTP deficits was delayed (1-24 hours post-exposure), and the deficit recovered over time (6-10 days post-exposure), depending on blast intensity. Primary blast exposure reduced expression and disrupted phosphorylation of proteins critical to LTP induction. Blast reduced phosphorylation of GluR1-Ser831 and expression of total GluR1. Blast also decreased PSD-95 expression and phosphorylation of stargazin-Ser239/240. Treatment with FDA-approved roflumilast immediately post-blast prevented LTP deficits measured at 24 hours. We hypothesize that a mechanism for blast-induced LTP deficits is the disruption of PSD-95, which prevents the increase and subsequent phosphorylation of synaptic AMPAR-GluR1 at the PSD, thereby preventing the induction of LTP.

Our study is the first to report that primary blast produced deficits in LTP at acute time points following injury. *In vivo* blast injury induced LTP deficits at 2 and 4 weeks following blast in mice[24, 81]. Non-blast, fluid percussion injury (FPI) models induce LTP deficits in rodents at 2-4 hours[82], 1-2 days[83, 255], and 1 week[85] post-injury. One study did not observe FPI-induced LTP deficits at 1 week post-injury, but did observe deficits at 8 weeks post-injury[84]. The difference in injury biomechanics between our injury model and FPI is important to note when interpreting results. Our blast model applied a pressure transient *in vitro* that leads to minimal tissue deformation[49], whereas FPI is a mix of pressure and deformation throughout the brain[237, 238].

Glycine-LTP is similar to high-frequency stimulus-induced LTP because they both directly activate NMDARs enabling an influx of Ca^{2+} ions[257]. Conversely, rolipram/forskolin-LTP activates secondary messengers (namely cAMP) to induce LTP[258]. In sham cultures, both protocols induced hallmark signs of LTP, including GluR1-containing AMPAR insertion into the PSD, phosphorylation of CaMKII, phosphorylation of GluR1-Ser831, and increased electrophysiological response[258, 260, 261]. No previous study has investigated the effect of TBI on glycine-LTP; however, one study observed that blast exposure significantly reduced rolipram/forskolin-LTP at 2 and 4 weeks following injury[24]. Although the results of our study contradict those findings, it is important to note the substantial differences between the studies including the post-injury time point, injury biomechanics, and concentration of rolipram.

We observed that primary blast affected postsynaptic receptors, specifically total GluR1 expression and phosphorylation of GluR1-Ser831 (Figure 18). Conversely, one non-blast TBI study observed an increase in phosphorylation of GluR1-Ser831 between 1 and 4 hours following stretch injury in cortical neurons; however, their findings corroborate our observations that total GluR1 expression or phosphorylation of GluR1-Ser845 did not change with injury[262]. This difference may be linked to different injury models, brain region, and use of chemical LTP induction. We observed that cAMP-aCSF increased the phosphorylation of GluR1-Ser845 over that of gly-aCSF for both blast and sham cultures. This difference suggests a mechanism for LTP-recovery with cAMP-aCSF treatment. We also chose to investigate the NMDAR-NR2B subunit, as previous studies reported this subunit governed NMDAR mechanosensitivity[108]. We observed no change to this subunit after blast exposure; however, previous non-blast TBI studies reported mixed results for this target [105, 263, 264]. The effect of primary blast on postsynaptic

receptors, namely the AMPAR-GluR1 subunit, is likely linked to the LTP deficits measured electrophysiologically.

CaMKII is a protein critical for induction of hippocampal LTP[265]. Our data suggested that blast did not affect either total CaMKII expression or phosphorylation at the Thr-286 site (Figure 19). These results suggest that the mechanism to phosphorylate CaMKII was not impacted by blast. Studies with non-blast TBI have reported a decrease in total CaMKII expression at varying time points after FPI[85, 266]. Conversely, CaMKII phosphorylation was reported to increase acutely following *in vivo* and *in vitro* non-blast TBI in rodents[131, 262, 263, 266]. Most of these studies reported resolution of altered phosphorylation of CaMKII by 24 hours post-injury, which corroborates our finding that CaMKII phosphorylation was not affected at 24 hours following primary blast exposure; however, reduction of total CaMKII by non-blast-TBI suggested a different injury cascade from blast. Interestingly, we observed that blasted cultures that were subsequently treated with cAMP-aCSF exhibited significantly increased phosphorylation of CaMKII-Thr286 over blasted cultures that subsequently were treated with gly-aCSF, suggesting that CaMKII phosphorylation may modulate LTP-rescue by rolipram/forskolin.

The immobilization of GluR1-containing AMPARs at the PSD through PSD-95 is a required step for LTP induction[267]. We observed that primary blast reduced PSD-95 expression, in both vehicle and glycine-LTP groups (Figure 20). PSD-95 was the only target for which blast, without subsequent LTP-induction, reduced expression. These findings corroborate our observation that blast did not affect all neuronal function, but rather that deficits after blast were LTP-specific. Combined primary and tertiary blast exposure did not affect cortical PSD-95

expression 2 weeks post-injury in rats[27]; however, the rise time of the pressure profile in that model was extended (~2ms) compared to typical shock exposures (~20μs)[49]. Several non-blast TBI reduced hippocampal PSD-95 expression between 18 hours and 7 days post-injury[132, 136, 268]. Stargazin is an auxiliary AMPA protein that mediates the binding of AMPARs to PSD-95 upon phosphorylation. We observed that blast exposure reduced pStargazin-Ser239/240 when LTP was induced with glycine, which could explain the reduction in total GluR1 after blast, as stargazin binds to the GluR1 subunit. Genetically-altered stargazin expression was shown to decrease the duration that AMPARs resided in the PSD[269]. Our study is the first to report that TBI affected stargazin

Our working hypothesis (Figure 22) is that blast disrupts PSD-95, which, in turn, reduces induction of LTP due to decreased GluR1 immobilization at the PSD and phosphorylation at the Ser831 site (Figure 22). Phosphorylation of GluR1-Ser831 requires immobilization of GluR1-containing AMPARs to PSD-95. We also investigated the effect of blast on protein expression when LTP was chemically induced through secondary messengers, specifically cAMP. We observed that modulation of the cAMP/PKA pathway restored phosphorylation of GluR1-Ser831 and PSD-95 expression. One study previously observed that activation of the cAMP pathway with forskolin prevented NMDA-induced PSD-95 loss[270]. Our findings, in conjunction with previously reported results, warrant further investigation into the modulation of cAMP/PKA pathway as a therapeutic target for primary blast injury.

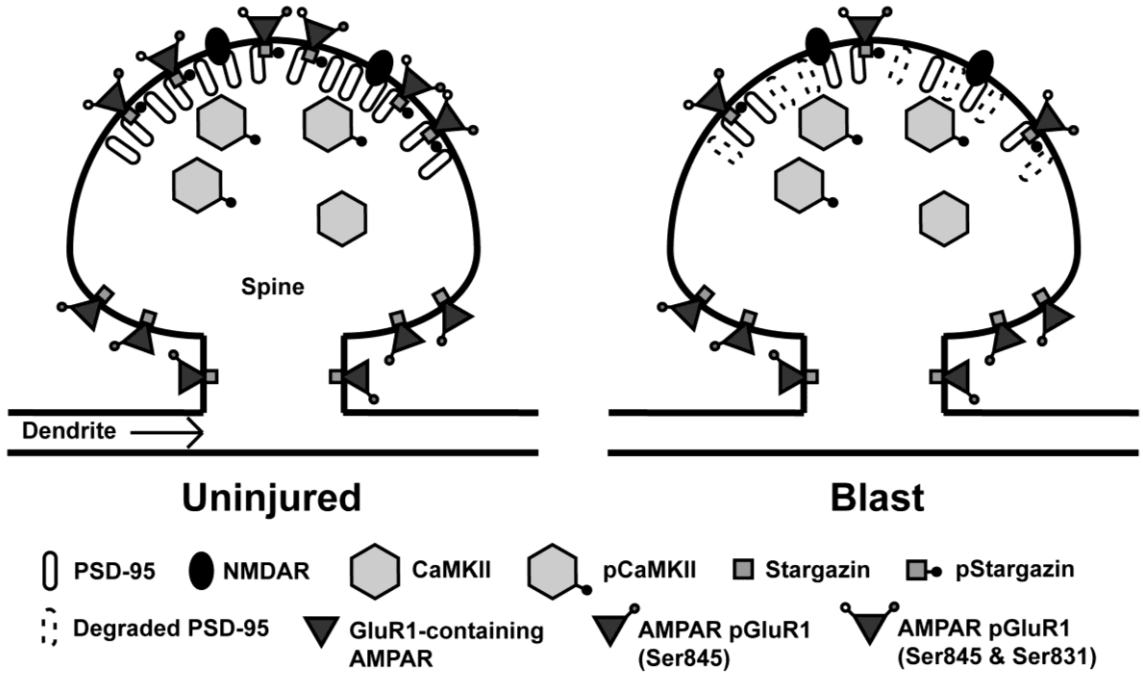

Figure 22 Hypothesized injury mechanism for primary blast-induced LTP deficits. This diagram compares an uninjured dendritic spine to a spine exposed to primary blast. Our findings suggest that primary blast exposure degrades or reduces the expression of PSD-95, the major post-synaptic membrane scaffolding protein. We hypothesize that when attempting to induce LTP after blast, GluR1-containing AMPARs are less able to immobilize at the PSD, a required step for the increase in AMPAR signaling that enables potentiation. Thus, pCaMKII is unable to phosphorylate GluR1 subunits at the Ser831 site and potentiation is reduced. Our data suggests that NR2B-containing NMDARs, CaMKII, and extrasynaptic AMPAR priming (via phosphorylation of Glur1-Ser845) were unaffected by primary blast.

In this study, we report that the PDE4 inhibitor, roflumilast, reduced LTP-deficits after blast (Figure 21). Although it has not been investigated in TBI, treatment with roflumilast improved cognition in hypertensive rats[155]. Another PDE4 inhibitor, rolipram, rescued FPI-induced LTP deficits in rats at two weeks post-injury[147]. Together, these studies suggest that the modulation of the cAMP pathway may hold therapeutic potential for TBI.

There are limitations to consider when interpreting these results. A goal of this study was to focus on the effects of primary blast injury in isolation. This approach required an *in vitro*

injury model to ensure precise control over the injury biomechanics. Subsequently, it is difficult to translate the observed functional deficits from this study to macroscopic behavioral and cognitive changes. In studying the time course of primary blast-induced LTP deficits, we chose to measure LTP out to 10 days post-injury. Although we did not observe spontaneous recovery for Level 9 exposed cultures in this period, it is possible that LTP could recover at later time points. As previously mentioned, PSD-95 was the only target for which blast reduced expression when LTP was not induced. This finding supports our observation that blast did not affect basal function, but rather affected an LTP-specific pathway. We concluded that modulation of the cAMP/PKA pathway might act therapeutically against primary blast-induced LTP loss; however, it is possible that the multiple stimulatory components within the cAMP-aCSF solution comprise a more powerful potentiating stimulus than electrical or glycine-induced LTP. In this case, our results suggest that a supra-physiological induction (i.e. non-synaptic) of LTP is required following primary blast exposure.

In summary, we report that primary blast disrupted hippocampal LTP in a delayed manner (>1 hour) and, depending on the severity of blast exposure, LTP spontaneously recovered by 10 days post-injury. We observed blast-induced deficits in phosphorylation or expression of proteins critical for LTP induction, namely AMPAR-GluR1 (total and pGluR1-Ser831), PSD-95, and pStargazin-Ser239/240. Finally, we observed that modulation of the cAMP/PKA pathway using PDE4 inhibitors ameliorated blast-induced deficits in LTP and protein expression. Future studies will investigate the potential of PDE4 inhibitors to prevent the effects of primary blast injury.

5 Phosphodiesterase-4 inhibition restored hippocampal long term potentiation after primary blast[4]

5.1 Introduction

Traumatic brain injury (TBI) is defined as a disruption of brain function due to mechanical forces acting on the head[1]. Since 2000, there have been approximately 350,000 diagnosed TBIs among U.S. military personnel, with 83% of these injuries considered mild TBI (mTBI)[3]. Exposure to blast is the leading cause of TBIs for military personnel[4, 271]. The biomechanics of blast-induced TBI (bTBI) are multi-phasic and can include penetrating injury and acceleration-based deformation[215, 272]; however, injury due to shock wave exposure, often referred to as primary blast injury, remains debated[13]. Studying primary blast injury using *in vivo* models can be difficult due to the associated challenges of eliminating head motion and providing adequate thoracic protection[30]. In comparison, our *in vitro* primary blast injury model isolates the shock wave component of blast from the other, confounding phases of injury [50]. The precisely controlled biomechanics of our injury model enables the study of neuronal dysfunction following primary blast injury in isolation[50, 54, 56, 176].

One common clinical symptom of bTBI is memory impairment[273]. Behavioral and ultrastructural changes in rodents following *in vivo* blast exposure suggest that the hippocampus is especially vulnerable to bTBI[35, 74, 274]. Long-term potentiation is the primary experimental model for investigating synaptic plasticity on a cellular level and is known to occur within the hippocampus[80]. It has been well-documented that blast exposure in animals negatively effects

[4] A modified version of this chapter previously appeared in print: **Vogel III E.W.**, Morales F.N., Meaney D.F., Bass C.D., Morrison III, B. Phosphodiesterase-4 inhibition restored hippocampal long term potentiation after primary blast, *Exp. Neurol*. 2016, In Revisions.

hippocampal LTP, but this observation is not universal among preclinical models of blast TBI[24, 55, 81, 176, 275]. We have previously reported that 24h post-injury, primary blast reduced the expression and phosphorylation of AMPA-GluR1 subunits[56], a key transmembrane receptor required for the induction and maintenance of LTP[103, 276, 277]. We also observed that modulation of the second messenger cyclic adenosine monophosphate (cAMP) rescued blast-induced deficits in LTP and the expression of key proteins involved in LTP maintenance[56]. Those results suggested that modulation of the cAMP pathway could have therapeutic potential in preventing memory deficits following primary bTBI. Intriguingly, increasing cAMP through phosphodiesterase-4 (PDE4) inhibition was effective in improving outcome in some experimental models of TBI and also reduced cognitive impairments associated with Alzheimer's disease, schizophrenia and aging[141, 278-281]. Currently, there are no clinically-approved treatments for TBI[282].

This study examined the ability of PDE4 inhibitors, including roflumilast, to prevent primary blast-induced deficits in LTP and protein expression. Roflumilast is FDA-approved for treatment of chronic obstructive pulmonary disorder (COPD), making it an attractive therapeutic candidate. We observed that delivery of a PDE4 inhibitor immediately post-blast prevented LTP deficits measured 24 hours following injury *in vitro*. When varying the time post-injury of drug delivery, the therapeutic window of PDE4 inhibitors following primary blast was 6 hours post-injury. PDE4 inhibition post-blast reversed blast-induced changes in protein expression/phosphorylation for key targets in the LTP pathway, including phosphorylation of AMPA-GluR1 subunits (pGluR1) at the serine-831 (Ser831) site, total GluR1 expression, and phosphorylation of stargazin (pStargazin) at the serine-239/240 (Ser239/240) site upon LTP induction. Roflumilast treatment significantly increased total postsynaptic density protein-95

(PSD-95) expression regardless of LTP induction. These findings indicate that further investigation into the therapeutic potential of PDE4 inhibition following bTBI is warranted.

5.2 Materials and Methods

5.2.1 Organotypic hippocampal slice culture

All animal procedures were approved by the Columbia University Institutional Animal Care and Use Committee (IACUC). OHSCs were generated from P8-P10 Sprague Dawley rats as previously described[50, 53, 55, 184]. In brief, the hippocampus was excised, cut into 400µm thick sections, and plated onto Millicell inserts (EMD Millipore, Billerica, MA) in Neurobasal medium supplemented with 2mM GlutaMAX^{TM}, 1X B27 supplement, 10mM 4-(2-hydroxyethyl)-1-piperazineethanesulfonic acid (HEPES), and 25mM D-glucose (Life Technologies, Grand Island, NY). Following plating, cultures were fed every 2-3 days with full serum medium, containing 50% MEM, 25% Hank's Balanced Salt Solution, 25% heat inactivated horse serum, 2mM GlutaMAX, 25mM D-glucose, and 10mM HEPES (Sigma). Prior to blast injury, cultures were maintained for 10-14 days.

5.2.2 Primary blast exposure

Blast injury methods have been described previously in detail[49, 50, 52-55]. Cultures were placed into sterile bags, filled with pre-warmed, serum-free medium, pre-equilibrated with 5% CO_2 at 37°C. Any air bubbles were removed from the bag, which was sealed and placed into the receiver column. The receiver column was filled with pre-warmed water (37°C), sealed with a

silicone membrane, and the shock tube was fired. Piezoresistive pressure transducers (Endevco 8530B-500, San Juan Capistrano, CA, USA) recorded incident pressure at the shock tube exit and inside the fluid-filled receiver. Peak overpressure, duration, and impulse were recorded, processed, and quantified as previously described[50, 52, 53, 55]. Sham cultures were treated identically except the shock tube was not fired.

Based on previous studies, a blast exposure was utilized that produced consistent deficits in LTP, which was characterized by the peak pressure, duration, and impulse of the in-air shock wave (336 ± 8 kPa, 0.84 ± 0.01 ms, 87 ± 2 kPa•ms) and the in-fluid pressure transient (598 ± 15 kPa, 1.85 ± 0.30 ms, 440± 13 kPa•ms)[55]. Following blast or sham exposure, cultures were immediately removed from the receiver and returned to the incubator in fresh, full serum medium. Cultures were maintained in full serum medium until the indicated time points.

5.2.3 Drug treatment

A stock solution of roflumilast (SML1099, Sigma-Aldrich) was dissolved in DMSO at a final concentration of 200μM. The drug was further diluted in fresh, full serum medium (≤ 0.07% DMSO) at indicated concentrations: 100pM, 1nM, 10nM, and 100nM. Cultures were placed into drug-containing medium immediately following blast injury. In a separate set of cultures, roflumilast (1nM) or DMSO vehicle was delivered to OHSCs at varying times following blast exposure: 0 hours, 1 hour, 6 hours, and 23 hours. To further evaluate the effect of delayed roflumilast delivery, a separate set of cultures were treated with roflumilast 24 hours following injury and function was evaluated 48 hours following injury.

A stock solution of piclamilast (SML0585, Sigma-Aldrich), another PDE4 inhibitor, was dissolved in DMSO at a final concentration of 10μM. The drug was further diluted in fresh, full serum medium (≤ 0.07% DMSO) to 5nM, which was used to treat cultures at the indicated time points following blast exposure.

A stock solution of ibudilast (I0157, Sigma-Aldrich), another PDE4 inhibitor, was dissolved in DMSO at a final concentration of 200mM. The drug was further diluted in fresh, full serum medium (≤ 0.07% DMSO) to 1μM, which was used to treat cultures at the indicated time points following blast exposure.

A stock solution of papaverine (CDS021481, Sigma-Aldrich), a partially selective PDE10A inhibitor, was dissolved in DMSO to 400μM. The drug was further diluted in fresh, full serum medium (≤ 0.07% DMSO) to 200nM, which was used to treat cultures at the indicated time points following blast exposure.

For all experiments, additional groups of injured or sham cultures were treated with DMSO vehicle (0.07%) for comparison to drug-treated cultures.

5.2.4 Electrophysiology

Electrophysiological activity within the OHSC was recorded using 60-channel MEAs (8×8 electrode grid without the corners, 30 μm electrode diameter, 200 μm electrode spacing) at the indicated time points following blast injury (60MEA200/30iR-Ti-gr, Multi-Channel Systems, Reutlingen, Germany). OHSCs were perfused with aCSF (norm-aCSF) containing 125 mM NaCl, 3.5 mM KCl, 26 mM $NaHCO_3$, 1.2 mM KH_2PO_4, 2.4 mM $CaCl_2$, 1.3 mM $MgCl_2$, 10mM

HEPES, and 10 mM glucose (pH = 7.40), which was bubbled with 5% CO_2/95% O_2 and warmed to 37°C, as previously described[97]. Recordings were acquired with an MEA1060-BC amplifier and data acquisition system (Multi-Channel Systems). Neural signals were recorded at 20 kHz with a 6kHz analog, anti-aliasing filter and then further filtered in MATLAB, using an eighth-order, digital low-pass (1000Hz) and a fourth-order, digital, high-pass (0.2Hz) Butterworth filter.

5.2.5 Spontaneous activity

Spontaneous neural activity was measured by recording continuously for 3 minutes from all electrodes within the hippocampus, as previously described[55]. In brief, neural event activity was detected based on the multi-resolution Teager energy operator[88, 115, 205, 222, 223]. Data from each electrode was segregated by anatomical ROI (DG, CA3, and CA1). The effect of blast injury and drug-treatment on spontaneous event rate, magnitude, and duration were analyzed by two-way ANOVA with statistical significance set as $p < 0.05$ (SPSS v22, IBM; Armonk, NY). It is important to note that there no significant difference between vehicle-treated cultures and roflumilast-treated cultures was observed for the number of electrodes per region.

Spontaneous network synchronization was also quantified using previously published methods[55, 115, 121, 224, 225]. In brief, correlation between neural events was calculated for each electrode pair based upon neural event-timing, where two events occurring within 1.5ms were considered synchronous, and the total number of events. A correlation matrix was constructed which represented the strength of correlation between electrode pairings. To determine statistical significance, this data was compared to randomized surrogate time-series data without correlated activity, but with an equal event-rate, to identify significantly synchronized clusters.

The GSI, ranging from 0 (random, uncorrelated activity) to 1 (perfectly synchronous, correlated activity on all electrodes), was calculated from the clusters of electrodes with the highest (significant) degree of synchronization. This analysis was based upon the eigenvalues of the correlation matrix, which represented correlation strength, and associated eigenvectors, which represented the cluster of electrodes. The effects of blast exposure and drug-treatment on GSI were analyzed by two-way ANOVA, with statistical significance set as $p < 0.05$.

5.2.6 Stimulus-response curves

Stimulus-response curves were generated by applying a constant current, biphasic, bi-polar stimulus (100 µs positive phase followed by 100 µs negative phase) of increasing magnitude (0-200 µA in 10 µA increments) to electrodes located in the SC pathway. As in previous studies, each electrode's response was fit to a sigmoidal curve, and three parameters were quantified: R_{max}, represented the maximum amplitude of the evoked response, I_{50} represented the current necessary to generate a half-maximal response, and the term *m*, represented the slope of the sigmoidal fit[97]. As before, data from each electrode was segregated by anatomical ROI. Each parameter (I_{50}, m, R_{max}) for an electrode was averaged within a region to determine that regional response for any given slice. Data reported for each region is the average across slices within a given experimental group. The effects of blast exposure and drug-treatment on individual SR parameters were analyzed by two-way ANOVA with statistical significance set as $p < 0.05$.

5.2.7 Long-term potentiation

Following SR recordings, the ability to induce LTP by electrical stimulus was measured as previously described[55]. Baseline response was evoked by stimulating at I_{50} across the SC pathway once per minute for 30 minutes. LTP was induced by stimulating with a HFS, which consisted of three trains of 100Hz pulses applied for 1 second at I_{50}, with each train separated by 10 seconds. Immediately following LTP induction, post-induction response was evoked by stimulating at I_{50} once every minute for 60 minutes. LTP induction was calculated as percent potentiation above baseline based on the last 10 minutes of recording in each recording window. To ensure only stable responses were included for analysis, electrodes were discounted if the coefficient of variance (pre or post-induction) was greater than 20%[235]. The average number of discounted electrodes was 12% and recordings where greater than 50% of electrodes were discounted were removed from analysis. This led to an average of LTP induction was averaged among electrodes within the CA1. The effect of drug treatment was analyzed by ANOVA, followed by Tukey HSD *post hoc* tests with statistical significance set as $p < 0.05$. For the dose response study, the effect of roflumilast concentration was analyzed by ANOVA, followed by Tukey HSD *post hoc* tests with statistical significance set as $p < 0.05$.

5.2.8 Cell death measurement

Propidium iodide fluorescence was used to observe the effect of roflumilast on cell viability. Cell death was measured immediately prior and 24 hours following injury using 2.5 µM PI (Life Technologies) in serum-free medium. Previous studies with this injury model have reported that blast injury caused minimal cell death[53, 55]. Cultures were treated with full serum medium containing either 1nM roflumilast or DMSO (0.07%) vehicle at 6 hours post-injury.

Cell death was determined for ROI, as previously described, using MetaMorph (Molecular Devices, Downingtown, PA), and reported as percentage area[50, 53, 55, 95]. To confirm OHSC viability, a subset of cultures were exposed to blast and either roflumilast or vehicle treatment, and subsequently subjected to an excitotoxic exposure of glutamate (10mM for 3 hours) 24 hours following blast exposure (18 hours following drug delivery). OHSC were returned to fresh serum-free medium following excitotoxic exposure, and cultures were imaged for cell death 24h later. Cell death was analyzed by ANOVA, followed by Tukey HSD *post hoc* tests with statistical significance set at $p < 0.05$.

5.2.9 Chemically-induced LTP (chemLTP)

In a separate set of cultures, LTP was chemically induced. The chemLTP protocol replaced electrical LTP induction with a 3 minute perfusion with a modified aCSF solution (gly-aCSF)[257]: norm-aCSF containing 200 µM glycine and 0 mM MgCl (reduced from 1.3mM). Perfusate was then switched back to norm-aCSF for 20 minutes prior to assessing LTP induction. LTP was quantified as described above. Chemically-induced LTP was averaged among electrodes within the CA1 and the effect of drug-treatment was analyzed by ANOVA with statistical significance set as $p < 0.05$.

5.2.10 Western blotting

For each condition tested by Western blotting, 8 slice cultures from 2 different animals were collected for protein extraction at the indicated time points. Protein concentrations were determined by the BCA assay according to the manufacturer's instructions (Thermo Fisher

Scientific, Waltham, MA, USA), and 50 µg of protein per sample was separated on a 4-12% Bis-Tris gel (Life Technologies) and transferred to a nitrocellulose membrane by semi-dry transfer, as previously described[55]. The membrane was blocked in TBS (pH 7.4) with 1% BSA for 1 hour. Membranes were incubated overnight at 4°C with primary Ab (total GluR1 [Millipore, #04-855, 1:1000], phosphorylated GluR1-Ser^{831} [Millipore, #04-823, 1:500], total PSD-95 [Thermo Fisher, MA1-046, 1:500], phosphorylated stargazin-Ser239/240 [Millipore, AB3713, 1:500], β-actin [Sigma, #A1978, 1:2000]) in TBS with Tween (TBS-T, 0.1% Tween-20, pH 7.4) and 0.25% BSA. To detect protein bands, the membranes were labeled with a corresponding secondary Ab (Donkey anti-Rabbit Alexa Fluor 488 or Goat anti-Mouse Alexa Fluor 647, Life Technologies). Fluorescence was detected using a CRi Maestro 2 Imaging System (Perkin Elmer). The bands were quantified using ImageJ software. Average fluorescence was quantified from, at minimum, 4 lysates per exposure group (8 slices per lane, 32 slices in total). All cultures were exposed to blast injury and received either 1nM roflumilast or DMSO vehicle at 6 hours post-injury. At 24 hours post-injury, cultures were exposed to aCSF containing 200uM glycine (LTP induction) or DMSO vehicle (No LTP induction) prior to cell lysis. The effects of drug-treatment and chemLTP treatment were analyzed by two-way ANOVA with statistical significance set as $p < 0.05$.

5.3 Results

5.3.1 PDE4 inhibitors prevented LTP deficits after blast

Our group previously observed that 1µM roflumilast delivered immediately post-blast prevented LTP deficits measured 24 hours following injury[56]. When delivered immediately

following blast exposure, roflumilast (concentrations ≥ 1nM) was efficacious in preventing blast-induced LTP deficits 24 hours post-injury (Figure 23), as compared to blast-injured cultures treated with vehicle or 100pM roflumilast. Alternative PDE4 inhibitors, ibudilast and piclamilast, were similarly effective in preventing blast-induced LTP deficits.

PDE4 enzymes are present in abundance across the hippocampus, including dendrites of CA1 neurons, and have been attributed with maintaining basal levels of cAMP[283-285]. This contrasts with PDE10A which also inhibits degradation of cAMP; however, basal expression of PDE10A within the hippocampus is limited to cell bodies, with no discernable expression in the dendritic or axonal processes[286]. We observed that treatment with the PDE10A inhibitor papaverine immediately following blast did not prevent LTP deficits measured 24 hours post-injury.

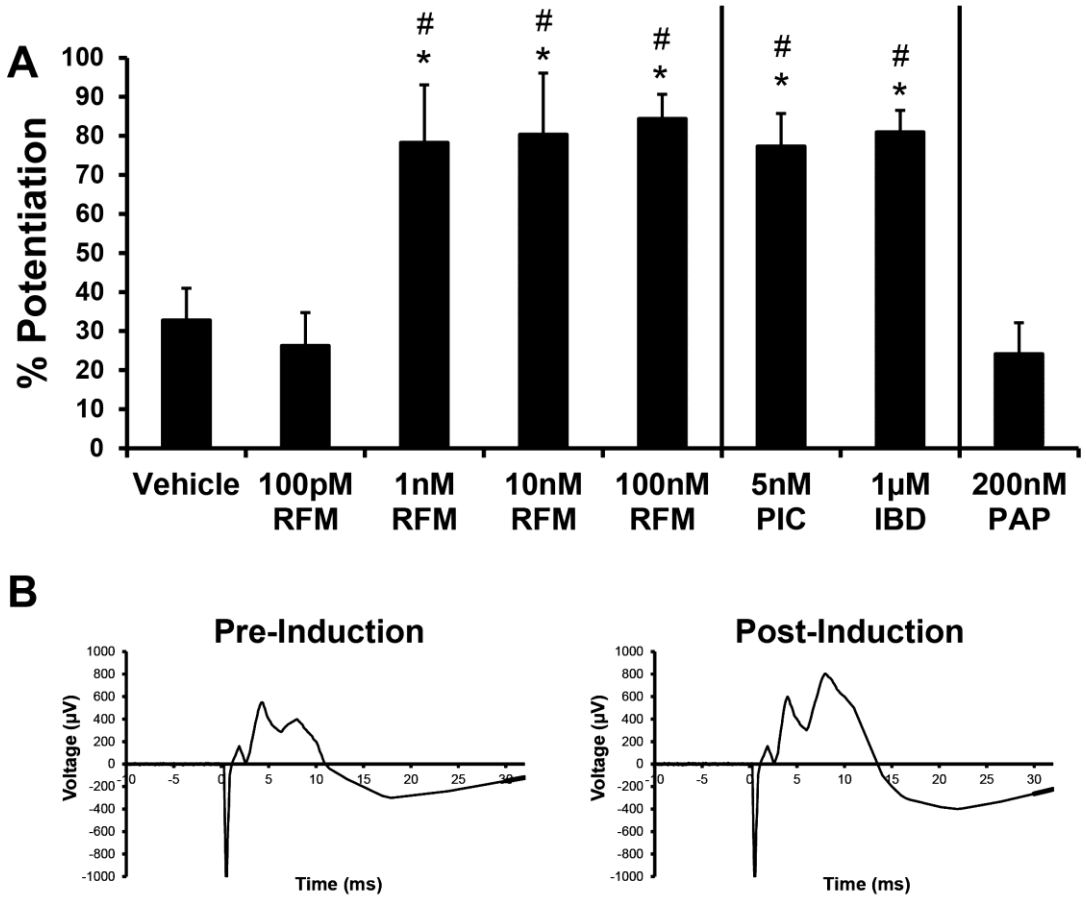

Figure 23 Effect of PDE inhibitors on LTP measured 24 hours following primary blast injury. (A) Cultures were treated with either DMSO (vehicle), roflumilast (RFM), piclamilast (PIC), ibudilast (IBD), or papaverine (PAP) immediately following blast exposure. LTP was significantly increased in cultures that received roflumilast (1nM or greater), piclamilast, or ibudilast compared to those receiving vehicle. LTP in cultures that received 100pM roflumilast or papaverine was not significantly different from those receiving vehicle. Potentiation was evaluated 60 minutes following HFS. (B) Examples of field potentials from a single electrode channel prior to and following LTP induction in a slice culture exposed to blast and subsequently treated with 1nM RFM. (mean ± S.E.M.; n≥6; * $p<0.05$, as compared to blast + vehicle, # $p<0.05$, as compared to blast + 100pM RFM)

5.3.2 Delayed roflumilast treatment prevented LTP deficits after blast

We varied the time of roflumilast delivery, using the minimum therapeutic roflumilast concentration (1nM), to determine the duration of the therapeutic window. Roflumilast delivered at 1 and 6 hours post-injury prevented LTP deficits 24 hours following blast exposure (Figure 24). In contrast, roflumilast delivered 23 hours post-injury did not prevent LTP deficits measured 1 hour later. To verify that inefficacy of 23h delayed drug delivery was not due to minimal exposure time, we delivered the drug 23 hours post-injury in a separate set of cultures and observed an LTP deficit when recording after an additional 24 hours (47 hours post-injury).

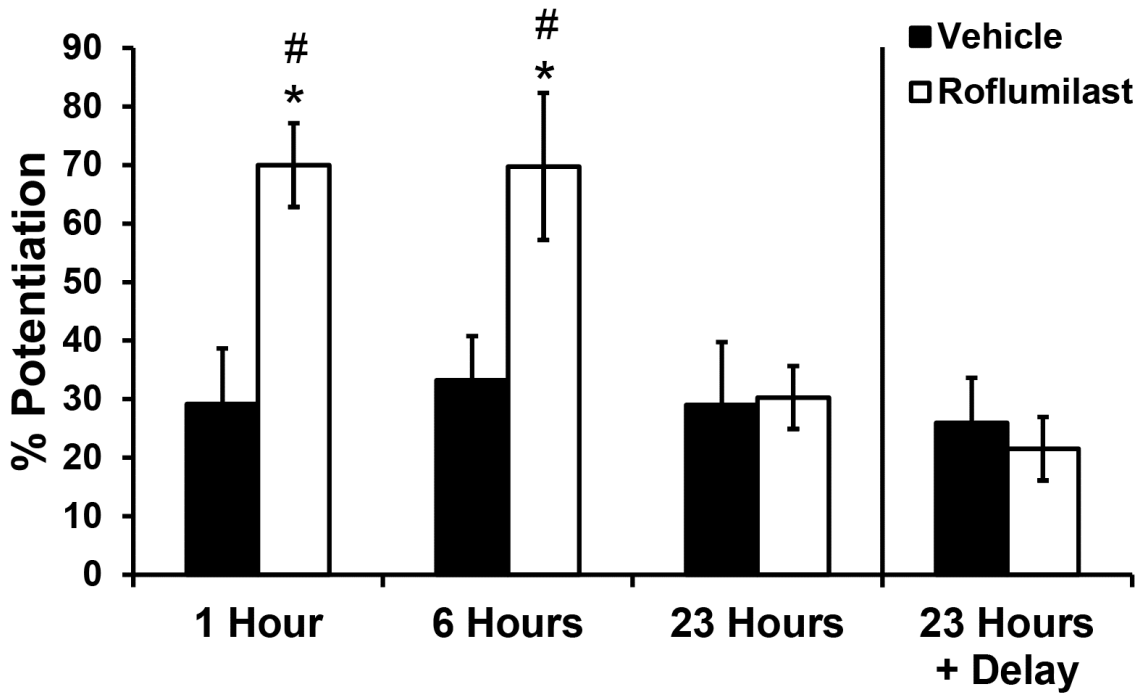

Figure 24 Effect of roflumilast delivery time on LTP measured after primary blast injury. Cultures were treated with either DMSO (vehicle) or 1nM roflumilast at increasing times post-blast exposure (1, 6 or 23 hours). LTP was significantly increased in cultures that received roflumilast at 1 or 6 hours post-blast, as compared to time-matched vehicle treatment. Cultures that received vehicle or roflumilast at 23 hours post-blast were unable to potentiate significantly. When cultures were treated with vehicle or roflumilast at 23 hours post-injury and LTP was evaluated after an additional 24 hours (47 hours post-blast), potentiation was not increased by treatment. Potentiation was evaluated 60 minutes following HFS. (mean ± S.E.M.; n≥6; * $p<0.05$, as compared to time-matched blast + vehicle, # $p<0.05$, as compared to blast + roflumilast delivered at 23 hours)

5.3.3 Roflumilast treatment prevented deficits in glycine-induced LTP after blast

We previously reported that primary blast exposure significantly reduced glycine-induced LTP[56]. The gly-aCSF activates synaptic NMDA receptors, allowing Ca^{2+} ions to enter the dendritic spine, similar to electrically-induced LTP[257]. Roflumilast (1nM) delivered 6 hours post-blast exposure significantly enhanced glycine-induced potentiation 24 hours post-blast, as compared to vehicle (Figure 25). We had previously reported that blast exposure significantly reduced glycine-induced potentiation 24 hours post-blast, as compared to a sham exposure, which was confirmed in the current study[56].

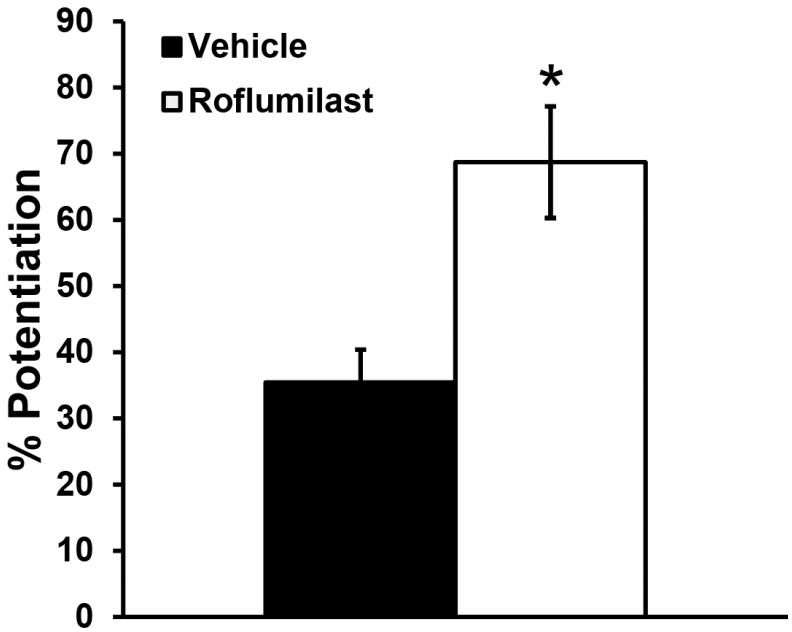

Figure 25 Roflumilast treatment significantly increased glycine-induced LTP 24 hours following blast exposure. LTP was significantly increased in injured, roflumilast-treated (1nM delivered 6 hours post-injury) cultures when induced by gly-aCSF at 24 hours following injury, as compared to injured, vehicle-treated cultures also induced by gly-aCSF. Potentiation was evaluated 60 minutes following end of chemical LTP induction protocol. (mean ± S.E.M.; n≥7, * $p<0.05$, as compared to blast + vehicle)

5.3.4 Roflumilast treatment prevented deficits in spontaneous activity after blast

Blast exposure significantly decreased spontaneous event rate across all ROI for vehicle-treated cultures as compared to vehicle-treated sham cultures (Figure 26). Roflumilast (1nM) delivered 6 hours post-blast, prevented the decrease in spontaneous event rate across all ROI at 24 hours, as compared to vehicle treated cultures. There was no effect of blast or drug exposure on spontaneous event magnitude for any ROI. Roflumilast significantly reduced event duration in all ROI, as compared to sham + vehicle, and in CA1 and CA3, as compared to blast + vehicle. Roflumilast also rescued blast-induced deficits in GSI.

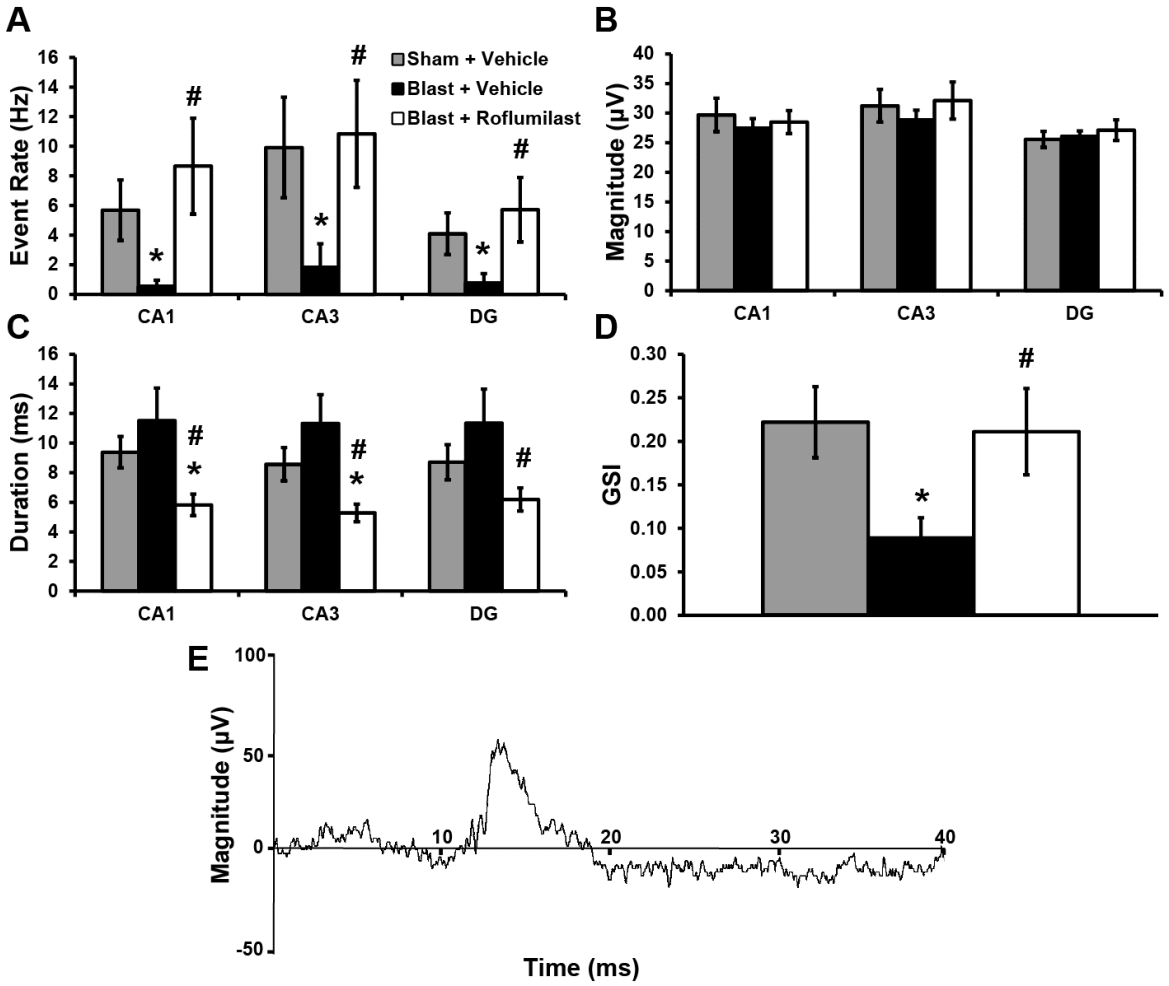

Figure 26 Roflumilast treatment affected spontaneous activity measured 24 hours following blast exposure. (A) Event rate (Hz) was significantly depressed across all regions for injured, vehicle-treated (6 hours) cultures, as compared to sham + vehicle treatment. Roflumilast (1nM) treatment 6 hours following blast significantly increased event rate, as compared to injured, vehicle-treated cultures, returning it to sham levels. (B) Event magnitude (µV) was unaffected by either blast exposure or roflumilast treatment. (C) Blast exposure did not significantly affect event duration (ms); however, roflumilast exposure 6 hours following blast significantly depressed event duration, as compared to vehicle-treated sham or blast cultures in CA1 and CA3 regions (only was significantly depressed in DG for blast + vehicle). (D) GSI was significantly depressed for injured, vehicle-treated cultures, as compared to sham + vehicle treated slices; however, roflumilast treatment following blast injury significantly increased GSI, as compared to injured, vehicle-treated cultures, returning it to sham levels. (E) An example of an identified spontaneous field event. (mean ± S.E.M.; n≥7, * $p<0.05$, as compared to sham + vehicle; # $p<0.05$, as compared to blast + vehicle)

5.3.5 Roflumilast treatment did not affect basal evoked function or cell variability

We previously reported that blast exposure had minimal effect on basal evoked function, measured through SR[55, 56]. We observed no significant effect of blast exposure or roflumilast delivery in any ROI on SR parameters 24 hours post-injury (data not shown). We observed no significant effect of blast exposure or roflumilast in any ROI on cell viability; exposure of cultures to excitotoxic concentrations of glutamate verified the presence of viable cells after blast (data not shown).

5.3.6 After blast, roflumilast preserved protein transduction pathways necessary for LTP induction

Phosphorylation of GluR1-Ser831 has been shown to be a key molecular step for induction of LTP[277]. We previously reported that blast exposure significantly reduced phosphorylation of GluR1-Ser831 and expression of total GluR1 after glycine-exposure 24 hours post-blast[56]. We found in this study that after blast exposure and LTP-induction, increased phosphorylation of GluR1-Ser831 was eliminated (Figure 27A). However, post-injury treatment with roflumilast restored GluR1-Ser831 phosphorylation after LTP induction. In the absence of LTP induction, roflumilast did not affect levels of phosphorylation for GluR1-Ser831.

Blast exposure eliminated the increase of total GluR1 expression normally observed after LTP induction[56]. However, post-injury treatment with roflumilast increased total GluR1 expression after LTP induction (Figure 27B). In the absence of LTP induction, roflumilast did not affect total expression of GluR1.

Our group has previously observed that primary blast exposure significantly reduced expression of PSD-95 and phosphorylation of stargazin at the Ser239/240 site 24 hours post-injury[56]. In this study, roflumilast significantly increased total expression of PSD-95 regardless of LTP induction (Figure 27C). PSD-95 expression after LTP induction was the same for either vehicle-treated or roflumilast-treated cultures. LTP induction was previously shown to not affect total PSD-95 expression[287]. Post-blast, phosphorylation of stargazin-Ser239/240 was not increased after LTP induction (Figure 27D). However, post-injury treatment with roflumilast restored stargazin-Ser239/240 phosphorylation after LTP induction. In the absence of LTP induction, roflumilast did not affect levels of phosphorylation for GluR1-Ser831.

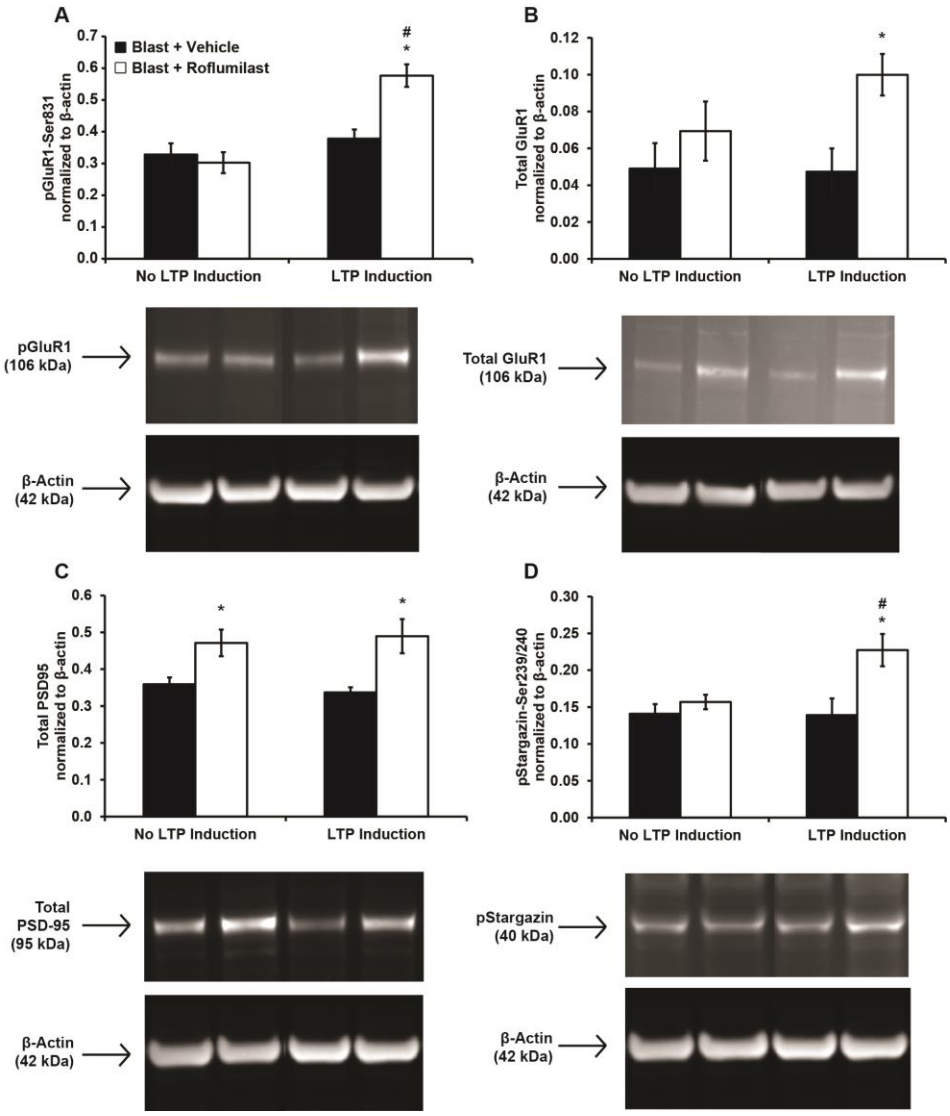

Figure 27 Roflumilast treatment 6 hours following blast injury altered protein expression measured 24 hours post-injury. Protein expression (normalized to loading control β-actin) was evaluated at 24 hours following blast for four protein targets critical to LTP: pGluR1-Ser831 (A), total GluR1 (B), total PSD-95 (C), and pStargazin-Ser239/240 (D). Cultures were exposed to blast and treated with either DMSO (vehicle) or 1nM roflumilast 6 hours following injury. At 24 hours post-injury, cultured were treated with either aCSF + DMSO (No LTP Induction) or aCSF + 200μM glycine (LTP induction) prior to cell lysis. Roflumilast treatment significantly increased pGluR1-Ser831, total GluR1, total PSD-95, and pStargazin-Ser239/240 when LTP was induced, as compared to injured, vehicle-treated cultures. Roflumilast treatment significantly increased total PSD-95 when LTP was not induced, as compared to injured, vehicle-treated cultures. LTP induction significantly increased pGluR1-Ser831and pStargazin-Ser239/240 in injured, roflumilast-treated cultures. Representative bands from each group are shown below the graphs, along with the size of the identified protein. (mean ± S.E.M.; n≥4, * $p<0.05$, as compared to LTP-matched vehicle treatment, # $p<0.05$ as compared to treatment-matched, non-LTP induction)

5.4 Discussion

We previously reported that a PDE4 inhibitor, roflumilast at high concentration, prevented neuronal dysfunction after primary blast exposure[56], and herein, we report molecular mechanisms by which PDE4 inhibitors may be preserving LTP induction. We observed that roflumilast (1nM) increased LTP when treatment was delayed by up to 6 hours post-injury but was not effective when delivered 23 hours post-injury. We also observed that roflumilast increased protein expression and phosphorylation caused by LTP induction that was previously lost when slices were exposed to blast[56]. Roflumilast restored the increase in pGluR1-Ser831, expression of total GluR1, and pStargazin-Ser239/240 upon LTP induction 24 hours following blast exposure. Additionally, roflumilast increased PSD-95 expression, regardless of LTP induction, at 24 hours following blast exposure. These observations suggest that modulation of the cAMP pathway through inhibition of PDE4 can prevent primary blast-induced alterations in LTP-induction.

Investigation of blast-induced alteration of cAMP has been limited. One study observed that 3',5'-cAMP did not significantly change in pre-frontal cortex using one rodent mild blast injury model[29]. Conversely, FPI studies observed hippocampal cAMP levels decreased between 15 minutes and 24 hours following injury[130, 144, 288]. Increased hippocampal PDE4 expression was observed between 1 and 24 hours following FPI in rats[289]. Studies using PDE4 inhibitors have demonstrated that a cAMP-dependent mechanism is a part of the pathogenesis of TBI and modulation of this pathway can prevent electrophysiological deficits measured *in vitro* and cognitive deficits measured *in vivo* after blast[147, 290].

Previous work showed PDE4 inhibitors could enhance hippocampal-dependent memory and LTP in animals[149, 291, 292]. The current study observed that roflumilast concentrations of at least 1nM prevented LTP deficits post-blast (Figure 23). Alternative PDE4 inhibitors (piclamilast, ibudilast) similarly preserved LTP induction. Although no other study has investigated the therapeutic potential of PDE4 inhibition after blast, several studies have observed that PDE4 inhibition preserved LTP measured 2 weeks and 12 weeks following FPI in rats[147, 293]. The effectiveness of either ibudilast or piclamilast following TBI is unknown; however, ibudilast prevented LTP-deficits in cortical cell cultures after microglia activation [294]. Similar findings across biomechanically distinct models provide greater confidence in the therapeutic potential of PDE4 inhibition following injury[49, 237, 238]. Conversely, we found that the PDE10A inhibitor papaverine was unable to rescue LTP after blast injury. A previous study observed that PDE10A expression decreased at 1 hour post-FPI in rats, whereas PDE4 expression increased[289]. It is possible that this change in expression leads to the observed deficits in in CA1 synaptic plasticity[292]. The contrasting abilities of PDE4 and PDE10A inhibitors to prevent blast-induced deficits in hippocampal LTP suggests that there may be an important subcellular effect and regulation of recovery following blast.

Previous studies found that PDE4 inhibition at 2 weeks[147] and 3 months[293] post-FPI improved both LTP *in vitro* and cognition *in vivo*. This contrasts with our observation that delayed PDE4 inhibition (23 hours post-injury) did not prevent blast-induced LTP deficits. One possible explanation is that our study delivered the PDE4 inhibitor at acute time points following injury, whereas the aforementioned non-blast studies delivered PDE4 inhibitors at sub-acute time points after injury and during LTP induction with electrical stimulation. Our findings showing efficacy with a 6 hour delayed treatment exceed the current target for an extended therapeutic

window within clinical trials (3 hours post-TBI)[295]. PDE4 inhibition may provide an extended delivery window making it an exciting prospect.

PDE4 inhibition by roflumilast reversed negative effects of blast on network synchronization and spontaneous event rate measured 24 hours following injury (Figure 26). In cortical neurons, PDE4 inhibition increased spontaneous spike-rate[296]. Increasing cAMP concentration increased spontaneous spike rate in the hippocampus, but decreased burst duration[297]. Niedringhaus and colleagues suggested collective network activity contracted and reorganized into shorter episodes following PKA activation, which could explain the observed changes in event rate and duration in our study. We observed that blast did not alter spontaneous event duration, but roflumilast treatment decreased duration. More research is needed to confirm if the protective effect of PDE4 inhibition on spontaneous neural function following TBI will translate to animal studies.

We observed that measures of basal evoked function were unaffected by PDE4 inhibition. Several studies observed that TBI-induced deficits in hippocampal input/output (I/O) curves were improved following PDE4 inhibition in rats, with no effect on paired pulse facilitation (PPF)[147]. There was no observable effect on I/O curves or PPF in *PDE4D* genetic KO mice[292]. These data suggest that PDE4 inhibition can repair deficits in synaptic plasticity without negatively affecting basal evoked function.

We observed that roflumilast significantly increased glycine-induced LTP measured 24 hours following blast exposure (Figure 4). PDE4 inhibitors' effect on chemical LTP is unclear. One study observed that *in vivo* blast injury decreased chemical LTP (via rolipram/forskolin) in hippocampal slices measured 2 weeks following injury[24]. Our group previously found that

rolipram/forskolin-induced LTP was not decreased by blast at 24 hours following *in vitro* primary blast[56]. The varied responses may be due to several differences between these studies, in terms of injury model, blast injury mechanics, and observation time post-injury.

This study is the first to report that PDE4 inhibitors prevented changes in protein expression after primary blast. Roflumilast treatment significantly increased phosphorylation of GluR1-Ser831 when LTP was induced, as compared to injured, vehicle-treated cultures. Several studies show that increasing cAMP concentration promotes AMPA receptor function, both directly and indirectly[140, 298]. We observed that when LTP was induced after injury, roflumilast treatment significantly increased expression of total GluR1 subunits compared to vehicle-treated cultures. However, this finding contrasts with another study in which rolipram did not increase total GluR1 expression in rat hippocampal neuronal cultures[299]. More studies are needed to understand the influence of PDE4 inhibitors on AMPARs following injury.

The proteins PSD-95 and stargazin are critical for anchoring AMPARs at the postsynaptic membrane during LTP[269, 270]. Here we observed that roflumilast treatment significantly increased expression of total PSD-95 after injury regardless of LTP induction. Forskolin activation of the cAMP pathway was found to prevent NMDA-induced loss of PSD-95, implicating cAMP in the regulation of PSD-95[270]. We also observed that roflumilast significantly increased pStargazin-Ser239/240 after injury when LTP was induced. Although the effect of PDE4 inhibitors on stargazin phosphorylation has not been studied previously, ghrelin, an activator of both PKA and protein kinase C (PKC), increased pStargazin-Ser239/240[300]. It is important to note that the Ser239/240 site is phosphorylated by PKC, but there is evidence of crosstalk between the PKA and PKC pathways[301, 302]. Our working hypothesis for blast-induced

LTP deficits is that degradation of PSD-95 led to a reduced ability of GluR1-containing AMPARs to immobilize at the PSD, which prevented phosphorylation of GluR1-Ser831 and thus reduced potentiation (Figure 22). It is possible that PDE4 inhibition restored LTP induction by preventing blast-induced PSD-95 degradation, which enables immobilization and phosphorylation of GluR1-containing AMPARs at the PSD and, ultimately, increased potentiation (Figure 28).

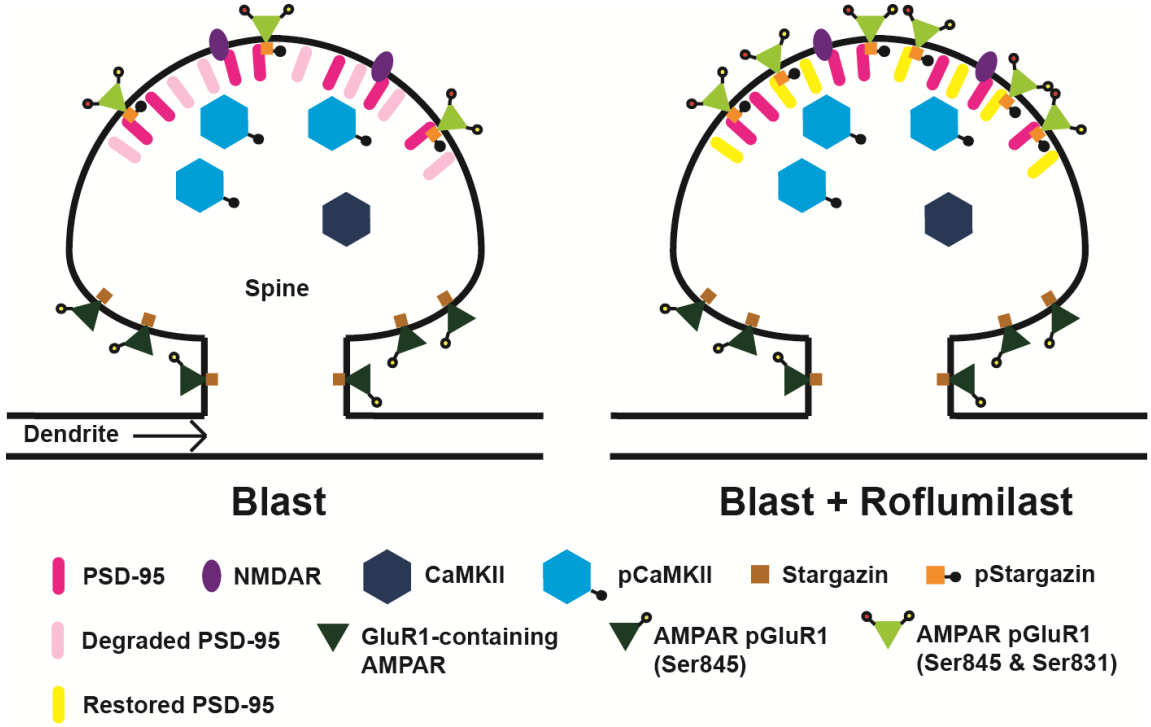

Figure 28 Hypothesized mechanism for the prevention of primary blast-induced long-term potentiation (LTP) deficits via phosphodiesterase-4 (PDE4) inhibition. On the left is a dendritic spine exposed to blast, and on the right, is a dendritic spine that has been treated with roflumilast after blast. Our findings suggest that primary blast exposure reduces expression of postsynaptic density protein-95 (PSD-95), which in turn prevents immobilization and phosphorylation of glutamate receptor-1 (GluR1)-containing α-amino-3-hydroxy-5-methyl-4-isoxazolepropionic acid receptors (AMPARs) at the PSD, a necessary step for potentiation. We hypothesize that PDE4 inhibition maintains expression of PSD-95 (by a mechanism to be determined), which then allows for the downstream immobilization and phosphorylation of GluR1 subunits necessary for LTP induction.

Although we report that PDE4 inhibition following primary blast injury preserves LTP, there are some limitations associated with this study. The use of an *in vitro* culture model prevents direct comparisons between electrophysiology and cognitive function observed *in vivo*[24, 73]. A benefit of our injury model is that it provides precise control over the injury biomechanics, which is difficult to achieve with *in vivo* injury models. Another limitation of this study is the induction of LTP via glycine exposure in cultures lysed for western blotting. This study required that chemical induction be employed due to the number of slices needed for western blotting. Glycine-induced LTP generated hallmark signs of electrically-induced LTP, including increased electrical response, phosphorylation of AMPA-GluR1 subunits, and activation of CaMKII[257]. Another limitation of this study is that we did not evaluate total stargazin expression. As phosphorylation of stargazin is necessary to bind AMPARs to PSD-95 at the postsynaptic density, we viewed phosphorylated stargazin as a surrogate for AMPAR translocation, which was the mechanism we wished to investigate. As such, we felt that total stargazin levels were not critical to the mechanism for blast-induced LTP dysfunction and chose not to include total stargazin. Another potential limitation of this study is the use of a pan-PDE4 inhibitor, like roflumilast, over a subtype-specific inhibitor. Pan-PDE4 inhibitors can induce emetic effects in patients, limiting their clinical effectiveness[293]; however, a recent study observed that non-emetic doses of roflumilast improved memory in rodents[156]. In that study, free brain concentrations of roflumilast were estimated to be 10.37nM, which is greater than our lowest effective concentration tested (1nM). Time scaling between slice cultures and humans may also be a necessary consideration moving forward[243].

In summary, we report that PDE4 inhibitors preserved LTP induction in the hippocampus after primary blast. We found the minimal therapeutic concentration of roflumilast was 1nM and

the therapeutic window was at least 6 hours, but less than 23 hours. Roflumilast treatment post-blast increased phosphorylation or expression of proteins critical for LTP induction including AMPAR-GluR1 (total and pGluR1-Ser831), and pStargazin-Ser239/240 when LTP was induced. Regardless of LTP induction, roflumilast treatment post-blast increased total PSD-95 expression. Future studies will investigate the potential of PDE4 inhibitors to prevent cognitive deficits after *in vivo* blast injury.

6 Summary and discussion

6.1 *In vitro* primary blast exposure delivered a low-strain, high-strain rate deformation to hippocampal slice cultures

In this thesis work, we utilized a shock tube and a custom-built sample receiver to expose OHSCs to isolated primary blast. Our shock tube produced a characteristic Friedlander waveform, measured at the shock tube exit[303]. The blast intensities utilized in this thesis work were similar to typical blast exposure conditions experienced in theater, ranging from a small mortar round for Level 1 blast (M49A4 60 mm mortar, standoff distance 0.25-2 m) to a large bomb for Level 4 blast (M118 bomb, standoff distance 10-32 m), according to ConWEP analysis. The *in vitro* receiver performed several necessary functions in this injury model: a surrogate for the surrounding skull-brain complex, translation of the shock wave into a fluid pressure transient that mimicked the intracranial pressure transient, immobilization of the sample to prevent inertial-driven deformation, and prevention of internal wave reflections[49, 50]. The pressure profile measured at the level of the tissue resembled those predicted by computational models and measured in mice intracranially during blast exposure *in vivo*[17, 49, 50, 304]. This model enabled precise control over the injury biomechanics, a feat that is difficult to achieve with *in vivo* blast injury models[49, 50].

In Chapter 2, we characterized the range of strain and strain rate profiles induced by our injury model using a stereoscopic high-speed camera system and DIC software. Finite element simulations of a human head under shock wave loading predicted that brain tissue experienced low maximal principal strain (5-10%) and high strain rates (100-1000 s^{-1})[17]. Computational

modeling of our *in vitro* receiver under shock loading similarly predicted that tissue experienced low-strain (< 5%) and high-strain rate (80 s^{-1}) deformation[49]. This type of loading is biomechanically distinct from blunt impact deformation profiles, which typically consist of higher maximum principal strains (>10%) at lower strain rates (<50 s^{-1})[95, 220].

Our experiments that measured tissue strain during blast validated our computational model of the injury. As blast exposure increased in severity, statistically significant strain magnitudes were induced in OHSCs; however, the strain magnitudes remained relatively low (<9%). Blast exposure induced statistically significant strain rates in OHSCs ranging from 25-86s^{-1}. It is important to note that we observed these maximum values after the pressure pulse had passed the sample (>5ms), suggesting potential influence of bulk fluid motion. We observed that both strain magnitude and rate strongly correlated with certain blast parameters, specifically in-air impulse and in-fluid peak pressure. When comparing blast-induced LTP deficits from Chapter 3 to observed strain magnitudes and rates at the same intensities, we observed a strain threshold for LTP deficits between 3.7-6.7% and a rate threshold for LTP deficits between 25-33s^{-1}. This finding suggested that even at high-rate loading, the strain threshold for functional deficits may be aligned with the threshold for electrophysiological dysfunction identified in non-blast TBI studies (5-10%)[97, 194, 204, 210]. Kang and colleagues previously reported that hippocampal electrophysiological function has a complex dependence on both strain magnitude and rate[88]. Another non-blast TBI study found that in cultured hippocampal neurons stretched at low strain magnitudes, intracellular [Ca^{2+}] increased in a rate-dependent fashion[194]. Our findings in Chapter 2 place our *in vitro* blast exposure data into biomechanical perspective with non-blast TBI studies.

There is much debate over the role of primary blast in the bTBI cascade. Some evidence has shown that functional changes following blast injury are wholly due to inertia effects[24]; however, many other studies have demonstrated that primary blast exposure in isolation initiates distinct effects[52, 53, 55, 74, 173, 305, 306]. One study investigated the neurocognitive deficits in U.S. Army Special Operations Command personnel with diagnosed blunt, blast, and blast-blunt mTBIs[273]. Kontos and colleagues found that patients with combination blast-blunt mTBIs exhibited significantly different residual symptoms (mTBI symptoms, PTSD symptoms, verbal memory, visual memory, visual processing speed, reaction time) versus blunt-only. This finding would suggest that primary blast exposure leads to separate and distinct consequences compared to blunt or inertia-driven TBI. Multiple *in vivo* studies observed that blast overpressure and rotational injury induce distinct patterns of cognitive deficits in rats[74, 175]. From a biomechanical perspective, our results suggest these observed differences between primary and tertiary blast outcomes may be a result of different strain profiles induced by each phase. A complete understanding of the biomechanics and pathobiology associated with the phases of blast exposure is necessary for designing protective helmet equipment and potential therapeutics.

6.2 *In vitro* primary blast exposure induced hippocampal electrophysiological dysfunction

6.2.1 LTP is more sensitive to primary blast than other electrophysiological parameters measured

Our blast injury model enabled extensive investigation into the effects of shock wave exposure on OHSC neurological function. We exposed OHSCs to a range of blast intensities and

measured functional outcomes in an effort to identify tolerance criteria for blast-induced functional change. In Chapter 3, we identified a threshold for primary blast-induced LTP deficits between Level 1 and Level 2 blast (Table 2), when measured 4-6 days following injury[55]. In previous studies with this injury model, we found that impulse, rather than peak pressure or duration, best predicted the significant, but minimal, cell death observed after primary blast exposure[53]. Impulse was similarly correlative to induced strain magnitudes and rates, as presented in Chapter 2. Hue and colleagues also found that primary blast-induced BBB disruption most correlated with the impulse parameter[52]. The shock wave parameters peak pressure and duration, along with the shape of the pressure history, define the impulse. In this study, LTP deficits best correlated with increasing blast impulse levels.

We found that LTP, induced by HFS, exhibited greater vulnerability to primary blast than network synchronization, spontaneous function, and basal evoked function. When we did observe deficits in measures other than LTP, the threshold for dysfunction was between Level 2 and Level 4 blast, which was higher than the threshold observed for LTP. This was the first study to report that isolated primary blast exposure disrupted LTP in OHSCs. This study suggests that low-level exposure intensities are capable of disrupting neurological function. While scaling of to the test species is a common topic in blast injury research, it is important to note that, regardless of scaling, the blast intensities used in this study are akin to realistic blast exposures[53]. We observed functional deficits without significant loss of cells, which verified previous findings from our group[53].

Other studies have investigated blast-induced electrophysiological dysfunction since we completed this research. Within our own group, Effgen and colleagues found that repetitive *in*

vitro primary blast exposure (two blasts delivered 24 hours apart) reduced LTP measured 3 days following the second exposure[176]. Additionally, they did not observe any overt changes to SR function or cell death, which corroborated our studies in Chapter 3. Another study observed that *in vivo* blast exposure in mice with restricted head motion reduced hippocampal CA1 excitability and increased $GABA_A$ signaling (inhibitory tone)[74]. Although those findings differs slightly from ours, it is important to note that their injury model was not pure primary blast, as the animal's head undergoes accelerations of almost 3,500 m/s^2, even with restraint of the shoulders and snout. This study reported no blast-induced deficits in PPRs, which corroborated our findings.

6.2.2 Primary blast exposure induced delayed LTP deficits

In Chapter 4, we explored the time course of primary blast-induced LTP deficits. To test our hypothesis that functional changes would occur more rapidly than blast-induced changes in cell death (which occur around 4 days following injury[53]), we evaluated LTP at increasing time points (1 hour, 1 day, 2 days, 4 days, 6 days, 10 days) following either Level 4 or Level 9 blast. We found that neither blast intensity induced LTP deficits when measured 1 hour following injury; however, both exposures led to significant reductions in LTP by 24 hours following injury[56]. These deficits were maintained through 6 days post-injury and, by day 10, only the group exposed to Level 4 blast recovered significantly. This study verified the findings from Chapter 3 that LTP was depressed between 4-6 days post-blast. The findings of this study suggested that altered memory function from increased shock intensities required a longer duration to recover, or that shock loading may in fact induce chronic deficits. The

aforementioned repetitive blast study from Effgen and colleagues reported heightened vulnerability to Level 2 blast exposure when they extended the inter-blast interval to 3 days; however, they did not observe this result upon extending the interval to 6 days[176]. Although we observed in Chapter 5 that a single, but more intense (Level 4), blast reduced LTP measured 6 days following exposure, these studies agree that at least 6-10 days are required to recover from primary blast exposure. Several *in vivo* studies have reported blast-induced LTP deficits as far out as 14-30 days post-injury; however, it is important to consider the varied injury biomechanics across these studies[24, 81]. The surrounding tissue and vasculature could also influence recovery times observed *in vivo*. Studies from Hue and colleagues observed that primary blast exposure caused BBB dysfunction both *in vitro* and *in vivo*[40, 52]. Breakdown of the BBB enables extravasation of various serum constituents, normally blocked from the brain, which may influence neurological function and network connectivity post-injury[307]. It is important to note that we did not observe any significant changes in basal evoked function at any time point, which further suggested that LTP exhibited greater sensitivity to primary blast exposure than other electrophysiological measures we measured.

6.2.3 Primary blast exposure depressed chemically-induced LTP

In addition to HFS, chemical exposures can also induce LTP[257, 258]. In Chapter 4, we examined the effect of primary blast exposure on glycine-induced LTP. We observed that Level 4 blast exposure significantly reduced glycine-induced LTP when measured 24 hours following injury; however, measured 10 days post-injury, primary blast did not reduce glycine-induced LTP. This result matched our findings from the time course of blast-induced LTP deficits when inducing LTP via HFS. Glycine activates NMDARs and causes an influx of Ca^{2+} ions that

triggers LTP in a manner similar to HFS[80, 257]. Thus, it is intuitive that blast would affect both HFS-induced and glycine-induced LTP in a similar manner

An alternative chemical LTP induction protocol that exposed cultures to aCSF with rolipram, forskolin, and picrotoxin, That induce synaptic potentiation supra-physiologically via activation of the cAMP/PKA pathway[258]. In Chapter 4, we found that primary blast exposure did not affect cAMP-induced LTP measured 24 hours following injury, which contradicted the results from HFS-induced and glycine-induced LTP measured at the same time point post-blast. This result suggested that modulation of the cAMP/PKA pathway could prevent primary blast-induced deficits in LTP. Pharmacological induction of LTP provides a powerful research tool to antagonize different aspects of the complicated cellular pathways that govern LTP.

6.2.4 Translating electrophysiological outcomes to clinical observations

There is limited clinical data for primary blast-induced brain injury. One clinical study observed the effect of repetitive primary blast exposure on "breachers," a military population routinely exposed to low-level primary blast through detonations on locked doorways[308]. Breachers had reduced neurocognitive performance when tested following a 2-week training course. Most mild bTBI patients' symptoms resolved within a few hours or days; however, some patients developed post-concussive syndrome in the following days, which leads to chronic cognitive deficits[5]. Clinicians observed residual mTBI symptoms in soldiers exposed to blast, which increased a dose-response manner to multiple blast exposures; these symptoms included altered consciousness, headache, anxiety, impaired balance, dizziness, attention difficulties, and memory deficits[273, 309].

The clinical sequelae of mild bTBI mainly consist of subtle deficits in cognitive function[273, 310, 311]. Blast injury research with animal models has verified these subtle cognitive deficits using behavioral tasks post-injury, including the MWM and NOR[31, 74, 312]. Although it is speculative to directly compare electrophysiological deficits to altered cognition and behavior, the electrophysiological deficits following blast reported in Chapters 2 and 3 appear to align with the subtle cognitive deficits observed clinically and *in vivo*.

One area where mild bTBI diverges from non-blast mTBI is the observation of cognitive deficits with no cell loss or overt damage to cell structure following blast. In Chapters 2 and 3, we observed that blast induced subtle changes to electrophysiological function (LTP deficits, limited basal function deficits) without significant cell death. Studies have shown that mild blast is capable of inducing deficits in hippocampal-dependent memory tasks with no changes in cell viability or gross anatomical damage (i.e. hemorrhage, atrophy, scarring, etc.)[24, 25, 35, 75]. If observed, pathology associated with mild bTBI is similarly subtle, including diffuse axonal injury, microtubule disruption, and glial activation between 24 hours and 30 days post-injury[24, 35, 275, 313].

6.3 PDE4 inhibition restored electrophysiological function after primary blast exposure

Rolipram, a component of the protocol used in the chemical induction of LTP, is a PDE4 inhibitor that prevents degradation of cAMP. The PDE4 inhibitor class has shown an ability to restore LTP and cognition following non-blast TBI in rats[147, 293]. Rolipram has limited clinical

potential due to its emetic potential[153, 154]; however, an alternative PDE4 inhibitor, roflumilast, is FDA-approved for treatment of COPD. In Chapter 4, we observed that a super-therapeutic concentration of roflumilast (1μM), delivered immediately following Level 4 blast injury, restored LTP measured 24 hours post-injury.

In Chapter 5, we examined the dose response of roflumilast delivered immediately following Level 4 blast by evaluating LTP 24 hours post-injury. We found that 1nM roflumilast (or greater) significantly increased LTP after blast as compared to cultures treated with 100pM roflumilast or DMSO vehicle. Alternative PDE4 inhibitors, piclamilast and ibudilast, produced a similar effect; however, the PDE10A inhibitor papaverine did not restore LTP. It is important to note, within the hippocampus, CA1 dendrites heavily express PDE4, but not PDE10A (primarily found in cell bodies)[283-286]. One non-blast TBI study observed that injury increased expression of PDE4 subunits in the hippocampus, but decreased expression of PDE10A[289]. Thus, PDE4 inhibition following injury may restore the levels of PDE4 activity following injury, while PDE10A inhibition may exacerbate the inhibitory effect of TBI. Phosphodiesterase subtype specificity is an important consideration when investigating new therapeutic targets for TBI. It is possible the positive effect of PDE4 inhibitors is due to subcellular localization of PDE4 in dendrites and/or to the presence of elevated PDE4 expression following injury.

We also investigated the therapeutic delivery-window for roflumilast. In Chapter 5, we observed that roflumilast (1nM) delivered 6 hours or earlier following Level 4 blast could restore LTP measured 24 hours post-injury; however, roflumilast delivered 23 hours post-injury could not restore LTP measured 1 hour later. In a separate set of cultures, we delivered roflumilast 23 hours post-injury and evaluated LTP after an additional 24 hours of exposure time (48 hours

post-injury). We again observed no restoration of LTP, confirming the negative result was not due to the brief exposure-time. The observed therapeutic delivery window of 6 hours following TBI is promising as the current target for an extended therapeutic window within clinical trials is 3 hours post-injury[295]. When using the minimum therapeutic roflumilast concentration (1nM) and the maximum therapeutic delivery time (6 hours post-injury), we observed that roflumilast treatment restored glycine-induced LTP measured 24 hours following Level 4 blast.

In Chapter 5, we found that post-blast roflumilast delivery influenced not only LTP, but spontaneous function as well. We found that roflumilast treatment restored hippocampal synchronization following primary blast. It is possible that roflumilast restored LTP and synchronization through similar pathways, as studies have shown that synchronized neural activity is the basis for working memory[241, 242]. Roflumilast prevented the blast-induced decrease in spontaneous event rate measured 24 hours following injury. Although we reported in Chapters 3 and 5 that blast exposure did not reduce event duration, we observed that roflumilast significantly reduced event duration. Increased cAMP concentration were previously shown to significantly increase spontaneous spike rate and decrease burst duration in uninjured hippocampal neurons[297]. In contrast, we did not see any significant effect of primary blast or roflumilast treatment on spontaneous event magnitudes, SR curves or cell viability, which adds to the potential of roflumilast as a clinical target.

Although we investigated PDE4 inhibition post-injury only, there is evidence that prophylactic caffeine exposure ameliorated spatial reference memory impairment, working memory impairment, and astrogliosis measured 1 week following bTBI[314]. Caffeine is a non-specific PDE inhibitor, which supports our *in vitro* findings; however, the shock duration used in

this study was 51 ms, which is more representative of a nuclear explosion than an IED blast event[243]. This study was unclear on controlling head motion and thoracic protection, which, as previously discussed, can greatly influence the injury response[38, 40].

Other pharmacological interventions have gained recent attention for ameliorating blast-induced cognitive deficits such as N-acetylcysteine (NAC). Hoffer and colleagues administered NAC to blast-exposed soldiers within 24 hours following injury (and then for 7 consecutive days) in a Phase II clinical study that found NAC treatment improved executive function[315]. NAC serves as a prodrug to L-cysteine, which subsequently replenishes glutathione stores[316]. As a result, NAC can influence a number of downstream targets including c-Jun N-terminal kinase, p38 MAP kinase, NF-κB, and synaptic membrane receptors like NMDARs[316, 317]. It is possible that NAC could improve hippocampal-dependent memory following blast, as one study found that NAC restored LTP in aged mice to that observed in adult mice[317]. Thus, NAC may be worth investigating following *in vitro* primary blast exposure. The next goal of the thesis was to determine the cellular mechanisms that mediated primary blast-induced neuronal dysfunction and prevention of dysfunction with roflumilast.

6.4 Primary blast-induced disruption of synaptic proteins influenced neurological function

In Chapter 4, we utilized western blotting to measure protein expression 24 hours following Level 4 blast exposure. We previously showed that LTP exhibited greater sensitivity to primary blast than other electrophysiological measures we studied[55]. This finding led us to

investigate specific protein targets critical to the induction of LTP, namely AMPA-GluR1 (total, Ser831 phosphorylation, Ser845 phosphorylation), total NMDA-NR2B, CaMKII (total, Thr286 phosphorylation), total PSD-95, and stargazin-Ser239/240 phosphorylation. We quantified protein expression with and without the induction of LTP using glycine. The first group of protein targets investigated was transmembrane glutamate receptors (AMPAR and NMDAR). We found that Level 4 blast exposure prevented an increase in GluR1-Ser831 phosphorylation induced by gly-aCSF. The effect of blast on glycine-induced Ser831 phosphorylation corroborated the effect of blast on chemical LTP measured electrophysiologically as LTP induction is associated with increased Ser831 phosphorylation[276, 277]. Blast exposure significantly decreased the expression of total GluR1 subunits with exposure to gly-aCSF. One study observed no change in hippocampal GluR1 at 24 hours following a single blast *in vitro*, but found decreased hippocampal GluR1 at 24 hours following two blast exposures[174]. The previous study applied an extremely short duration (50μs) shock exposure to OHSCs, which may explain the difference with our findings.

An alternative GluR1 phosphorylation site, Ser845, controls insertion of GluR1-containing AMPARs into the synaptic membrane[298, 318]. We found that Level 4 blast did not influence Ser845 phosphorylation; however, gly-aCSF treatment significantly increased phosphorylation over vehicle treatment. The lack of blast effects on Ser845 phosphorylation suggested that blast exposure did not affect the mechanism controlling GluR1-containing AMPAR insertion into the synaptic membrane, although channel insertion was not directly measured. Lastly, we did not observe any effect of blast or chemical LTP induction on total NMDA-NR2B expression levels. We concluded that primary blast exposure influenced the AMPA-GluR1 subunit.

The next target we investigated in Chapter 4 was CaMKII, the protein kinase that, upon phosphorylation, initiates the biochemical cascade that ultimately phosphorylates the GluR1-Ser831 site and potentiates synaptic transmission[140, 259, 319, 320]. We found that chemical LTP induction significantly increased CaMKII-Thr286 phosphorylation, but blast exposure had no effect. We did not see any influence of blast or chemical LTP on total CaMKII expression. The lack of blast effects on CaMKII suggests that the mechanism to phosphorylate the GluR1-Ser831 site was intact after blast and that the disruption must be with another step in the complicated pathway, perhaps translocation of GluR1-containing AMPARs to the PSD.

The final targets we investigated in Chapter 4 addressed translocation of the GluR1 receptors to the PSD. The first target was PSD-95, a synaptic scaffolding protein that associates with both receptors and cytoskeletal elements at the PSD[321]. The second target was stargazin, a transmembrane protein associated with AMPARs that regulate their synaptic targeting by PSD-95[322]. Multiple studies have shown that the interactions between PSD-95 and phosphorylated stargazin protein govern the number of synaptic AMPARs[322, 323]. We observed that Level 4 blast exposure significantly reduced total PSD-95 expression for both vehicle and gly-aCSF treated cultures. A recent *in vivo* study found that blast exposure in mice did not affect cerebellar PSD-95 expression at 24 hours following blast, but did significantly reduce expression at 30 days following blast[324]. Blast exposure prevented the increase in pStargazin-Ser239/240 when treating cultures with gly-aCSF. Our hypothesis for a cellular mechanism that drives primary blast-induced LTP deficits is blast-induced disruption of PSD-95. Disruption of PSD-95 prevents immobilization of GluR1-containing AMPARs at the PSD and subsequently prevents GluR1-Ser831 phosphorylation.

As mentioned in Section 6.3, blast exposure had no effect on potentiation induced via activation of the cAMP/PKA pathway. We examined the effect of blast on protein expression after treatment with cAMP-aCSF. We found that primary blast did not affect GluR1-Ser831 phosphorylation, total GluR1 expression, or GluR1-Ser845 phosphorylation when treated with cAMP-aCSF. For all three targets, the group exposed to cAMP-aCSF exhibited significantly higher phosphorylation or expression than blasted cultures treated with either vehicle or gly-aCSF. Neither blast nor cAMP-aCSF affected total NMDA-NR2B expression. Although cAMP-aCSF significantly increased CaMKII-Thr286 phosphorylation over vehicle and gly-aCSF treatment, cAMP activation did not influence total CaMKII expression. There was no effect of blast on total PSD-95 expression for cAMP-aCSF treated cultures. Additionally, this group exhibited significantly higher expression than cultures receiving vehicle or gly-aCSF treatment following blast. Blast exposure had no effect on phosphorylated stargazin when treating cultures with cAMP-aCSF; however, this group exhibited significantly higher phosphorylation than cultures receiving vehicle or gly-aCSF following blast. These findings suggested that modulation of the cAMP/PKA pathway prevents changes to key proteins involved in LTP induction that blast exposure disrupted. The positive effect of PKA activation on protein expression/phosphorylation following blast could explain the restorative effect of roflumilast on LTP following blast, as one component of the cAMP-aCSF treatment (rolipram) is a PDE4 inhibitor.

6.5 PDE4 inhibition following primary blast exposure restored expression of key proteins for LTP induction

In Chapter 5, we explored the effect of delivering roflumilast after blast injury on the proteins exhibiting sensitivity to primary blast from Chapter 4 (pGluR1-Ser831, total GluR1, total PSD-95, and pStargazin-Ser239/240). We quantified protein expression or phosphorylation at 24 hours following blast exposure in OHSCs that received 1nM roflumilast or DMSO vehicle 6 hours post-injury. As in Chapter 4, we quantified protein expression with and without the induction of LTP using glycine. Roflumilast significantly increased GluR1-Ser831 phosphorylation and total GluR1 expression upon induction of LTP, as compared to vehicle. This finding explained the recovery in electrically- and glycine-induced LTP following blast exposure and subsequent roflumilast treatment observed in Chapter 5. Roflumilast significantly increased total PSD-95 expression, as compared to vehicle, regardless of LTP induction. Finally, we found that roflumilast increased stargazin-Ser239/240 phosphorylation upon induction of LTP, as compared to vehicle. These findings suggested that PDE4 inhibition restored LTP induction by preventing blast-induced PSD-95 degradation, which enables immobilization and phosphorylation of GluR1-containing AMPARs at the PSD and, ultimately, increased potentiation.

6.6 Potential cellular mechanisms for blast-induced PSD-95 disruption and cAMP-induced restoration

Although Chapters 4 and 5 demonstrated that synaptic protein disruption (specifically GluR1, PSD-95, and stargazin) is associated with LTP deficits following primary blast, we did not explore the mechanisms by which the proteins are degraded. We also did not explore the mechanisms by which roflumilast treatment restored protein expression/phosphorylation. The

following sections outline two pathways that may be involved in this process: 1) the ubiquitin-proteasome system (UPS) and 2) calpain-mediated degradation.

6.6.1 Blast-induced PSD-95 degradation by ubiquitin-proteasome system

Most proteins in the PSD are degraded via the UPS[325]. This pathway regulates synaptic strength, plasticity, and structure in mammals[326]. Previous research found involvement of the UPS in memory consolidation of a hippocampal-dependent learning task in rats[327]. In Chapter 4, we reported that PSD-95 was the only target investigated for which blast exposure reduced expression, regardless of LTP induction. The UPS is an important regulator of PSD-95; the protein is first ubiquitinated, or "tagged", for degradation by the E3 ligase Mdm2 and subsequently degraded by the 26S proteasome[270]. This process causes a resultant reduction in AMPAR surface expression due to reduced interactions with PSD-95. A possible theory for blast-induced degradation of PSD-95 is that blast exposure activates the UPS. Studies found that primary and combined primary-tertiary blast exposure increased levels of ubiquitin-C-terminal hydrolase-L1 (UCH-L1), a marker of UPS activation, in both human[308, 328] and rat[19, 313] serum and cerebral spinal fluid (CSF) as early as 24 hours and as late as 48 hours post-injury. Non-blast TBI studies have similarly identified increased levels of UCH-L1 as a potential injury biomarker[329-334].

If UPS activation were the injury mechanism following primary blast, one possible therapeutic mechanism of PDE4 inhibition could be the prevention of ubiquitination of PSD-95 prior to digestion. One study found that PKA activation inhibited ubiquitination of the protein β-catenin through phosphorylation of β-catenin[335]. Increased PKA activation, via treatment with forskolin/rolipram, increased phosphorylation of PSD-95 at the serine-295 site[287]. It is possible

that PDE4 inhibition blocks the mechanism that tags PSD-95 for digestion by inducing phosphorylation of PSD-95.

It is also possible that blast exposure prevents phosphorylation of PSD-95 by increasing the protein phosphatase calcineurin (CaN). Calcineurin is co-localized with PKA on A-kinase associated proteins (AKAPs) at the PSD and, when activated, CaN reduces the open probability of GluR1-containing AMPARs[336, 337]. Under basal activity, AKAP79/150 anchors both PKA and CaN; while PKA is partially active, CaN is normally inhibited[336, 338, 339]. When the ratio of active PKA:CaN shifts, such as during LTD induction, the resultant dephosphorylation of PKA substrates leads to relocalization of AKAP-PKA complexes away from the PSD in a process that is driven by actin depolymerization[277, 340, 341]. It is possible that this ratio shifts following TBI as studies have shown that TBI increased CaN in CA1 dendrites as early as 2 hours and as long as 4 weeks following injury, and TBI decreased PKA in the same time frame[130, 342, 343]. Increased PKA activity antagonized the inhibitory effects of CaN on excitatory postsynaptic current amplitude in rat hippocampal cultures[344]. Enhancing activated PKA to outcompete CaN could explain another possible therapeutic mechanism for PDE4 inhibition following primary blast. Activated PKA would prevent degradation of AKAP-PKA complexes and enable greater phosphorylation of PSD-95, thus preventing ubiquitination. We could test this hypothesis by applying an inhibitor of CaN following blast exposure, such as the FDA-approved FK506 compound.

An alternative therapeutic mechanism for PDE4 inhibition following primary blast could be preventing the digestion of PSD-95 by the 26S proteasome. The UPS degrades ubiquitinated proteins via the 26S proteasome. Although there is limited research on the 26S proteasome

following TBI, one study did find that blast injury in humans reduced gene expression for proteasome inhibitor subunit 1, which suggested that proteasome activity increased following injury[345]. Proteasome inhibition, in combination with dexamethasone treatment, prevented proteasomal degradation of the glucocorticoid receptor following TBI[346]. However, it is unlikely that PDE4 inhibition ameliorates any increase in proteasomal degradation, as elevated cAMP concentrations increased 26S proteasome activity in a PKA-dependent manner in rat spinal cord neurons[347]. Although PDE4 inhibition may not address this mechanism, therapeutics targeting proteasomal dysfunction after TBI may also be efficacious and perhaps even additive to PDE4 inhibition.

6.6.2 Calpain-mediated PSD-95 degradation following blast

The calpain protease mediates a second mechanism that degrades cytoskeletal proteins within the PSD. Calpains are calcium-dependent proteases known to be critical to LTP induction. The calpain-1 isoform is located in dendrites, soma, axons, and glia, where the calpain-2 isoform is located only in axons[348]. Cytoskeletal proteins, including microtubule-associated proteins (MAPs), neurofilaments, spectrin, and actin, are preferred substrates for calpain[349]. Researchers have demonstrated that calpain-mediated degradation of PSD-95 and AMPARs occurs in hippocampal neurons and slice cultures[350-352]. There is evidence that certain cytoskeletal proteins are more sensitive to calpain degradation than other cytoskeletal proteins[353]. This differential sensitivity could explain the lack of blast-induced cell death that large-scale calpain activation induces[354].

Studies observed that bTBI increased calpain activation and the presence of calpain-breakdown products in the hippocampus as early as 12 hours post-injury[22]. Blast exposure in rats cleaved calpain-regulated caspase-3 and caspase-12 at 24 hours post-injury[355]. One study did not observe any calpain-mediated proteolysis of spectrin following bTBI in rats; however, the pressure waveform exhibited a much longer rise time (~1ms) than the typical Friedlander waveform (~100ns)[27]. Multiple non-blast studies observed calpain-breakdown products as early as 6 hours post-injury[123, 125, 356, 357]. Functionally, calpain activation after TBI is associated with reduced LTP and network synchronization[121]. It is possible that primary blast-induced PSD-95 digestion is calpain-mediated.

Calpain inhibition following TBI in rats attenuated observed cognitive deficits[358]. There is evidence that the PKA pathway can modulate calpain activity. Over-activation of calpain was found to downregulate PKA; PDE5 inhibitors, which enhance cAMP, reduced calpain activation[134, 359, 360]. Interestingly, a current patent application exists for the use of a PDE5 inhibitor in treating blast-induced tinnitus[361]. No studies have tested the effect of PDE4 inhibition on calpain activation; however, it is possible that PDE inhibitors out-compete calpains to increase PKA activation or, more simply, reduce calpain activation on their own. Greater investigation is necessary to determine if primary blast-induced PSD-95 loss, and restoration with PDE4 inhibition, is calpain-mediated.

6.7 Strategies to prevent primary blast-induced neurological dysfunction

6.7.1 Improving safe-working guidelines and clinical care

While in active combat and training, military personnel frequently encounter high-intensity blast exposures, which can lead to a mTBI[4, 166, 308]. The diagnosis of mTBI within the military can often be subjective, depending on self-reporting of neurological symptoms[309]. In some cases, soldiers who have sustained a TBI will deny their symptoms to remain in the field, and physicians who evaluate soldiers post-deployment may over-report symptoms in order to be conservative. Efforts have been made to more accurately diagnose acute bTBI such as by using the Military Acute Concussion Evaluation (MACE) protocol[362], computer-assisted cognitive testing[363, 364], eye tracking/balance testing[363, 365], and blast dosimeters[366] to name a few. Blast dosimetry presents a non-biased approach for alerting medical professionals of a potential bTBI; however, it requires accurate injury thresholds for correct diagnosis. This thesis (Chapters 2 and 3) advances the development of these thresholds; identifying strain, strain rate, and impulse levels that disrupted memory function (LTP). Here we identified that blast intensities similar to those commonly seen in theater are capable of inducing neurological dysfunction[55]. These thresholds will help curtail underreporting of mild bTBI from soldiers and inform physicians' protocols on removal-from-duty.

Upon diagnosis, physicians remove soldiers from duty until all indicators of mTBI/concussion have resolved completely. Evidence from sports medicine and animal studies suggests a period of increased vulnerability for repeat injury exists for approximately 10 days post-injury[367-369]. Current Veteran Affairs/Department of Defense guidelines for patients who complain of mTBI/concussion symptoms is removal from activity for at least 7 days post-injury; however, this timeline is based on findings from non-blast TBI studies[364, 370]. Although researchers have previously investigated the window of vulnerability for civilian mTBIs, more research is necessary to determine if the same timeline holds for mild bTBI[367, 368, 371-373]. The

window of vulnerability following bTBI is critical information that is necessary for military physicians to gauge when soldiers can safely return-to-duty.

In Chapter 5, we investigated the time course of blast-induced LTP deficits and found that deficits could spontaneously resolve between 7 and 10 days post-injury; however, this recovery was dependent on blast intensity[56]. Other research from our group (not presented in this thesis) reported that the window of heightened vulnerability for LTP deficits to subsequent primary blast in OHSCs may be 72 to 144 hours long[176]. For comparison, our group (not presented in this thesis) identified the same window of heightened vulnerability for LTP deficits to subsequent mild stretch injury in OHSCs[204]. This research suggests that the timeline for spontaneous recovery from mild bTBI is about 6-10 days, which closely aligns with LTP and behavioral research from non-blast TBI studies[256, 367, 374, 375].

6.7.2 Enhancing military helmet technology

Another route to protect soldiers from the effects of primary blast injury is altering helmet design to mitigate the biomechanical forces of the shock wave. Current helmet technology, known as the Advanced Combat Helmet (ACH), in combination with advances in personal protective equipment for other areas of the body (i.e. thoracic protection), have increased survival rates in the current military conflicts as compared to previous conflicts[5, 14, 376]. Although fewer soldiers are perishing from blast exposure, increased survival has resulted in increased diagnosis of TBI[57, 377]. Engineers designed the ACH to protect against penetrative injury, blunt impact, and skull fracture[188, 378]. Its design consists of an outer shell, composed of a polymer-matrix and Kevlar fibers, and an inner-suspension system, composted of elastomeric

foam pads derived from ethylene vinyl acetate[379]. Due to the lack of understanding of primary blast injury, it is unclear how the ACH protects the brain against primary blast (shock wave) exposure. Additionally, researchers continue to debate whether primary blast exposure can cause injury and if this capability is even necessary. Chapters 3-5 of this thesis have demonstrated that primary blast forces, in isolation, are indeed capable of disrupting neurological function and protein pathways, suggesting that engineers may need to redesign military helmets to account for the shock wave.

Computational simulations investigating the protective ability of the ACH against primary blast exposure have come to mixed conclusions. One study modeled an non-helmeted human head, a head wearing the ACH, and a head wearing the ACH with a conceptual face shield and exposed each to a frontal blast wave with incident overpressure of 10atm (~1000kPa)[188]. The ACH slightly mitigated intracranial stresses as compared to the non-helmeted head; however, it did not prevent direct transmission of stress waves into the intracranial cavity. In contrast, the ACH and face shield combination impeded direct transmission of stress waves to the face and resulted in lower intracranial stresses. Another computational study predicted that the ACH provided efficient protection against tertiary phase bTBI, but only partial protection against the shock wave by reducing its intensity in the intracranial cavity by about 5-7%[380]. Conversely, investigation into directional-dependence of blast exposure revealed that, regardless of head protection, maximum principal strains within the brain from shock exposure remained below 8%[381]. This strain level corroborates computational simulations of our *in vitro* injury model[49] and our *in vitro* data from Chapter 2. While our findings indicate 8% strain delivered at a high rate can initiate LTP deficits, this strain level is

less than the threshold for inertia-induced functional deficiencies defined by non-blast TBI studies[95, 97].

Another design concern for helmet technologies is potential underwash overpressures that develop due to the way in which the shock wave envelops protective equipment. A computational study predicted that while a helmet with an attached face shield mitigated underwash overpressures for front and side blasts, the helmet/face shield gap entrapped pressure waves and caused additional reflections when the blast was initiated behind the subject[382]. Helmet designers will need to be cognizant of this phenomenon when adapting equipment for shock exposure.

Another approach to reduce shock wave-induced injury that has demonstrated both computational and experimental success was the use of a polyurea-based external coating on the ACH[379]. When exposing head-forms to 67 grams of pentolite explosive at a 1.07m standoff distance (SOD), the polyurea-coated ACH reduced intracranial levels of impulse and acceleration by approximately 50%, as compared to an uncoated ACH. Interestingly, the rate-sensitivity of the polyurea material provided for improved protection at shorter SOD versus longer, i.e. shorter duration shock exposures. Other studies have found that the current ACH helmet is more effective in mitigating high intensity-short duration blast waves versus lower intensity-longer duration pulses[381].

It is challenging to compare computational studies as material properties and head models vary between studies. Groups often extract inconsistent biomechanical data (ICP, strain, stress, acceleration, etc.), which hinders comparisons between models and comparisons to experimentally determined injury threshold data. Although computational models provide

insight into experimental designs that are too expensive, difficult, or dangerous to conduct in the laboratory, experimental validation of data is critical. This thesis provides insight into strain/rate (Chapter 2) and blast overpressure/impulse (Chapters 3-4) design criteria to incorporate into computational and experimental models, thus providing guidelines for preventing shock-induced neurological deficits.

6.7.3 Identification of new therapeutic targets

At present, no pharmacotherapy has been clinically approved to ameliorate neurocognitive effects attributed to mild TBI[370]. Some cognitive benefits have been found for TBI patients with off-label pharmaceuticals known to improve cognition in neurodegenerative disease, such as methylphenidate or amantadine[383]. Doctors prescribe medications only for presented symptoms such as headaches, musculoskeletal pain, depression/anxiety, sleep disturbance, fatigue, or poor emotional control. To date, more than 30 clinical trials investigating neuroprotection in TBI patients have already failed and there are over 300 more that are currently active[384]. As previously mentioned, a Phase II clinical study of NAC in blast-exposed soldiers found that executive function improved after a week of treatment; however, they did not examine any hippocampal dependent tasks[315]. Most successful pre-clinical therapies have focused on severe TBI, but have not translated from bench-to-bedside[385]. The present lack of approved therapies demonstrates the need to identify and investigate new pharmacological therapies for memory deficits following mild bTBI.

One therapeutic category currently under clinical investigation for reversal of memory deficits in a number of neurological disorders is PDE4 inhibitors. Although PDE4 inhibitors

have yet to be clinically investigated for TBI, a recent Phase II study has begun to investigate whether the pan-PDE4 inhibitor roflumilast improves memory, attention, information processing, or executive function in healthy humans[386]. Two other PDE4 inhibitors (MK0952 and HT07152) have reached Phase II clinical trials investigating whether treatment improves cognition for Alzheimer's disease and age-associated memory impairment, respectively[387, 388].

No pre-clinical study has investigated PDE4 inhibition following blast exposure, but PDE4 inhibition reversed LTP and cognitive deficits in rats following FPI[147, 293]. In Chapter 5, we found that the roflumilast restored LTP when delivered 6 hours (or less) following TBI. We also identified that roflumilast could restore protein expression or phosphorylation that was altered by primary blast. Roflumilast was specifically chosen for this thesis as it is a PDE4 inhibitor that is already FDA-approved for treating chronic obstructive pulmonary disorder[157]. This finding demonstrates that the safety of roflumilast is not a concern, but proof of clinical efficacy is necessary. Although additional studies are necessary to verify roflumilast efficacy using *in vivo* blast injury models, it presents significant therapeutic potential in a field where no pharmacotherapies currently exist.

6.8 Limitations

This thesis employed the OHSC model for all experiments. Although there are many benefits to using this model, one drawback is that we only capture the response of the hippocampus to blast forces. In reality, blast exposure loads the entire brain, head, and body, which all could potentially influence the hippocampal injury response. Hippocampal slice

cultures also lack vasculature that could further influence response. The lack of vasculature limits the thickness of slice cultures to below 500μm, thus limiting the layers of cells[389]. One way to account for this limitation is to implement a complex tissue model, such as endothelial BBB cells co-cultured with OHSCs[390]. Another alternative is to implement an *in vivo* injury model to capture the entire brain response. This step is necessary for rigorously defining the onset of blast-induced functional deficits, safe rest and return-to-duty periods, and therapeutic efficacy established within this thesis. Although as mentioned previously, one benefit of the *in vitro* model that is extremely difficult with *in vivo* models is the fine control of the injury biomechanics.

For this research, we harvested cultures at P8-10 and maintained some cultures out to P10 + 27 days *in vitro*. Sprague-Dawley rats do not develop to sexual maturity until P42[391], which indicates that the cultures used in this thesis are representative of juvenile rat hippocampi. For a better developmental comparison to adult brains, older OHSCs would be more appropriate; however, brain slice cultures are healthiest when cultured from P8-10 pups and maintaining cultures past P40 before testing would be difficult[389]. Thus, the conclusions of this thesis are limited to the response of juvenile rat brains.

As mentioned in Chapter 1, we utilized a shock tube to expose our custom-built *in vitro* receiver, and the OHSCs housed within the receiver, to blast. Exposure levels used in this thesis fall within the range of human-relevant exposures and those physiologically scaled for the rat[53, 55]. There is much debate within the bTBI community regarding proper scaling of injury conditions for animal studies[13, 243]. Within our receiver, tissue samples are positioned 8 cm from the top of the cylindrical PVC column and surrounded by water, which mimics the physiological

barrier from the shock wave provided by surrounding brain tissue, fluid, and skull. The column sits on a drum of water, totaling 57L in volume, which hinders reflections of the blast wave. Due to this unique design, the applied scaling relationships may need adjusting for our custom-built receiver.

Our injury model delivers a single Friedlander waveform, the classic free-field blast injury input[392]. Although this is beneficial for gaining initial understanding of the injury response and mechanisms, it does not represent the complexity of blast exposures experienced in combat. For soldiers, blast exposure(s) often occurs in tight urban environments where there are many surfaces for wave reflections (e.g. buildings, vehicles, etc.)[392]. Although blast intensities used in this thesis represent realistic exposures, the waveforms may need added complexity to mimic real world battlefield conditions more closely.

In Chapters 3-5, we quantified the electrophysiological response of brain tissue to primary blast exposure. We represented spontaneous function with GSI, basal evoked function with SR curves and PPF, and synaptic plasticity with LTP. Although these measures have correlation to higher-order cognitive function, it is difficult to extrapolate *in vitro* electrophysiological changes to behavioral changes *in vivo*. The observed changes in this thesis require further verification with *in vivo* behavioral studies.

A major finding of this thesis is that LTP is more sensitive to blast exposure than other measures we tested, and that primary blast alters proteins involved in LTP induction. The LTP induction pathway is very complex, involving many different presynaptic and postsynaptic components[80, 393]. For this study, we chose to focus only on critical components for LTP

induction that previous studies had demonstrated susceptibility to non-blast TBI. It is possible that primary blast exposure could influence many other components involved in LTP induction.

In Chapters 4 & 5, we explored the therapeutic potential of the PDE4 inhibitor roflumilast against blast-induced neurological deficits. Although we observed efficacy in these experiments, one major limitation of roflumilast is that it does not readily pass the BBB, which could limit its effectiveness when orally-administered after *in vivo* injury[158]. Our group demonstrated (data not shown here) poor extravasation of sodium fluorescein (376 Da) in control animals, which corroborates the reduced passage of roflumilast (400 Da) across healthy BBB[40]. The same study observed that 70kDa molecules can extravasate into the brain due to acute BBB opening after *in vivo* blast injury in mice, suggesting that oral delivery of roflumilast acutely after bTBI may be possible due to blast-induced opening of the BBB[40]. Previous studies have reported blast-induced BBB opening to last at least 6 hours after injury[355, 394]. This suggests that the BBB will not limit oral delivery of roflumilast in animals or humans following blast.

6.9 Future Directions

Soldiers in combat often are exposed to complex blast waveforms when encountering explosions in spatially confined environments. Future work is necessary to understand the pathobiology and biological mechanisms of complex loading conditions. Previous studies have investigated the effect of a complex blast waveform on brain histology following *in vivo* injury[395, 396]. This concept could be adapted using our *in vitro* injury model by altering the shock tube or introducing surfaces for reflections within the sample receiver.

Another future study could explore other complex loading conditions in which *in vitro* cultures are exposed to both primary and tertiary phase blast in controlled isolation. Studies have shown that blast-only loading versus combined blast-blunt loading leads to distinct symptoms in humans, while others have demonstrated that blast overpressure and rotational acceleration lead to different behavioral etiologies in rats[74, 175, 273]. Current *in vivo* blast injury models expose animals to combined primary-tertiary blast loading[24, 30, 40]. In these studies, the influence of inertial blast forces is limited by varying the level of head restraint, although it is extremely difficult to remove this component completely. Our group has already established a stretch model of inertial-driven TBI (tertiary) that we can employ following primary blast exposure[16, 95]. It is possible that the initial primary blast exposure will alter the tolerance of OHSCs to subsequent tertiary blast. One experimental concern is that the temporal delay between injuries is limited due to the need for transitioning the sample between injury devices (seconds to minutes), whereas in reality the phases occur within milliseconds of each other. Additionally, we grow cultures for stretch injury on non-porous, silicone membranes, whereas we grow cultures for blast injury on porous Teflon membranes. Adjustments to the experimental protocol will be necessary to combine these injury models.

Another future area to study is expanding the *in vitro* blast model to alternative brain regions. Other brain regions known to be vulnerable to TBI include the cortex, prefrontal cortex, cerebellum, amygdala, and the brain stem[397]. Our group has previously generated tolerance criteria for *in vitro* stretch injury in cortical slice cultures[205] and other groups have developed either slice culture models for the cerebellum, amygdala, and brain stem[398-400]. As mentioned previously, studies could implement a co-culture model of the hippocampus (or alternative regions) and BBB endothelial cells in order to investigate how blast affects more complex tissue

cultures. Future work could apply the methodologies and results from this thesis to other biological tissue explants to further the understanding of brain tolerance to primary blast exposure.

In this thesis, we investigated how primary blast exposure affected LTP using electrophysiology and western blotting techniques; however, information could also be gained from observing structural changes to the neuron. Changes to hippocampal dendritic spine structure and composition underlie the development of LTP, ultimately contributing to learning and memory[401]. The focus of this thesis was on key LTP proteins localized in and around the PSD; however, it is known that the overall spine size, spine density along the dendrite, and internal stabilization of the spine change during LTP[401, 402]. These changes can be quantified using confocal microscopy or quantitative electron microscopy. Researchers previously observed that non-blast TBI in rats altered spine anatomy in both the hippocampus and forebrain, with one study observing concomitant deficits in LTP[85, 403]. Researchers have yet to investigate spine changes following blast injury, making it an intriguing future line of research.

We found in this thesis that PDE4 inhibition restored PSD-95 expression following blast exposure, which we hypothesized was key to restoring LTP post-treatment. However, we did not extend the study to investigate the mechanism by which this restoration occurs. As suggested in Section 6.5, future studies could explore ubiquitination inhibition, blocked calcineurin signaling, proteasome inhibition, or calpain deactivation as possible therapeutic mechanisms of PDE4 inhibition.

Finally, another line of future research is to replicate the studies of this thesis with an *in vivo* blast injury model to verify if our conclusions translate to the whole brain and animal. The

first necessary step is to confirm the findings from Chapters 3-4, including blast-induced thresholds for electrophysiological dysfunction, onset time of functional deficits, and spontaneous recovery of function following *in vivo* blast injury with acute slice culture electrophysiology. Next, researchers can investigate blast-induced cognitive dysfunction with behavioral tasks that target hippocampal-dependent memory, such as MWM, Radial Arm Maze, or NOR[404-406]. This experimental process enables translation of primary blast-induced electrophysiological deficits into whole-animal cognitive dysfunction. It is also important to examine if the reported cellular injury mechanisms also translate to *in vivo* injury, as protein alterations ultimately define the resulting electrophysiological dysfunction. This transition defines critical implications for improving soldier protective equipment and pharmacotherapies at the human level.

Similarly, the PDE4 inhibitor treatment paradigm should be investigated following *in vivo* injury. The first step is to determine if PDE4 inhibition prevents *in vivo* blast-induced LTP deficits using acute slice electrophysiology. As stated above, the next step would be to test the therapeutic efficacy of PDE4 inhibitors by transitioning to hippocampal-dependent behavioral tasks. PDE4 inhibitor efficacy following *in vivo* blast lends further support to the treatment paradigm, as well as increases confidence in our *in vitro* primary blast model. Successive experiments should investigate drug efficacy against aforementioned blast-induced cognitive dysfunction, while at the same time determining proper dosing and duration of the therapeutic window.

References

1. Ommaya, A.K. and Gennarelli, T.A. (1974). Cerebral concussion and traumatic unconsciousness. Brain 97, 633-654.

2. Morrison, B., 3rd, Elkin, B.S., Dolle, J.P. and Yarmush, M.L. (2011). In vitro models of traumatic brain injury. Annual review of biomedical engineering 13, 91-126.

3. DVBIC (2016). Department of Defense Numbers for Traumatic Brain Injury. Armed Forces Health Surveillance Center: Defense and Veterans Brain Injury Center (DVBIC).

4. Hoge, C.W., McGurk, D., Thomas, J.L., Cox, A.L., Engel, C.C. and Castro, C.A. (2008). Mild traumatic brain injury in U.S. soldiers returning from Iraq. The New England Journal of Medicine 358, 453-463.

5. Ling, G., Bandak, F., Armonda, R., Grant, G. and Ecklund, J. (2009). Explosive blast neurotrauma. J Neurotrauma 26, 815-825.

6. Magnuson, J., Leonessa, F. and Ling, G.S.F. (2012). Neuropathology of explosive blast traumatic brain injury. Curr Neurol Neurosci Rep 12, 570-579.

7. Huang, M., Risling, M. and Baker, D.G. (2015). The role of biomarkers and MEG-based imaging markers in the diagnosis of post-traumatic stress disorder and blast-induced mild traumatic brain injury. Psychoneuroendocrinology.

8. Taylor, P.A. and Ford, C.C. (2009). Simulation of blast-induced early-time intracranial wave physics leading to traumatic brain injury. J Biomech Eng 131, 061007.

9. (START), N.C.f.t.S.o.T.a.R.t.T. (2014). Global Terrorism Database.

10. Bilukha, O.O., Brennan, M. and Anderson, M. (2008). The lasting legacy of war: epidemiology of injuries from landmines and unexploded ordnance in Afghanistan, 2002-2006. Prehospital Disast Med 23, 493-499.

11. Bandak, F.A., Ling, G., Bandak, A. and De Lanerolle, N.C. (2015). Injury biomechanics, neuropathology, and simplifeid physics of explosive blast and impact mild traumatic brain injury. In: *Handbook of Clinical Neurology*. Grafman, J., Salazar, A.M. (eds). Elsevier, pps. 89-104.

12. Chen, Y.C., Smith, D.H. and Meaney, D.F. (2009). In-Vitro Approaches for Studying Blast-Induced Traumatic Brain Injury. Journal of Neurotrauma 26, 861-876.

13. Bass, C.R., Panzer, M.B., Rafaels, K.A., Wood, G., Shridharani, J. and Capeheart, B.P. (2012). Brain injuries from blast. Annals of Biomedical Engineering 40, 185-202.

14. Warden, D. (2006). Military TBI during the Iraq and Afghanistan Wars. J Head Trauma Rehabil 21, 398-402.

15. Wallace, D. and Rayner, S. (2012). Combat helmets and blast traumatic brain injury. Journal of Military and Veterans Health 20, 10-17.

16. Morrison III, B., Cater, H.L., Wang, C.C.B., Thomas, F.C., Hung, C.T., Ateshian, G.A. and Sundstrom, L.E. (2003). A tissue level tolerance criterion for living brain developed with an *in vitro* model of traumatic mechanical loading. Stapp Car Crash Journal 47, 93-105.

17. Panzer, M.B., Myers, B.S., Capehart, B.P. and Bass, C.R. (2012). Development of a finite element model for blast brain injury and the effects of CSF cavitation. Annals of Biomedical Engineering 40, 1530-1544.

18. Long, J.B., Bentley, T.L., Wessner, K.A., Cerrone, C., Sweeney, S. and Bauman, R.A. (2009). Blast overpressure in rats: recreating a battlefield injury in the laboratory. J Neurotrauma 26, 827-840.

19. Svetlov, S.I., Prima, V., Kirk, D.R., Gutierrez, H., Curley, K.C., Hayes, R.L. and Wang, K.K.W. (2010). Morphologic and Biochemical Characterization of Brain Injury in a Model of Controlled Blast Overpressure Exposure. Journal of Trauma and Acute Care Surgery 69, 795-804 710.1097/TA.1090b1013e3181bbd1885.

20. Readnower, R.D., M. Chavko, S. Adeeb, M.D. Conroy, J.R. Pauly, R.M. McCarron, P.G. Sullivan (2010). Increase in blood–brain barrier permeability, oxidative stress, and activated microglia in a rat model of blast-induced traumatic brain injury. Journal of Neuroscience Research 88, 3530-3539.

21. Garman, R.H., Jenkins, L.W., Switzer, R.C., Bauman, R.A., Tong, L.C., Swauger, P.V., Parks, S.A., Ritzel, D.V., Dixon, C.E., Clark, R.S.B., Bayır, H., Kagan, V., Jackson, E.K. and Kochanek, P.M. (2011). Blast Exposure in Rats with Body Shielding Is Characterized Primarily by Diffuse Axonal Injury. Journal of Neurotrauma 28, 947-959.

22. Park, E., Gottlieb, J.J., Cheung, B., Shek, P.N. and Baker, A.J. (2011). A model of low-level primary blast brain trauma results in cytoskeletal proteolysis and chronic functional impairment in the absence of lung barotrauma. Journal Of Neurotrauma 28, 343-357.

23. Vandevord, P.J., Bolander, R., Sajja, V.S.S.S., Hay, K. and Bir, C.A. (2012). Mild Neurotrauma Indicates a Range-Specific Pressure Response to Low Level Shock Wave Exposure. Ann Biomed Eng 40, 227-236.

24. Goldstein, L.E., Fisher, A.M., Tagge, C.A., Zhang, X.L., Velisek, L., Sullivan, J.A., Upreti, C., Kracht, J.M., Ericsson, M., Wojnarowicz, M.W., Goletiani, C.J., Maglakelidze, G.M., Casey, N., Moncaster, J.A., Minaeva, O., Moir, R.D., Nowinski, C.J., Stern, R.A., Cantu, R.C., Geiling, J., Blusztajn, J.K., Wolozin, B.L., Ikezu, T., Stein, T.D., Budson, A.E., Kowall, N.W., Chargin, D., Sharon, A., Saman, S., Hall, G.F., Moss, W.C., Cleveland, R.O., Tanzi, R.E., Stanton, P.K.

and McKee, A.C. (2012). Chronic traumatic encephalopathy in blast-exposed military veterans and a blast neurotrauma mouse model. Sci Transl Med 4, 134ra160.

25. Elder, G.A., Dorr, N.P., De Gasperi, R., Gama Sosa, M.A., Shaughness, M.C., Maudlin-Jeronimo, E., Hall, A.A., McCarron, R.M. and Ahlers, S.T. (2012). Blast Exposure Induces Post-Traumatic Stress Disorder-Related Traits in a Rat Model of Mild Traumatic Brain Injury. J Neurotrauma 29, 2564-2575.

26. Shridharani, J.K., Wood, G.W., Panzer, M.B., Capehart, B.P., Nyein, M.K., Radovitzky, R.A. and Bass, C.R. (2012). Porcine head response to blast. Frontiers in Neurology 3.

27. Baalman, K.L., Cotton, R.J., Rasband, S.N. and Rasband, M.N. (2013). Blast Wave Exposure Impairs Memory and Decreases Axon Initial Segment Length. J Neurotrauma 30, 741-751.

28. Tompkins, P., Tesiram, Y., Lerner, M., Gonzalez, L.P., Lightfoot, S., Rabb, C.H. and Brackett, D.J. (2013). Brain injury: neuro-inflammation, cognitive deficit, and magnetic resonance imaging in a model of blast induced traumatic brain injury. J Neurotrauma 30, 1888-1897.

29. Kochanek, P.M., Dixon, C.E., Shellington, D.K., Shin, S.S., Bayir, H., Jackson, E.K., Kagan, V.E., Yan, H.Q., Swauger, P.V., Parks, S.A., Ritzel, D.V., Bauman, R., Clark, R.S.B., Garman, R.H., Bandak, F., Ling, G. and Jenkins, L.W. (2013). Screening of biochemical and molecular mechanisms of secondary injury and repair in the brain after experimental blast-induced traumatic brain injury in rats. J Neurotrauma 30, 920-937.

30. Gullotti, D.M., Beamer, M., Panzer, M.B., Chia Chen, Y., Patel, T.P., Yu, A., Jaumard, N., Winkelstein, B., Bass, C.R., Morrison, B. and Meaney, D.F. (2014). Significant Head Accelerations Can Influence Immediate Neurological Impairments in a Murine Model of Blast-Induced Traumatic Brain Injury. Journal of Biomechanical Engineering 136, 091004-091004.

31. Awwad, H.O., Gonzalez, L.P., Tompkins, P., Lerner, M., Brackett, D.J., Awasthi, V. and Standifer, K.M. (2015). Blast overpressure waves induce transient anxiety and regional changes in cerebral glucose metabolism and delayed hyperarousal in rats. Frontiers in Neurology 6, 1-13.

32. Saljo, A., Bao, F., Hamberger, A., Haglid, K.G. and Hansson, H.A. (2001). Exposure to short-lasting impulse noise causes microglial and astroglial cell activation in the adult rat brain. Pathophysiology 8, 105-111.

33. Bauman, R.A., Ling, G., Tong, L., Januszkiewicz, A., Agoston, D., Delanerolle, N., Kim, Y., Ritzel, D., Bell, R., Ecklund, J., Armonda, R., Bandak, F. and Parks, S. (2009). An introductory characterization of a combat-casualty-care relevant swine model of closed head injury resulting from exposure to explosive blast. J Neurotrauma 26, 841-860.

34. Pun, P.B.L., Kan, E.M., Salim, A., Li, Z., Ng, K.C., Moochhala, S.M., Ling, E., Tan, M.H. and Lu, J. (2011). Low level primary blast injury in rodent brain. Frontiers in Neurology 2.

35. Rubovitch, V., M. Ten-Bosch, O. Zohar, C.R. Harrison, C. Tempel-Brami, E. Stein, B.J. Hoffer, C.D. Balaban, S. Schreiber, W. Chiu, C.G. Pick (2011). A mouse model of blast-induced mild traumatic brain injury. Experimental Neurology 232, 280-289.

36. Kuehn, R., Simard, P.F., Driscoll, I., Keledjian, K., Ivanova, S., Tosun, C., Williams, A., Bochicchio, G., Gerzanich, V. and Simard, J.M. (2011). Rodent model of direct cranial blast injury. J Neurotrauma 28, 2155-2169.

37. Heldt, S.A., Elberger, A.J., Deng, Y., Guley, N.H., Del Mar, N., Rogers, J., Choi, G.C., Ferrell, J., Rex, T.S., Honig, M.G. and Reiner, A. (2014). A novel closed-head model of mild traumatic brain injury caused by primary overpressure blast to the cranium produces sustained emotional deficits in mice. Frontiers in Neurology 5, 1-14.

38. Bass, C.R., Rafaels, K.A. and Salazar, R.S. (2008). Pulmonary injury risk assessment for short-duration blasts. J Trauma 65, 604-615.

39. Wood, G.W., Panzer, M.B., Shridharani, J.K., Matthews, K.A., Capehart, B.P., Myers, B.S. and Bass, C.R. (2013). Attenuation of blast pressure behind ballistic protective vests. Injury Prevention 19, 19-25.

40. Hue, C.D., Cho, F.S., Cao, S., Nicholls, R.E., Vogel III, E.W., Sibindi, C., Arancio, O., Bass, C.R., Meaney, D.F. and Morrison III, B. (2016). Time course and size of blood-brain barrier opening in a mouse model of blast-induced traumatic brain injury. J Neurotrauma 33, 1202-1211.

41. Divani, A.A., Murphy, A.J., Meints, J., Sadeghi-Barzargani, H., Nordberg, J., Monga, M., Low, W.C., Bhatia, P.M., Beilman, G.J. and SantaCruz, K.S. (2015). A novel preclinical model of primary blast-induced traumatic brain injury. J Neurotrauma 32, 1109-1116.

42. Shepard, S.R., Ghajar, J.B.G., Giannuzzi, R., Kupferman, S. and Hariri, R.J. (1991). Fluid percussion barotrauma chamber: a new *in vitro* model for traumatic brain injury. J Surg Res 51, 417-424.

43. Murphy, E.J. and Horrocks, L.A. (1993). A model for compression trauma: pressure induced injury in cell cultures. Journal of Neurotrauma 10, 431-444.

44. Wallis, R.A. and Panizzon, K.L. (1995). Felbamate neuroprotection against CA1 traumatic neuronal injury. European Journal of Pharmacology 294, 475-482.

45. Salvador-Silva, M., Aioi, S., Parker, A., Yang, P., Pecen, P. and Hernandez, M.R. (2004). Responses and signaling pathways in human optic nerve head astrocytes exposed to hydrostatic pressure in vitro. Glia 45, 364-377.

46. Connell, S., Gao, J., Chen, J. and Shi, R. (2011). Novel model to investigate blast injury in the central nervous system. J Neurotrauma 28, 1229-1236.

47. Zander, N.E., Piehler, T., Boggs, M.E., Banton, R. and Benjamin, R. (2015). In vitro studies of primary blast loading on neurons. J Neurosci Res 93, 1353-1363.

48. Arun, P., J. Spadaro, J. John, R.B. Gharavi, T.B. Bentley, M.P. Nambiar (2011). Studies on blast traumatic brain injury using in-vitro model with shock tube. NeuroReport 22, 379-384.

49. Panzer, M.B., Matthews, K.A., Yu, A.W., Morrison III, B., Meaney, D.F. and Bass, C.R. (2012). A Multiscale Approach to Blast Neurotrauma Modeling: Part I – Development of Novel Test Devices for in vivo and in vitro Blast Injury Models. Frontiers in Neurology 3.

50. Effgen, G.B., Hue, C.D., Vogel III, E.W., Panzer, M.B., Bass, C.R., Meaney, D.F. and Morrison III, B. (2012). A multiscale approach to blast neurotrauma modeling: part II: methodology for inducing blast injury to in vitro models. Frontiers in Neurology 3, 1-10.

51. Miller, A.P., Shah, A.S., Aperi, B.V., Budde, M.D., Pintar, F.A., Tarima, S., Kurpad, S.N., Stemper, B.D. and Glavaski-Josimovic, A. (2015). Effects of blast overpressure on neurons and glial cells in rat organotypic hippocampal slice cultures. Frontiers in Neurology 6.

52. Hue, C.D., Cao, S., Haider, S.F., Vo, K.V., Effgen, G.B., Vogel III, E.W., Panzer, M.B., Bass, C.R., Meaney, D.F. and Morrison III, B. (2013). Blood-Brain Barrier Dysfunction after Primary Blast Injury in vitro. Journal of Neurotrauma 30, 1652-1663.

53. Effgen, G.B., Vogel III, E.W., Lynch, K.A., Lobel, A., Hue, C.D., Meaney, D.F., C.R., B. and Morrison III, B. (2014). Isolated Primary Blast Alters Neuronal Function with Minimal Cell Death in Organotypic Hippocampal Slice Cultures. J Neurotrauma 31, 1202-1210.

54. Hue, C.D., Cao, S., Bass, C.R., Meaney, D.F. and Morrison III, B. (2014). Repeated primary blast injury causes delayed recovery, but not additive disruption, in an in vitro blood–brain barrier model. J Neurotrauma 31, 951-960.

55. Vogel III, E.W., Effgen, G.B., Patel, T.P., Meaney, D.F., Bass, C.R. and Morrison III, B. (2016). Isolated primary blast inhibits long-term potentiation in organotypic hippocampal slice cultures. J Neurotrauma 33, 652-661.

56. Vogel III, E.W., Rwema, S.H., Meaney, D.F., Bass, C.R. and Morrison III, B. (2016). Primary blast injury depressed hippocampal long-term potentiation through disruption of synaptic proteins. J Neurotrauma Available online.

57. Terrio, H., Brenner, L.A., Ivins, B.J., Cho, J.M., Helmick, K., Schwab, K., Scally, K., Bretthauer, R. and Warden, D. (2009). Traumatic brain injury screening: preliminary findings in a US Army brigade combat team. J Head Trauma Rehabil 24, 14-23.

58. Wilk, J.E., Thomas, J.L., McGurk, D.M., Riviere, L.A., Castro, C.A. and Hoge, C.W. (2010). Mild traumatic brain injury (concussion) during combat: lack of assocaition of blast mechanism with persistent postconcussive symptoms. J Head Trauma Rehabil 25, 9-14.

59. Luethcke, C.A., Bryan, C.J., Morrow, C.E. and Isler, W.C. (2011). Comparison of concussive symptoms, cognitive performance, and psychological symptoms between acute blast-versus nonblast-induced mild traumatic brain injury. J Int Neuropsych Soc 17, 36-45.

60. Miyazaki, S., Newlon, P.G., Goldberg, S.J., Jenkins, L.W., Lyeth, B.G., Katayama, Y. and Hayes, R.L. (1989). Cerebral concussion supresses hippocampal long-term potentiation (LTP) in rats. In: *Intracranial Pressure VII*. Hoff, J.T., Betz, A.L. (eds). Springer-Verlag, pps. 651-653.

61. Lyeth, B.G., Jenkins, L.W., Hamm, R.J., Dixon, C.E., Phillips, L.L., Clifton, G.L., Young, H.F. and Hayes, R.L. (1990). Prolonged memory impairment in the absence of hippocampal cell death following traumatic brain injury in the rat. Brain Res 526, 249-258.

62. Squire, L.R. (1992). Memory and the hippocampus: a synthesis form findings with rats, monkeys, and humans. Psychol Rev 99, 195-231.

63. Tulving, E., Kapur, S., Markowitsch, H.J., Craik, F.I.M., Habib, R. and Houle, S. (1994). Neuroanatomical correlates of retrieval of episodic memory: auditory sentence recognition. Proc Natl Acad Sci U S A 91, 2012-2015.

64. Knight, R.T. (1996). Contribution of human hippocampal region to novelty detection. Nature 383, 256-259.

65. Ekstrom, A.D., Kahana, M.J., Caplan, J.B., Fields, T.A., Isham, E.A., Newman, E.L. and Fried, I. (2003). Cellular networks underlying human spatial navigation. Nature 425, 184-187.

66. Cohen, A.S., Pfister, B.J., Schwarzbach, E., Grady, M.S., Goforth, P.B. and Satin, L.S. (2007). Injury-induced alterations in CNS electrophysiology. Prog Brain Res 161, 143-169.

67. Kitamura, T., Tsuchihashi, Y. and Fujita, S. (1978). Initial response of silver-impregnated "resting microglia" to stab wounding in rabbit hippocampus. Acta Neuropathol 44, 31-39.

68. Lowenstein, D.H., Thomas, M.J., Smith, D.H. and McIntosh, T.K. (1992). Selective vulnerability of dentate hilar neurons following traumatic brain injury: a potential mechanistic link between head trauma and disorders of the hippocampus. J Neurosci 12, 4846-4853.

69. Hicks, R.R., Smith, D.H., Lowenstein, D.H., Saint Marie, R. and McIntosh, T.K. (1993). Mild experimental brain injury in the rat induces cognitive deficts associated with regional neuronal loss in the hippocampus. J Neurotrauma 10, 405-414.

70. Smith, D.H., Chen, X., Xu, B., McIntosh, T.K., Gennarelli, T.A. and Meaney, D.F. (1997). Characterization of diffuse axonal pathology and selective hippocampal damage following inertial brain trauma in the pig. J Neuropathol Exp Neurol 56, 822-834.

71. Cernak, I., Merkle, A.C., Koliatsos, V.E., Bilik, J.M., Luong, Q.T., Mahota, T.M., Xu, L., Slack, N., Windle, D. and Ahmed, F.A. (2011). The pathobiology of blast injuries and blast-induced neurotrauma as identified using a new experimental model of injury in mice. Neurobiology of disease 41, 538-551.

72. Wang, Y., Wei., Y., Oguntayo, S., Wilkins, W., Arun, P., Valiyaveettil, M., Song, J., Long, J.B. and Nambiar, M.P. (2011). Tightly Coupled Repetitive Blast-Induced Traumatic Brain Injury: Development and Characterization in Mice. J Neurotrauma 28, 2171-2183.

73. Patel, T.P., Gullotti, D.M., Hernandez, P., O'Brien, W.T., Capeheart, B.P., Morrison III, B., Bass, C.R., Eberwine, J.H., Abel, T. and Meaney, D.F. (2014). An open-source toolbox for automated phenotyping of mice in behavioral tasks. Frontiers in Behavioral Neuroscience 8, 1-16.

74. Beamer, M., Tummala, S.R., Gullotti, D., Kopil, K., Gorka, S., Abel, T., Bass, C.R., Morrison III, B., Cohen, A.S. and Meaney, D.F. (2016). Primary blast injury causes cognitive impairments and hippocampal circuit alterations. Exp Neurol 283, 16-28.

75. Saljo, A., Svensson, B., Mayorga, M., Hamberger, A. and Bolouri, H. (2009). Low-Level Blasts Raise Intracranial Pressure and Impair Cognitive Function in Rats. J Neurotrauma 26, 1345-1352.

76. Cho, H.J., Sajja, V.S.S.S., VandeVord, P.J. and Lee, Y.W. (2013). Blast induces oxidative stress, inflammation, neuronal loss and subsequent short-term memory impairments in rats. J Neurosci 253, 9-20.

77. Sajja, V.S.S.S., Perrine, S.A., Ghodoussi, F., Hall, C.S., Galloway, M.P. and VandeVord, P.J. (2014). Blast neurotrauma impairs working memory and disrupts prefrontal myo-inositol levels in rats. Molecular and Cellular Neuroscience 59, 119-126.

78. Morris, R.G.M., Davis, S. and Butcher, S.P. (1990). Hippocampal synaptic plasticity and NMDA receptors: a role in information storage? Phil Trans R Society Lond 329, 187-204.

79. Doyere, V. and Laroche, S. (1992). Linear relationship between the maintenance of hippocampal long-term potentiation and retention of an associative memory. Hippocampus 2, 39-48.

80. Bliss, T.V.P. and Collingridge, G.L. (1993). A synaptic model of memory: long-term potentiation in the hippocampus. Nature 361, 31-39.

81. Yin, T.C., Britt, J.K., Ready, J.M. and Pieper, A.A. (2014). P7C3 neuroprotective chemicals block axonal degeneration and preserve function after traumatic brain injury. Cell Reports 8, 1731-1740.

82. Miyazaki, S., Katayama, Y., Lyeth, B.G., Jenkins, L.W., DeWitt, D.S., Goldberg, S.J., Newlon, P.G. and Hayes, R.L. (1992). Enduring suppression of hippocampal long-term potentiation following traumatic brain injury in rat. Brain Res 585, 335-339.

83. D'Ambrosio, R., Maris, D.O., Grady, M.S., Winn, H.R. and Janigro, D. (1998). Selective loss of hippocampal long-term potentiation, but not depression, following fluid percussion injury. Brain Research 786, 64-79.

84. Sanders, M.J., Sick, T.J., Perez-Pinzon, M.A., Dietrich, W.D. and Green, E.J. (2000). Chronic failure in the maintenance of long-term potentiation following fluid-percussion injury in the rat. Brain Research 861, 69-76.

85. Schwarzbach, E., Bonislawski, B.P., Xiong, G. and Cohen, A.S. (2006). Mechanisms underlying the ability to induce area CA1 LTP in the mouse after traumatic brain injury. Hippocampus 16, 541-550.

86. Zhang, B., Chen, X., Lin, Y., Tan, T., Yang, Z., Dayao, C., Liu, L., Jiang, R. and Zhang, J. (2011). Impairment of synaptic plasticity in hippocampus is exacerbated by methylprednisolone in a rat model of traumatic brain injury. Brain Research 1382, 165-172.

87. Reeves, T.M., Lyeth, B.G., Phillips, L.L., Hamm, R.J. and Povlishock, J.T. (1997). The effect of traumatic brain injury on inhibition in the hippocampus and dentate gyrus. Brain Research 757, 119-132.

88. Kang, W.H. and Morrison III, B. (2014). Functional tolerance to mechanical deformation developed from organotypic hippocampal slice cultures. Biomech Model Mechanobiol.

89. Griesemer, D. and Mautes, A.M. (2007). Closed head injury causes hyperexcitability in rat hippocampal CA1 but not in CA3 pyramidal cells. Journal Of Neurotrauma 24, 1823-1832.

90. Cater, H.L., Gitterman, D.P., Davis, S.M., Benham, C.D., Morrison III, B. and Sundstrom, L.E. (2007). Stretch-induced injury in organotypic hippocampal slice cultures reproduces in vivo post-traumatic neurodegeneration: role of glutamate receptors and voltage-dependent calcium channels. Journal of Neurochemistry 101, 434-447.

91. Akasu, T., Muraoka, N. and Hasuo, H. (2002). Hyperexcitability of hippocampal CA1 neurons after fluid percussion injury of the rat cerebral cortex. Neuroscience Letters 329, 305-308.

92. Witgen, B.M., Lifshitz, J., Smith, M.L., Schwarzbach, E., Liang, S.-L., Grady, M.S. and Cohen, A.S. (2005). Regional hippocampal alteration associated with cognitive deficit following experimental traumatic brain injury: a systems, network, and cellular evaluation. Neuroscience 133, 1-15.

93. Tran, L.D., Lifshitz, J., Witgen, B.M., Schwarzbach, E., Cohen, A.S. and Grady, M.S. (2006). Response of the contralateral hippocampus to lateral fluid percussion brain injury. Journal of Neurotrauma 23, 1330-1342.

94. Perez-Polo, J.R., Rea, H.C., Johnson, K.M., Parsley, M.A., Unabia, G.C., Xu, G.Y., Prough, D., DeWitt, D.S., Spratt, H. and Hulsebosch, C.E. (2015). A rodent model of mild traumatic brain blast injury. Journal of Neuroscience Research 93, 549-561.

95. Cater, H.L., Sundstrom, L.E. and Morrison III, B. (2006). Temporal development of hippocampal cell death is dependent on tissue strain but not strain rate. Journal of Biomechanics 39, 2810-2818.

96. Elkin, B.S. and Morrison III, B. (2007). Region-specific tolerance criteria for the living brain. Stapp Car Crash Journal 51, 127-138.

97. Yu, Z. and Morrison III, B. (2010). Experimental mild traumatic brain injury induces functional alteration of the developing hippocampus. Journal of Neurophysiology 103, 499-510.

98. Lamprecht, M.R. and Morrison III, B. (2015). A combination therapy of 17B-estradiol and memantine is more neuroprotective than monotherapies in an organotypic brain slice culture model of traumatic brain injury. J Neurotrauma 32, 1361-1368.

99. Gurkoff, G.G., Giza, C.C. and Hovda, D.A. (2006). Lateral fluid percussion injury in the developing rat causes an acute, mild behavioral dysfunction in the absence of significant cell death. Brain Res 1077, 24-36.

100. Eakin, K. and Miller, J.P. (2012). Mild Traumatic Brain Injury Is Associated with Impaired Hippocampal Spatiotemporal Representation in the Absence of Histological Changes. J Neurotrauma 29, 1180-1187.

101. Park, E., Eisen, R., Kinio, A. and Baker, A.J. (2013). Electrophysiological white matter dysfunction and association with neurobehavioral deficits following low-level primary blast trauma. Neurobiology of disease 52, 150-159.

102. Kelleher III, R.J., Govindarajan, A. and Tonegawa, S. (2004). Translational regulatory mechanisms in persistent forms of synaptic plasticity. Neuron 44, 59-73.

103. Makino, H. and Malinow, R. (2009). AMPA receptor incorporation into synapses during LTP: the role of lateral movement and exocytosis. Neuron 64, 381-390.

104. Lisman, J., Yasuda, R. and Raghavachari, S. (2012). Mechanisms of CaMKII action in long-term potentiation. Nature Reviews Neuroscience 13, 169-182.

105. Kumar, A., Zou, L., Yuan, X., Long, Y. and Yang, K. (2002). N-methyl-D-aspartate receptors: transient loss of NR1/NR2A/NR2B subunits after traumatic brain injury in a rodent model. J Neurosci Res 67, 781-786.

106. Zhang, L., Rzigalinski, B.A., Ellis, E.F. and Satin, L.S. (1996). Reduction of voltage-dependent Mg 2+ blockade of NMDA current in mechanically injured neurons. Science 274, 1921-1923.

107. Schumann, J., Alexandrovich, G.A., Biegon, A. and Yaka, R. (2008). Inhibition of NR2B phosphorylation restores alterations in NMDA receptor expression and improves functional recovery following traumatic brain injury in mice. J Neurotrauma 25, 945-957.

108. Singh, P., Doshi, S., Spaethling, J.M., Hockenberry, A.J., Patel, T.P., Geddes-Klein, D.M., Lynch, D.R. and Meaney, D.F. (2012). N-methyl-D-aspartate receptor mechanosensitivity is governed by C terminus of NR2B subunit. J Biol Chem 287, 4348-4359.

109. Goforth, P.B., Ellis, E.F. and Satin, L.S. (2004). Mechanical injury modulates AMPA receptor kinetics via an NMDA receptor-dependent pathway. Journal of Neurotrauma 21, 719-732.

110. Spaethling, J.M., Klein, D.M., Singh, P. and Meaney, D.F. (2008). Calcium-permeable AMPA receptors appear in cortical neurons after traumatic mechanical injury and contribute to neuronal fate. J Neurotrauma 25, 1207-1216.

111. Matzilevich, D.A., Rall, J.M., Moore, A.N., Grill, R.J. and Dash, P.K. (2002). High-density microarray analysis of hippocampal gnee expression following experimental brain injury. J Neurosci Res 67, 646-663.

112. Kharlamov, E.A., Lepsveridze, E., Meparishvili, M., Solomonia, R.O., Lu, B., Miller, E.R., Kelly, K.M. and Mtchedlishvili, Z. (2011). Alterations of $GABA_A$ and glutamate receptor subunits and heat shock protein in rat hippocampus following traumatic brain injury and in posttraumatic epilepsy. Epilepsy Research 95, 20-34.

113. Mtchedlishvili, Z., Lepsveridze, E., Xu, H., Kharlamov, E.A., Lu, B. and Kelly, K.M. (2010). Increase of $GABA_A$ receptor-mediated tonic inhibition in dentate granule cells after traumatic brain injury. Neurobiology of disease 38, 464-475.

114. Kao, C.Q., Goforth, P.B., Ellis, E.F. and Satin, L.S. (2004). Potentiation of GABA(A) currents after mechanical injury of cortical neurons. Journal of Neurotrauma 21, 259-270.

115. Kang, W.H., Cao, W., Graudejus, O., Patel, T.P., Wagner, S., Meaney, D.F. and Morrison III, B. (2014). Alterations in hippocampal network activity after *in vitro* traumatic brain injury. Journal of Neurotrauma.

116. Gibson, C.J., Meyer, R.C. and Hamm, R.J. (2010). Traumatic brain injury and the effects of diazepam, diltiazem, and MK-801 on GABA-A receptor subunit expression in rat hippocampus. J Biomed Sci 17, 1-11.

117. Raible, D.J., Frey, L.C., Cruz Del Angel, Y., Russek, S.J. and Brooks-Kayal, A.R. (2012). $GABA_A$ receptor regulation after experimental traumatic brain injury. J Neurotrauma 29, 2548-2554.

118. Panickar, K.S., Jayakumar, A.R. and Norenberg, M.D. (2002). Differential response of neural cells to trauma-induced free radical production in vitro. Neurochem.Res. 27, 161-166.

119. Osteen, C.L., Giza, C.C. and Hovda, D.A. (2004). Injury-induced alterations in N-methyl-D-aspartate receptor subunit composition contribute to prolonged ^{45}calcium accumulation following lateral fluid percussion. J Neurosci 128, 305-322.

120. Deshplande, L.S., Sun, D.A., Sombati, S., Baranova, A., Wilson, M.S., Attkisson, E., Hamm, R.J. and DeLorenzo, R.J. (2008). Alterations in neuronal calcium levels are associated with cognitive deficits after traumatic brain injury. Neuroscience Letters 441, 115-119.

121. Patel, T.P., Ventre, S.C. and Meaney, D.F. (2012). Dynamic changes in neural circuit topology following mild mechanical injury in vitro. Ann Biomed Eng 40, 23-36.

122. Guerriero, R.M., Giza, C.C. and Rotenberg, A. (2015). Glutamate and GABA imbalance following traumatic brain injury. Curr Neurol Neurosci Rep 15, 1-11.

123. Taft, W.C., Yang, K., Dixon, C.E. and Hayes, R.L. (1992). Microtubule-associated protein 2 levels decrease in hippocampus following traumatic brain injury. J Neurotrauma 9, 281-290.

124. Yang, K., Taft, W.C., Dixon, C.E., Todaro, C.A., Yu, R.K. and Hayes, R.L. (1993). Alterations of protein kinase C in rat hippocampus following traumatic brain injury. Journal of Neurotrauma 10, 287-295.

125. Posmantur, R., Hayes, R.L., Dixon, C.E. and Taft, W.C. (1994). Neurofilament 68 and Neurofilament 200 Protein Levels Decrease After Traumatic Brain Injury. Journal of Neurotrauma 11, 533-545.

126. Dash, P.K., Moore, A.N. and Dixon, C.E. (1995). Spatial memory deficits, increased phosphorylation of the transcription factor CREB, and induction of the AP-1 complex following experimental brain injury. J Neurosci 15.

127. Folkerts, M.M., Berman, R.F., Muizelaar, J.P. and Rafols, J.A. (1998). Disruption of MAP-2 Immunostaining in Rat Hippocampus After Traumatic Brain Injury. Journal of Neurotrauma 15, 349-363.

128. Dash, P.K., Mach, S.A. and Moore, A.N. (2002). The role of extracellular signal-regulated kinase in cognitive and motor deficits following experimental traumatic brain injury. J Neurosci 114, 755-767.

129. Mori, T., X. Wang, J.C. Jung, T. Sumii, A.B. Singhal, M.E. Fini, C.E. Dixon, A. Alessandrini, E.H. Lo (2002). Mitogen-activated protein kinase inhibition in traumatic brain injury: in vitro and in vivo effects. Journal of Cerebral Blood FLow and Metabolism 22, 444-452.

130. Atkins, C.M., Oliva Jr, A.A., Alonso, O.F., Pearse, D.D., Bramlett, H.M. and Dietrich, W.D. (2007). Modulation of the cAMP signaling pathway after traumatic brain injury. Exp Neurol 208, 145-158.

131. Folkerts, M.M., Parks, E.A., Dedman, J.R., Kaetzel, M.A., Lyeth, B.G. and Berman, R.F. (2007). Phosphorylation of calcium calmodulin-dependent protein kinase II following lateral fluid percussion brain injury in rats. J Neurotrauma 24, 638-650.

132. Ansari, M.A., Roberts, K.N. and Scheff, S.W. (2008). Oxidative stress and modification of synaptic proteins in hippocampus after traumatic brain injury. Free Radical Biology and Medicine 45, 443-452.

133. Atkins, C.M., Falo, M.C., Alonso, O.F., Bramlett, H.M. and Dietrich, W.D. (2009). Deficits in ERK and CREB activation in the hippocampus after traumatic brain injury. Neuroscience Letters 459, 52-56.

134. Griesbach, G.S., Sutton, R.L., Hovda, D.A., Ying, Z. and Gomez-Pinilla, F. (2009). Controlled contusion injury alters molecular systems associated with cognitive performance. J Neurosci Res 87, 795-805.

135. Bales, J.W., Ma, X., Yan, H.Q., Jenkins, L.W. and Dixon, C.E. (2010). Expression of protein phosphatase 2B (calcineurin) subunit A isoforms in rat hippocampus after traumatic brain injury. J Neurotrauma 27, 109-120.

136. Wakade, C., Sangeetha, S.R., Laird, M.D., Dhandapani, M. and Vender, J.R. (2010). Delayed reduction in hippocampal post-synaptic density protein-95 expression temporally correlates with cognitive dysfunction following controlled cortical impact in mice. J Neurosurg 113, 1195-1201.

137. Wang, J.H. and Feng, D.P. (1992). Postsynaptic protein kinase C essential to induction and maintenance of long-term potentiation in the hippocampal CA1 region. Proc Natl Acad Sci U S A 89, 2576-2580.

138. Mayford, M., Wang, J., Kandel, E.R. and O'Dell, T.J. (1995). CaMKII regulates the frequency-response function of hippocampal synapses for the production of both LTD and LTP. Cell 81, 891-904.

139. Roche, K.W., O'Brien, R.J., Mammen, A.L., Bernhardt, J. and Huganir, R.L. (1996). Characterization of multiple phosphorylation sites on the AMPA receptor GluR1 subunit. Neuron 16, 1179-1188.

140. Blitzer, R.D., Connor, J.H., Brown, G.P., Wong, T., Shenolikar, S., Iyengar, R. and Landau, E.M. (1998). Gating of CaMKII by cAMP-regulated protein phosphatase activity during LTP. Science 280.

141. Titus, D.J., Oliva, A.A., Wilson, N.M. and Atkins, C.M. (2014). Phosphodiesterase inhibitors as therapeutics for traumatic brain injury. Curr Pharm Des 21, 332-342.

142. Huai, Q., Colicelli, J. and Ke., H. (2003). The crystal structure of AMP-bound PDE4 suggests a mechanism for phosphodiesterase catalysis. Biochemistry 42, 13220-13226.

143. Conti, M., Richter, W., Mehats, C., Livera, G., Park, J.Y. and Jin, C. (2003). Cyclic AMP-specifc PDE4 phosphodiesterases as critical components of cyclic AMP signaling. J Biol Chem 278, 5493-5496.

144. Titus, D.J., Furones, C., Kang, Y. and Atkins, C.M. (2013). Age-dependent alterations in cAMP signaling contribute to synaptic plasticity deficits following traumatic brain injury. Neuroscience 231, 182-194.

145. Kobori, N., Moore, A.N. and Dash, P.K. (2015). Altered regulation of protein kinase A activity in the medial prefrontal cortex of normal and Brain-injured animals actively engaged in a working memory task. J Neurotrauma 32, 139-148.

146. Armstead, W.M., Kiessling, J.W., Cines, D.B. and Higazi, A.A. (2011). Glucagon Protects Against Impaired NMDA-Mediated Cerebrovasodilation and Cerebral Autoregulation during Hypotension after Brain Injury by Activating cAMP Protein Kinase A and Inhibiting Upregulation of tPA. J Neurotrauma 28, 451-457.

147. Titus, D.J., Sakurai, A., Kang, Y., Furones, C., Jergova, S., Santos, R., Sick, T.J. and Atkins, C.M. (2013). Phosphodiesterase inhibition rescues chronic cognitive deficits induced by traumatic brain injury. J Neurosci 33, 5216-5226.

148. Atkins, C.M., Cepero, M.L., Kang, Y., Liebl, D.J. and Dietrich, W.D. (2013). Effects of early rolipram treatment on histopathological outcome after controlled cortical impact injury in mice. Neuroscience Letters 532, 1-6.

149. Wang, C., Yang, X., Zhuo, Y., Zhou, H., Lin, H., Cheng, Y., Xu, J. and Zhang, H. (2012). The phosphodiesterase-4 inhibitor rolipram reverses Aβ-induced cognitive impairment and neuroinflammatory and apoptotic responses in rats. International Journal of Neuropsychopharmacology 15, 749-766.

150. Kanes, S.J., Tokarczyk, J., Siegel, S.J., Bilker, W., Abel, T. and Kelly, M.P. (2007). Rolipram: a specific phosphodiesterase 4 inhibitor with potential antipsychotic activity. Neuroscience 144, 239-246.

151. Rodefer, J.S., Saland, S.K. and Eckrich, S.J. (2012). Selective phosphodiesterase inhibitors improve performance on the ED/ID cognitive task in rats. Neuropharmacology 62, 1182-1190.

152. de Lima, M.N., Presti-Torres, J., Garcia, V.A., Guimães, M.R., Scalco, F.S., Roesler, R. and Schröder, N. (2008). Amelioration of recognition memory impairment associated with iron loading or aging by the type 4-specific phosphodiesterase inhibitor rolipram in rats. Neuropharmacology 55, 788-792.

153. Zhu, J., Mix, E. and Winbald, B. (2001). The antidepressant and antiinflammatory effects of rolipram in the central nervous system. CNS Drug Reviews 7, 387-398.

154. O'Donnell, J.M. and Zhang, H.T. (2004). Antidepressant effects of inhibitors of cAMP phosphodiesterase (PDE4). Trends in Pharmacological Sciences 25, 158-163.

155. Jabaris, S.G.S.L., Sumathy, H., Kumar, R.S., Narayanan, S., Thanikachalam, S. and Babu, C.S. (2015). Effects of rolipram and roflumilast, phosphodiesterase-4 inhibitors, on hypertension-induced defects in memory function in rats. Eur J Pharma 746, 138-147.

156. Vanmierlo, T., Creemers, P., Akkerman, S., van Duinen, M., Sambeth, A., De Vry, J., Uz, T., Blokland, A. and Prickaerts, J. (2016). The PDE4 inhibitor roflumilast improves memory in rodents at non-emetic doses. Behavioural Brain Research 303, 26-33.

157. Giembycz, M.A. and Field, S.K. (2010). Roflumilast: first phosphodiesterase 4 inhibitor approved for treatment of COPD. Drug Design, Development and Therapy 4, 147-158.

158. Takeda (2014). Daliresp® (roflumilast tablets): US prescribing information.

159. Faul, M.D., Xu, L., Wald, M.M. and Coronado, V.G. (2010). Traumatic brain injury in the United States: emergency department visits, hospitalizations, and deaths, 2002-2006. Center for Disease Control and Prevention.

160. Selassie, A.W., Zaloshnja, E., Langlois, J.A., Miller, T., Jones, P. and Steiner, C. (2008). Incidence of long-term disability following traumatic brain injury hospitalization, United States, 2003. J Head Trauma Rehabil 23, 123-131.

161. Finkelstein, E.A., Corso, P.S. and Miller, T.R. (2006). The Incidence and Economic Burden of Injuries in the United States. Oxford University Press: New York.

162. Coronado, V.G., McGuire, L.C., Faul, M.F., Sugerman, D.E. and Pearson, W.S. (2012). Traumatic brain injury epidemiology and public health issues. In: *Brain injury medicine: principles and practice. 2nd ed.* Zasler, N.D., Katz, D.I., Zafonte, R.D. (eds). Demos Medical Publishing: New York, NY, pps. 84-100.

163. Taylor, B.C., Hagel, E.M., Carlson, K.F., Cifu, D.X., Cutting, A., Bidelspach, D.E. and Sayer, N.A. (2012). Prevalence and costs of co-occurring traumatic brain injury with and without psychiatric disturbance and pain among Afghanistan and Iraq War Veteran VA Users. Med Care 50, 342-346.

164. Defense, D.o. (2011). Report to congress on expenditures for activities on traumatic brain injury and psychological health, including posttraumatic stress disorder, for 2010. Department of Defense.

165. Coupland, R.M. and Meddings, D.R. (1999). Mortality associated with use of weapons in armed conflicts, wartime atrocities, and civilian mass shootings: literature review. BMJ 319, 407-410.

166. Galarneau, M.R., Woodruff, S.I., Dye, J.L., Mohrle, C.R. and Wade, A.L. (2008). Traumatic brain injury during Operation Iraqi Freedom: findings from the United States Navy-Marine Corps Combat Trauma Registry. J Neurosurg 108, 950-957.

167. Xydakis, M.S., Fravell, M.D., Nasser, K.E. and Casler, J.D. (2005). Analysis of battlefield head and neck injuries in Iraq and Afghanistan. Otolaryngology-Head and Neck Surgery 133, 497-504.

168. Heltemes, K.J., Holbrook, T.L., MacGregor, A.J. and Galarneau, M.R. (2012). Blast-related mild traumatic brain injury is associated with a decline in self-rated health amongst US military personnel. Injury Int J Care Injured 43, 1990-1995.

169. Xiong, Y., Zhang, Y., Mahmood, A. and Chopp, M. (2015). Investigational agents for treatment of traumatic brain injury. Expert Opinion on Investigational Drugs 24, 743-760.

170. Ling, G.S.F., Hawley, J., Grimes, J., Macedonia, C., Hancock, J., Jaffee, M., Dombroski, T. and Ecklund, J.M. (2013). Traumatic brain injury in modern war. In: *SPIE*. Southern, S.O. (ed): Baltimore, MD, USA.

171. Povlishock, J.T. and Katz, D.I. (2005). Update of neuropathology and neurological recovery after traumatic brain injury. J Head Trauma Rehabil 20, 76-94.

172. Bidelspach, D. and Scholten, J. (2016). VA's TBI Screening and Evaluation Program. U.S. Department of Veterans Affairs: Mild TBI Diagnosis and Management Series.

173. Budde, M.D., Shah, A., McCrea, M., Cullinan, W.E., Pintar, F.A. and Stemper, B.D. (2013). Primary blast traumatic brain injury in the rat: relating diffusion tensor imaging and behavior. Frontiers in Neurology 4, 1-12.

174. Smith, M., Piehler, T., Benjamin, R., Farizatto, K.L., Pait, M.C., Almeida, M.F., Ghukasyan, V.V. and Bahr, B.A. (2016). Blast waves from detonated military explosive reduce GluR1 and synaptophysin levels in hippocampal slice cultures. Exp Neurol 286, 107-115.

175. Stemper, B.D., Shah, A.S., Budde, M.D., Olsen, C.M., Glavaski-Josimovic, A., Kurpad, S.N., McCrea, M. and Pintar, F.A. (2016). Behavioral outcomes differ between rotational acceleration and blast mechanisms of mild traumatic brain injury. Frontiers in Neurology 7, 1-13.

176. Effgen, G.B., Ong, T., Nammalwar, S., Ortuno, A.I., Meaney, D.F., Bass, C.R. and Morrison III, B. (2016). Primary blast exposure increases hippocampal vulnerability to subsequent exposure: reducing long-term potentiation. J Neurotrauma.

177. Morrison III, B., Meaney, D.F., Margulies, S.S. and McIntosh, T.K. (2000). Dynamic mechanical stretch of organotypic brain slice cultures induces differential genomic expression: relationship to mechanical parameters. J Biomech Eng 122, 224-230.

178. Pfister, B.J., Weihs, T.P., Betenbaugh, M. and Bao, G. (2003). An in vitro uniaxial stretch model for axonal injury. Annals of Biomedical Engineering 31, 589-598.

179. McAllister, T.W., Ford, J.C., Ji, S., Beckwith, J.G., Flashman, L.A., Paulsen, K. and Greenwald, R.M. (2012). Maximum principal strain and strain rate associated with concussion diagnosis correlates with changes in corpus callosum white matter indices. Annals of Biomedical Engineering 40, 127-140.

180. Lamy, M., Baumgartner, D., Yoganandan, N., Stemper, B.D. and Willinger, R. (2013). Experimentally validated three-dimensional finite element model of the rat for mild traumatic brain injury. Med Biol Eng Comput 51, 353-365.

181. Chen, Y.C., Mao, H., Yang, K.H., Abel, T. and Meaney, D.F. (2014). A modified controlled cortical impact technique to model mild traumatic brain injury mechanics in mice. Frontiers in Neurology 5, 1-14.

182. Yoganandan, N., Li, J., Zhang, J., Pintar, F.A. and Gennarelli, T.A. (2008). Influence of angular acceleration-deceleration pulse shapes on regional brain strains. J Biomech 41, 2253-2262.

183. Singh, D., Cronin, D.S. and Haladuick, T.N. (2014). Head and brain response to blast using sagittal and transverse finite element models. Int J Numer Meth Biomed Engng 30, 470-489.

184. Morrison, B., 3rd, Cater, H.L., Benham, C.D. and Sundstrom, L.E. (2006). An in vitro model of traumatic brain injury utilising two-dimensional stretch of organotypic hippocampal slice cultures. J Neurosci Methods 150, 192-201.

185. Alley, M.D., Schimizze, B.R. and Son, S.F. (2011). Experimental modeling of explosive blast-related traumatic brain injuries. NeuroImage 54, 545-554.

186. Sarnitoranont, M., Lee, S.J., Hong, Y., King, M.A., Subhash, G., Kwon, J. and Moore, D.F. (2012). High-strain-rate brain injury model using submerged acute rat brain tissue slice. J Neurotrauma 29, 418-429.

187. Chafi, M.S., G. Karami, M. Ziejewski (2010). Biomechanical Assessment of Brain Dynamic Responses Due to Blast Pressure Waves. Annals of Biomedical Engineering 38, 490-504.

188. Nyein, M.K., Jason, A.M., Pita, C.M., Johannopoulos, J.D., Moore, D.F. and Radovitzky, R.A. (2010). In silico investigation of intracranial blast mitigation with relevance to military traumatic brain injury. Proc Natl Acad Sci U S A 107, 20703-20708.

189. Zhu, F., Skelton, P., Chou, C.C., Mao, H., Yang, K.H. and King, A.I. (2013). Biomechanical responses of a pig head under blast loading: a computational simulation. Int J Numer Meth Biomed Engng 29, 392-407.

190. Suresh, K. and Regalla, S.R. (2014). Effect of mesh parameters in finite element simulation of single point incremental sheet forming process. Procedia Materials Science 6, 376-382.

191. Cargill, R.S. and Thibault, L.E. (1996). Acute alterations in [Ca 2+] i in NG108-15 cells subjected to high strain rate deformation and chemical hypoxia: an in vitro model for neural trauma. Journal of Neurotrauma 13, 396-407.

192. Ahmed, S.M., Weber, J.T., Liang, S., Willoughby, K.A., Sitterding, H.A., Rzigalinski, B.A. and Ellis, E.F. (2002). NMDA receptor activation contributes to a portion of the decreased mitochondrial membrane potential and elevated intracellular free calcium in strain-injured neurons. Journal of Neurotrauma 19, 1619-1629.

193. Geddes, D.M., Cargill, R.S. and LaPlaca, M.C. (2003). Mechanical stretch to neurons results in a strain rate and magnitude-dependent increase in plasma membrane permeability. J Neurotrauma 20, 1039-1049.

194. Lusardi, T.A., Wolf, J.A., Putt, M.E., Smith, D.H. and Meaney, D.F. (2004). Effect of acute calcium influx after mechanical stretch injury in vitro on the viability of hippocampal neurons. Journal of Neurotrauma 21, 61-72.

195. Morrison III, B., H.L. Cater, C.D. Benham, L.E. Sundstrom (2006). An in vitro model of traumatic brain injury utilising two-dimensional stretch of organotypic hippocampal slice cultures. Journal of Neuroscience Methods 150, 192-201.

196. Skotak, M., Wang, F. and Chandra, N. (2012). An *in vitro* injury model for SH-SY5Y neuroblastoma cells: effect of strain and strain rate. J Neurosci Methods 205, 159-168.

197. LaPlaca, M.C., Cullen, D.K., McLoughlin, J.J. and Cargill, R.S. (2005). High rate shear strain of three-dimensional neural cell cultures: a new in vitro traumatic brain injury model. Journal of Biomechanics 38, 1093-1105.

198. Bayly, P.V., Black, E.B., Pedersen, R.C., Leister, E.P. and Genin, G.M. (2006). In vivo imaging of rapid deformation and strain in an animal model of traumatic brain injury. J Biomech 39, 1086-1095.

199. Zhang, L., K.H. Yang, A.I. King (2001). Comparison of Brain Responses Between Frontal and Lateral Impacts by Finite Element Modeling. Journal of Neurotrauma 18, 21-30.

200. Takhounts, E., Ridella, S.A., Hasija, V., Tannous, R.E., Campbell, J.Q., Malone, D., Danelson, K., Stitzel, J., Rowson, S. and Duma, S. (2008). Investigation of traumatic brain injuries using the next generation of simulated injury monitor (SIMon) finite element head model. Stapp Car Crash Journal 52, 1-31.

201. Wright, R.M., Post, A., Hoshizaki, B. and Ramesh, K.T. (2013). A multiscale computational approach to estimating axonal damage under inertial loading of the head. J Neurotrauma 30, 102-118.

202. Cloots, R.J.H., van Dommelen, J.A.W., Kleiven, S. and Geers, M.G.D. (2013). Multi-scale mechanics of traumatic brain injury: predicting axonal strains from head loads. Biomech Model Mechanobiol 12, 137-150.

203. Mao, H., Zhang, L., Yang, K.H. and King, A.I. (2006). Application of a finite element model of the brain to study traumatic brain injury mechanisms in the rat. Stapp Car Crash Journal 50, 583-600.

204. Effgen, G.B. and Morrison III, B. (2016). Electrophysiological and pathological characterization of the period of heightened vulnerability to repetitive injury in an *in vitro* stretch model. J Neurotrauma In Press.

205. Kang, W.H. and Morrison III, B. (2015). Predicting changes in cortical electrophysiological function after in vitro traumatic brain injury. Biomech Model Mechanobiol, 1-12.

206. Barria, A., Derkach, V. and Soderling, T. (1997). Identification of the Ca^{2+}/calmodulin-dependent protein kinase II regulatory phosphorylation site in the α-amino-3-hydroxyl-5-methyl-4-isoxazole-propionate-type glutamate receptor. J Biol Chem 272, 32727-32730.

207. Gupta, R.K. and Prezekwas, A. (2013). Mathematical models of blast-induced TBI: current status, challenges, and prospects. Frontiers in Neurology 4, 1-21.

208. Elkin, B.S., Azeloglu, E.U., Costa, K.D. and Morrison III, B. (2007). Mechanical heterogeneity of the rat hippocampus measured by AFM indentation. Journal of Neurotrauma 24, 812-822.

209. Rashid, B., Destrade, M. and Gilchrist, M.D. (2014). Mechanical characterization of brain tissue in tension at dynamic strain rates. J Mech Behav Biomed Mater 33, 43-54.

210. Bain, A.C. and Meaney, D.F. (2000). Tissue-level thresholds for axonal damage in an experimental model of central nervous system white matter injury. J Biomech Eng 122, 615-622.

211. Cullen, D.K., Simon, C.M. and LaPlaca, M.C. (2007). Strain rate-dependent induction of reactive astrogliosis and cell death in three-dimensional neuronal-astrocytic co-cultures. Brain Research.

212. Kraft, R.H., Mckee, P.J., Dagro, A.M. and Grafton, S.T. (2012). Combining the finite element method with structural connectome-based analysis for modeling neurotrauma: connectome neurotrauma mechanics. PLoS Computational Biology 8, 1-15.

213. Lamprecht, M.R. and Morrison III, B. (2014). GPR30 activation is neither necessary nor sufficient for acute neuroprotection by 17β-estradiol after an ischemic injury in organotypic hippocampal slice cultures. Brain Res 1563, 131-137.

214. Keyes, D.C. (2005). Medical Response to Terrorism: Preparedness and Clinical Practice. Lippincott Williams & Wilkins: Philadelphia, PA, USA.

215. McIntosh, T.K., Vink, R., Noble, L., Yamakami, I., Fernyak, S., Soares, H. and Faden, A.L. (1989). Traumatic brain injury in the rat: Characterization of a lateral fluid-percusssion model. Neuroscience 28, 233-244.

216. Panzer, M.B., Matthews, K.A., Yu, A.W., Morrison, B., 3rd, Meaney, D.F. and Bass, C.R. (2012). A Multiscale Approach to Blast Neurotrauma Modeling: Part I - Development of Novel Test Devices for in vivo and in vitro Blast Injury Models. Frontiers in neurology 3, 46.

217. Effgen, G.B., Hue, C.D., Vogel, E., 3rd, Panzer, M.B., Meaney, D.F., Bass, C.R. and Morrison, B., 3rd (2012). A Multiscale Approach to Blast Neurotrauma Modeling: Part II: Methodology for Inducing Blast Injury to in vitro Models. Frontiers in neurology 3, 23.

218. Cater, H.L., Sundstrom, L.E. and Morrison, B., III (2006). Temporal development of hippocampal cell death is dependent on tissue strain but not strain rate. J Biomech 39, 2810-2818.

219. Morrison, B., III, Cater, H.L., Benham, C.D. and Sundstrom, L.E. (2006). An in vitro model of traumatic brain injury utilising two-dimensional stretch of organotypic hippocampal slice cultures. J Neurosci Meth 150, 192-201.

220. Morrison, B., III, Cater, H.L., Wang, C.C.-B., Thomas, F.C., Hung, C.T., Ateshian, G.A. and Sundstrom, L.E. (2003). A Tissue Level Tolerance Criterion for Living Brain Developed with an In Vitro Model of Traumatic Mechanical Loading. Stapp 47, 93-105.

221. Cater, H.L., Sundstrom, L.E. and Morrison, B., 3rd (2006). Temporal development of hippocampal cell death is dependent on tissue strain but not strain rate. J Biomech 39, 2810-2818.

222. Choi, J.H., Jung, H.K. and Kim, T. (2006). A new action potential detector using the MTEO and its effects on spike sorting systems at low signal-to-noise ratios. IEEE Trans Biomed Eng 53, 738-746.

223. Patel, T.P., Man, K., Firestein, B.L. and Meaney, D.F. (2015). Automated quantification of neuronal networks and single-cell calcium dynamics using calcium imaging. Journal of Neuroscience Methods 243, 26-38.

224. Li, X., Cui, D., Jiruska, P., Fox, J.E., Yao, X. and Jefferys, J.G. (2007). Synchronization measurement of multiple neuronal populations. J Neurophysiol 98, 3341-3348.

225. Li, X., Ouyang, G., Usami, A., Ikegaya, Y. and Sik, A. (2010). Scale-free topology of the CA3 hippocampal network: a novel method to analyze functional neuronal assemblies. Biophys J 98, 1733-1741.

226. Fueta, Y., Kawano, H., Ono, T., Mita, T., Fukata, K. and Ohno, K. (1998). Regional differences in hippocampal excitability manifested by paired-pulse stimulation of genetically epileptic El mice. Brain Res 779, 324-328.

227. Stanford, I.M., Wheal, H.V. and Chad, J.E. (1995). Bicuculline enhances the late GABAB receptor-mediated paired-pulse inhibition observed in rat hippocampal slices. Eur J Pharmacol 277, 229-234.

228. Margineanu, D.G. and Wulfert, E. (2000). Differential paired-pulse effects of gabazine and bicuculline in rat hippocampal CA3 area. Brain research bulletin 51, 69-74.

229. Joy, R.M. and Albertson, T.E. (1993). NMDA receptors have a dominant role in population spike-paired pulse facilitation in the dentate gyrus of urethane-anesthetized rats. Brain Res 604, 273-282.

230. DiScenna, P.G. and Teyler, T.J. (1994). Development of inhibitory and excitatory synaptic transmission in the rat dentate gyrus. Hippocampus 4, 569-576.

231. Commins, S., Gigg, J., Anderson, M. and O'Mara, S.M. (1998). Interaction between paired-pulse facilitation and long-term potentiation in the projection from hippocampal area CA1 to the subiculum. Neuroreport 9, 4109-4113.

232. Zucker, R.S. (1989). Short-term synaptic plasticity. Annual review of neuroscience 12, 13-31.

233. Hu, D., Cao, P., Thiels, E., Chu, C.T., Wu, G., Oury, T.D. and Klann, E. (2007). Hippocampal long-term potentiation, memory, and longevity in mice that overexpress mitochondrial superoxide dismutase. Neurobiology of Learning and Memory 87, 372-384.

234. Swant, J. and Wagner, J.J. (2006). Dopamine transporter blockade increases LTP in the CA1 region of the rat hippocampus via activation of the D3 dopamine receptor. Learn. Mem. 13, 161-167.

235. Heuschkel, M.O., Fejtl, M., Raggenbass, M., Bertrand, D. and Renaud, P. (2002). A three-dimensional multi-electrode array for multi-site stimulation and recording in acute brain slices. J Neurosci Methods 114, 135-148.

236. Axmacher, N., Mormann, F., Fernández, G., Elger, C.E. and Fell, J. (2006). Memory formation by neuronal synchronization. Brain Research Reviews 52, 170-182.

237. Thibault, L.E., Meaney, D.F., Anderson, B.J. and Marmarou, A. (1992). Biomechanical aspects of a fluid percussion model of brain injury. J Neurotrauma 9, 311-322.

238. Dixon, C.E., Lyeth, B.G., Povlishock, J.T., Findling, R.L., Hamm, R.J., Marmarou, A., Young, H.F. and Hayes, R.L. (1987). A fluid percussion model of experimental brain injury in the rat. Journal of Neurosurgery 67, 110-119.

239. Sponheim, S.R., McGuire, K.A., Kang, S.S., Davenport, N.D., Aviyente, S., Bernat, E.M. and Lim, K.O. (2011). Evidence of disrupted functional connectivity in the brain after combat-related blast injury. NeuroImage 54, 521-529.

240. Tsirka, V., Simos, P.G., Vakis, A., Kanatsouli, K., Vourkas, M., Erimaki, S., Pachou, E., Stam, C.J. and Micheloyannis, S. (2011). Mild traumatic brain injury: Graph-model characterization of brain networks for episodic memory. International Journal of Psychophysiology 79, 89-96.

241. Wang, X.J. (2001). Synaptic reverberation underlying mnemonic persistent activity. Trends in Neurosciences 24, 455-463.

242. Compte, A. (2006). Computational and *in vitro* studies of persistent activity: edging towards cellular and synaptic mechanisms of working memory. Neuroscience 139, 135-151.

243. Panzer, M.B., Wood, G.W. and Bass, C.R. (2014). Scaling in neurotrauma: How do we apply animal experiments to people? Experimental Neurology 261, 120-126.

244. Salin, P.A., Scanziani, M., Malenka, R.C. and Nicoll, R.A. (1996). Distinct short-term plasticity at two excitatory synapses in the hippocampus. Proceedings of the National Academy of Sciences 93, 13304-13309.

245. Schulz, P.E., Cook, E.P. and Johnston, D. (1994). Changes in paired-pulse facilitation suggests presynaptic involvement in long-term potentiation. Neuroscience 14, 5325-5337.

246. Wu, L.G. and Saggau, P. (1994). Presynaptic calcium is increased during normal synaptic transmission and paired-pulse facilitation, but not in long-term potentiation in area CA1 of hippocampus. Neuroscience 14, 645-654.

247. Schulz, P.E., Cook, E.P. and Johnston, D. (1995). Using paired-pulse facilitation to probe the mechanisms for long-term potentiation (LTP). J Physiol 89, 3-9.

248. Abdul-Muneer, P.M., Schuetz, H., Wang, F., Skotak, M., Jones, J., Gorantla, S., Zimmerman, M.C., Chandra, N. and Haorah, J. (2013). Induction of oxidative and nitrosative damage leads to cerebrovascular inflammation in an animal model of mild traumatic brain injury induced by primary blast. Free Radical Biology and Medicine 60, 282-291.

249. Yeoh, S., Bell, E.D. and Monson, K.L. (2013). Distribution of Blood–Brain Barrier Disruption in Primary Blast Injury. Annals of Biomedical Engineering 41, 2206-2214.

250. Hue, C.D., Cao, S., Bass, C.R., Meaney, D.F. and Morrison III, B. (2014). Repeated primary blast injury causes delayed recovery, but not additive disruption, in an in vitro blood-brain barrier model. J Neurotrauma 31, 951-960.

251. Morrison III, B., B.S. Elkin, J Dolle, M.L Yarmush (2011). In Vitro Models of Traumatic Brain Injury. Annual Reviews of Biomedical Engineering 13, 91-126.

252. Walls, M.K., Race, N., Zheng, L., Vega-Alvarez, S.M., Acosta, G., Park, J. and Shi, R. (2015). Structural and biochemical abnomalities in the absence of acute deficits in mild primary blast-induced head trauma. J Neurosurg, 1-12.

253. Davis, S., Butcher, S.P. and Morris, R.G.M. (1992). The NMDA receptor antagonist D-2-amino-5-phosphonopentanoate (D-AP5) impairs spatial learning and LTP in vivo at intracerebral concentrations comparable to those that block LTP in vitro J Neurosci 12, 21-34.

254. Takahashi, T., Svoboda, K. and Malinow, R. (2003). Experience strengthening transmission by driving AMPA receptors into synapses. Science 299, 1585-1588.

255. Sick, T.J., Perez-Pinzon, M.A. and Feng, Z.Z. (1998). Impaired expression of long-term potentiation in hippocampal slices 4 and 48h following mild fluid-percussion brain injury in vivo. Brain Res 785, 287-292.

256. Norris, C.M. and Scheff, S.W. (2009). Recovery of afferent function and synaptic strength in hippocampal CA1 following traumatic brain injury. J Neurotrauma 26, 2269-2278.

257. Lu, W., Man, H., Ju, W., Trimble, W.S., MacDonald, J.F. and Wang, Y.T. (2001). Activation of synaptic NMDA receptors induces membrane insertion of new AMPA receptors and LTP in cultured hippocampal neurons. Neuron 29, 243-254.

258. Otmakhov, N., Khibnik, L., Otmakhova, N., Carpenter, S.R., S., Asrican, B. and Lisman, J. (2004). Forskolin-Induced LTP in the CA1 Hippocampal Region is NMDA Receptor Dependent. J Neurophysiol 91, 1955-1962.

259. Sanhueza, M., Fernandez-Villalobos, G., Stein, I.S., Kasumova, G., Zhang, P., Bayer, K.U., Otmakhov, N., Hell, J.W. and Lisman, J. (2011). Role of CaMKII/NMDA receptor complex in the maintenance of synaptic strength. J Neurosci 31, 9170-9178.

260. Liao, D., Scannevin, R.H. and Huganir, R.L. (2001). Activation of silent synapses by rapid activity-dependent synaptic recruitment of AMPA receptors. Neuroscience 21, 6008-6017.

261. Kopec, C.D., Li, B., Wei, W., Boehm, J. and Malinow, R. (2006). Glutamate Receptor Exocytosis and Spine Enlargement during Chemically Induced Long-Term Potentiation. Journal of Neuroscience 26, 2000-2009.

262. Spaethling, J.M., Le, L. and Meaney, D.F. (2012). NMDA receptor mediated phosphorylation of GluR1 subunits contributes to the appearance of calcium-permeable AMPA receptors after mechanical stretch injury. Neurobiology of disease 46, 646-654.

263. Bigford, G.E., Alonso, O.F., Dietrich, W.D. and Keane, R.W. (2009). A novel protein complex in membrane rafts linking the NR2B glutamate receptor and autophagy is disrupted following traumatic brain injury. J Neurotrauma 26, 703-720.

264. Park, Y., Luo, T., Zhang, F., Liu, C., Bramlett, H.M., Dietrich, W.D. and Hu, B. (2013). Downregulation of Src-kinase and glutamate-receptor phosphorylation after traumatic brain injury. J Cereb Blood Flow Metab 33, 1642-1649.

265. Nicoll, R.A. and Malenka, R.C. (1995). Contrasting properties of two forms of long-term potentiation in the hippocampus. Nature 377, 115-118.

266. Atkins, C.M., Chen, S., Alonso, O.F., Dietrich, W.D. and Hu, B.R. (2006). Activation of calcium/calmodulin-dependent protein kinases after traumatic brain injury. J Cereb Blood Flow Metab 26, 1507-1518.

267. Ehrlich, I. and Malinow, R. (2004). Postsynaptic density 95 controls AMPA receptor incorporation during long-term potentiation and experience-driven synaptic plasticity. J Neurosci 24, 916-927.

268. Campbell, J.N., Low, B., Kurz, J.E., Patel, S.S., Young, M.T. and Churn, S.B. (2012). Mechanisms of dendritic spine remodeling in a rat model of traumatic brain injury. J Neurotrauma 29, 218-234.

269. Bats, C., Groc, L. and Choquet, D. (2007). The interaction between stargazin and PSD-95 regulates AMPA receptor surface trafficking. Neuron 53, 719-734.

270. Colledge, M., Snyder, E.M., Crozier, R.A., Soderling, J.A., Jin, Y., Langeberg, L.K., Lu, H., Bear, M.F. and Scott, J.D. (2003). Ubiquitination regulates PSD-95 degradation and AMPA receptor surface expression. Neuron 40, 595-607.

271. Rigg, J.L. and Mooney, S.R. (2011). Concussions and the military: Issues specific to service members. PM R 3, S380-S386.

272. Tecoma, E.S., Monyer, H., Goldberg, M.P. and Choi, D.W. (1989). Traumatic neuronal injury *in vitro* is attenuated by NMDA antagonists. Neuron 2, 1541-1545.

273. Kontos, A.P., Kotwal, R.S., Elbin, R.J., Lutz, R.H., Forsten, R.D., Benson, P.J. and Guskiewicz, K.M. (2013). Residual effects of combat-related mild traumatic brain injury. J Neurotrauma 30, 680-686.

274. Cernak, I., Wang, Z., Jiang, J., Bian, X. and Savic, J. (2001). Ultrastructural and functional characteristics of blast injury-induced neurotrauma. J Trauma 50, 695-706.

275. Huber, B.R., Meabon, J.S., Martin, T.J., Mourad, P.D., Bennett, R., Kraemer, B.C., Cernak, I., Petrie, E.C., Emery, M.J., Swenson, E.R., Mayer, C., Mehic, E., Peskind, E.R. and Cook, D.G. (2013). Blast exposure causes early and persistent aberrant phospho- and cleaved-tau expression in a murine model of mild blast-induced traumatic brain injury. J Alzheimer's Disease 37, 309-323.

276. Mammen, A.L., Kameyama, K., Roche, K.W. and Huganir, R.L. (1997). Phosphorylation of the a-Amino-3-hydroxy-5-methylisoxazole-4-propionic Acid Receptor GluR1 Subunit by Calcium/Calmodulin-dependent Kinase II. J Biol Chem 272, 32528-32533.

277. Lee, H., Barbarosie, M., Kameyama, K., Bear, M.F. and Huganir, R.L. (2000). Regulation of distinct AMPA receptor phosphorylation sites during bidirectional synaptic plasticity. Nature 405, 955-959.

278. Gong, B., Vitolo, O.V., Trinchese, F., Liu, S., Shelanski, M. and Arancio, O. (2004). Persistent improvement in synaptic and cognitive functions in an Alzheimer mouse model after rolipram treatment. J Clin Invest 114, 1624-1634.

279. Maxwell, C.R., Kanes, S.J., Abel, T. and Siegel, S.J. (2004). Phosphodiesterase inhibitors: a novel mechanism for receptor-independent antipsychotic medications. Neuroscience 129, 101-107.

280. Smith, D.L., Pozueta, J., Gong, B., Arancio, O. and Shelanski, M. (2009). Reversal of long-term dendritic spine alterations in Alzheimer disease models. Proc Natl Acad Sci U S A 106, 16877-16882.

281. Wiescholleck, V. and Manahan-Vaughan, D. (2012). PDE4 inhibition enhances hippocampal synaptic plasticity *in vivo* and rescues MK801-induced impairment of long-term potentiation and object recognition memory in an animal model of psychosis. Transl Psychiatry 2.

282. Silverberg, N.D., Crane, P.K., Dams-O'Connor, K., Holdnack, J., Ivins, B.J., Lange, R.T., Manley, G.T., McCrea, M. and Iverson, G.L. (2016). Developing a cognition endpoint for traumatic brain injury clinical trials. J Neurotrauma.

283. Cherry, J.A. and Davis, R.L. (1999). Cyclic AMP phosphodiesterases are localized in regions of the mouse brain associated wiht reinforcement, movement, and affect. Journal of Comparative Neurology 407, 287-301.

284. Perez-Torres, S., Miro, X., Palacios, J.M., Cortes, R., Puigdomenech, P. and Mengod, G. (2000). Phosphodiesterase type 4 isozymes expression in human brain examined by in situ hybridization histochemistry and [^{3}H]rolipram binding autoradiography comparison with monkey and rat brain. Journal of Chemical Neuroanatomy 20, 349-374.

285. Ahmed, T. and Frey, J.U. (2003). Expression of the specific type IV phosphodiesterase gene *PDE4B3* during different phases of long-term potentiation in single hippocampal slices of rats *in vitro*. Neuroscience 117, 627-638.

286. Seeger, T.F., Bartlett, B., Coskran, T.M., Culp, J.S., James, L.C., Krull, D.L., Lanfear, J., Ryan, A.M., Schmidt, C.J., Strick, C.A., Varghese, A.H., Williams, R.D., Wylie, P.G. and Menniti, F.S. (2003). Immunohistochemical localization of PDE10A in the rat brain. Brain Res 985, 113-126.

287. Kim, M.J., Futai, K., Jo, J., Hayashi, Y., Cho, K. and Sheng, M. (2007). Synaptic accumulation of PSD-95 and synaptic function regulated by phosphorylation of serine-295 of PSD-95. Neuron 56, 488-502.

288. Dhillon, H.S., Yang, L., Padmaperuma, B., Dempsey, R.J., Fiscus, R.R. and Prasad, M.R. (1995). Regional concentrations of cyclic nucleotides after experimental brain injury. J Neurotrauma 12, 1035-1043.

289. Wilson, N.M., Titus, D.J., Oliva Jr, A.A., Furones, C. and Atkins, C.M. (2016). Traumatic brain injury upregulates phosphodiesterase expression in the hippocampus. Frontiers in Systems Neuroscience 10.

290. Eakin, K., Li, Y., Chiang, Y.H., Hoffer, B.J., Rosenheim, H., Greig, N.H. and Miller, J.P. (2013). Exendin-4 ameliorates traumatic brain injury-induced cognitive impairments in rats. PLoS One 8, 82016.

291. Randt, C.T., Judge, M.E., Bonnet, K.A. and Quatermain, D. (1982). Brain cyclic AMP and memory in mice. Pharmacol.Biochem.Behav. 17, 677-680.

292. Rutten, K., Misner, D.L., Works, M., Blokland, A., Novak, T.J., Santarelli, L. and Wallace, T.L. (2008). Enhanced long-term potentiation and impaired learning in phosphodiesterase 4D-knockout (*PDE4D*$^{-/-}$) mice. Eur.J Neurosci. 28, 625-632.

293. Titus, D.J., Wilson, N.M., Freund, J.E., Carballosa, M.M., Sikah, K.E., Furones, C., Dietrich, W.D., Gurney, M.E. and Atkins, C.M. (2016). Chronic cognitive dysfunction after traumatic brain injury is improved with a phoshodiesterase 4B inhibitor. J Neurosci 36, 7095-7108.

294. Mizuno, T., Kurotani, T., Komatsu, Y., Kawanokuchi, J., Kato, H., Mitsuma, N. and Suzumura, A. (2004). Neuroprotective role of phosphodiesterase inhibitor ibudilast on neuronal cell death induced by activated microglia. Neuropharmacology 46, 404-411.

295. Wang, K.K.W., Larner, S.F., Robinson, G. and Hayes, R.L. (2006). Neuroprotection targets after traumatic brain injury. Curr Opin Neurol 19, 514-519.

296. Castro, L.R.V., Gervasi, N., Guiot, E., Cavellini, L., Nikolaeva, V.O., Paupardin-Tritsch, D. and Vincent, P. (2010). Type 4 phosphodiesterase plays different integrating roles in different cellular domains in pyramidal cortical neurons. J Neurosci 30, 6143-6151.

297. Niedringhaus, M., Chen, X., Conant, K. and Dzakpasu, R. (2013). Synaptic potentiation facilitates memory-like attractor dynamics in cultured *in vitro* hippocampal networks. PLoS One 8, e57144.

298. Oh, M.C., Derkach, V.A., Guire, E.S. and Soderling, T.R. (2006). Extrasynaptic membrane trafficking regulated by GluR1 serine phosphorylation primes AMPA receptors for long-term potentiation. J Biol Chem 281, 752-758.

299. Andreetta, F., Carboni, L., Grafton, G., Jeggo, R., Whyment, A.D., van den Top, M., Hoyer, D., Spanswick, D. and Barnes, N.M. (2016). Hippocampal 5-HT_7 receptors signal phosphorylation of the GluA1 subunit to facilitate AMPA receptor mediated neurotransmission *in vitro* and *in vivo*. British Journal of Pharmacology 173, 1438-1451.

300. Ribeiro, L.F., Catarino, T., Santos, S.D., Benoist, M., van Leeuwen, J.F., Esteban, J.A. and Carvalho, A.L. (2013). Ghrelin triggers the synaptic incorporation of AMPA receptors in the hippocampus. Proc Natl Acad Sci U S A 111, 149-158.

301. Roberson, E.D., English, J.D., Adams, J.P., Selcher, J.C., Kondratick, C. and Sweatt, J.D. (1999). The mitogen-activated protein kinase cascade couples PKA and PKC to cAMP response element binding protein phosphorylation in area CA1 of hippocampus. J Neurosci 19, 4337-4348.

302. Mao, L., Tang, Q. and Wang, J.Q. (2007). Protein kinase C-regulated cAMP response element-binding protein phosphorylation in cultured rat striatal neurons. Brain research bulletin 72, 302-308.

303. Baker, W.E. (1973). Explosions in air. University of Texas Press: Austin, TX.

304. Leonardi, A.D.C., Keane, N.J., Bir, C.A., Ryan, A.G., Xu, B. and VandeVord, P.J. (2012). Head orientation affects the intracranial pressure response resulting from shock wave loading in the rat. J Biomech 45, 2595-2602.

305. Taber, K.H., Hurley, R.A., Haswell, C.C., Rowland, J.A., Hurt, S.D., Lamar, C.D. and Morey, R.A. (2015). White matter compromise in veterans exposed to primary blast forces. J Head Trauma Rehabil 30, E15-E25.

306. Sawyer, T.W., Wang, Y., Ritzel, D.V., Josey, T., Villanueva, M., Shei, Y., Nelson, P., Hennes, G., Weiss, T., Vair, C., Fan, C. and Barnes, J. (2016). High-fidelity simulation of primary blast: direct effects on the head. J Neurotrauma 33, 1181-1193.

307. Abbott, N.J. and Friedman, A. (2012). Overview and introduction: the blood-brain barrier in health and disease. Epilepsia 53, 1-6.

308. Tate, C.M., Wang, K.K.W., Eonta, S., Zhang, Y., Carr, W., Tortella, F.C., Hayes, R.L. and Kamimori, G.H. (2013). Serum Brain Biomarker Level, Neurocognitive Performance, and Self-Reported Symptom Changes in Soldiers Repeatedly Exposed to Low Level Blast: A Breacher Pilot Study. J Neurotrauma 30, 1620-1630.

309. Rosenfeld, J.V., McFarlane, A.C., Bragge, P., Armonda, R.A., Grimes, J.B. and Ling, G.S. (2013). Blast-related traumatic brain injury. The Lancet Neurology 12, 882-893.

310. Karr, J.E., Areshenkoff, C.N., Duggan, E.C. and Garcia-Barrera, M.A. (2014). Blast-related mild traumatic brain injury: a bayesian random-effects meta-analysis on the cognitive outcomes of concussion among military personnel. Neuropsychol Rev 24, 428-444.

311. Stocker, R.P.J., Cieply, M.A., Paul, B., Khan, H., Henry, L., Kontos, A.P. and Germain, A. (2014). Combat-related blast exposure and traumatic brain injury influence brain glucose metabolism during REM sleep in military veterans. NeuroImage 99, 207-214.

312. Perez-Garcia, G., Sosa, M.A.G., De Gasperi, R., Lashof-Sullivan, M., Maudlin-Jeronimo, E., Stone, J.R., Haghighi, F., Ahlers, S.T. and Elder, G.A. (2016). Chronic post-traumatic stress disorder-related traits in a rat model of low-level blast exposure. Behavioural Brain Research In press.

313. Svetlov, S.I., Prima, V., Glushakova, O., Svetlov, A., Kirk, D.R., Gutierrez, H., Serebruany, V.L., Curley, K.C., Wang, K.K.W. and Hayes, R.L. (2012). Neuro-glial and systemic mechanisms of pathological responses in rat models of primary blast overpressure compared to "composite" blast. Frontiers in Neurology 3, 1-12.

314. Ning, Y.L., Yang, N., Chen, X., Zhao, Z.A., Chen, X.Y., Li, P., Zhao, Y. and Zhou, Y.G. (2015). Chronic caffeine exposure attenuates blast-induced memory deficit in mice. Chinese Journal of Traumatology 18, 204-211.

315. Hoffer, M.E., Balaban, C., Slade, M.D., Tsao, J.W. and Hoffer, B. (2013). Amelioration of acute sequelae of blast induced mild traumatic brain injury by N-acetyl cysteine: a double-blind, placebo controlled study. PLoS One 8, 1-10.

316. Zafarullah, M., Li, W.Q. and Ahmad, M. (2003). Molecular mechanisms of N-acetylcysteine actions. Cellular and Molecular Life Sciences 60, 6-20.

317. Robillard, J.M., Gordon, G.R., Choi, H.B., Christie, B.R. and MacVicar, B.A. (2011). Glutathione restores the mechanism of synaptic plasticity in aged mice to that of the adult. PLoS One 6, 1-7.

318. Esteban, J.A., Shi, S., Wilson, C., Nuriya, M., Huganir, R.L. and Malinow, R. (2003). PKA phosphorylation of AMPA receptor subunits controls synaptic trafficking underlying plasticity. Nat Neurosci 6, 136-143.

319. Hayashi, Y., Shi, S.H., Esteban, J.A., Piccini, A., Poncer, J.C. and Malinow, R. (2000). Driving AMPA receptors into synapses by LTP and CaMKII: Requirement for GluR1 and PDZ domain interaction. Science 287, 2262-2267.

320. Lisman, J., Schulman, H. and Cline, H. (2002). The molecular basis of CaMKII function in synaptic and behavioural memory. Nat Neurosci 3, 175-190.

321. El-Husseini, A.E.D., Schnell, E., Chetkovich, D.M., Nicoll, R.A. and Bredt, D.S. (2000). PSD-95 involvement in maturation of excitatory synapses. Science 290, 1364-1368.

322. Choi, J., Ko, J., Park, E., Lee, J.R., Yoon, J., Lim, S. and Kim, E. (2002). Phosphorylation of stargazin by protein kinase A regulates its interaction with PSD-95. J Biol Chem 277, 12359-12363.

323. Schnell, E., Sizemore, M., Karlmazadegan, S., Chen, L., Bredt, D.S. and Nicoll, R.A. (2002). Direct interactions between PSD-95 and stargazin control synaptic AMPA receptor number. Proc Natl Acad Sci U S A 99, 13902-13907.

324. Meabon, J.S., Huber, B.R., Cross, D.J., Richards, T.L., Minoshima, S., Pagulayan, K.F., Li, G., Meeker, K.D., Kraemer, B.C., Petrie, E.C., Raskind, M.A., Peskind, E.R. and Cook, D.G. (2016). Repetitive blast exposure in mice and combat veterans causes persistent cerebellar dysfunction. Science Translational Medicine 8, 1-15.

325. Bingol, B. and Schuman, E.M. (2005). Synaptic protein degradation by the ubiquitin proteasome system. Curr Opin Neurobio 15, 536-541.

326. Ehlers, M.D. (2003). Activity level controls postsynaptic composition and signaling via the ubiquitin-proteasome system. Nat Neurosci 6, 231-242.

327. Foley, A.G., Hartz, B.P., Gallagher, H.C., Ronn, L.C.B., Berezin, V., Bock, E. and Regan, C.M. (2000). A synthetic peptide ligand of neural cell adhesion molecule (NCAM) IgI domain

prevents NCAM internalization and disrupts passive avoidance learning. J Neurochem 74, 2607-2613.

328. Carr, W., Yarnell, A.M., Ong, R., Walilko, T., Kamimori, G.H., da Silva, U., McCarron, R.M. and LoPresti, M.L. (2015). Ubiquitin carboxy-terminal hydrolase-L1 as a serum neurotrauma biomarker for exposure to occupational low-level blast. Frontiers in Neurology 6, 1-11.

329. Yao, X., Liu, J. and McCabe, J.T. (2007). Ubiquitin and ubiquitin-conjugated protein expression in the rat cerebral cortex and hippocampus following traumatic brain injury (TBI). Brain Res 1182, 116-122.

330. Papa, L., Akinyi, L., Liu, M.C., Pineda, J.A., Tepas III, J.J., Oli, M.W., Zheng, W., Robinson, G., Robicsek, S.A., Gabrielli, A., Heaton, S.C., Hannay, H.J., Demery, J.A., Brophy, G.M., Layon, J., Robertson, C.S., Hayes, R.L. and Wang, K.K.W. (2010). Ubiquitin c-terminal hydrolase is a novel biomarker for humans for severe traumatic brain injury. Crit Care Med 38, 138-144.

331. Liu, M.C., Akinyi, L., Scharf, D., Mo, J., Larner, S.F., Muller, U., Oli, M.W., Zheng, W.R., Kobeissy, F., Papa, L., Lu, X.C., Dave, J.R., Tortella, F.C., Hayes, R.L. and Wang, K.K.W. (2010). Ubiquitin c-terminal hydrolase-L1 as a biomarker for ischemic and traumatic brain injury in rats. Eur J Pharma 31, 722-732.

332. Brophy, G.M., Mondello, S., Papa, L., Robicsek, S.A., Gabrielli, A., Tepas III, J.J., Buki, A., Robertson, C., Tortella, F.C., Hayes, R.L. and Wang, K.K.W. (2011). Biokinetic analysis of ubiquitin c-terminal hydrolase-L1 (UCH-L1) in severe traumatic brain injury patient biofluids. J Neurotrauma 28, 861-870.

333. Berger, R.P., Hayes, R.L., Richichi, R., Beers, S.R. and Wang, K.K.W. (2012). Serum concentrations of ubiquitin c-terminal hydrolase-L1 and αII-spectrin breakdown product 145 kDa correlate with outcome after pediatric TBI. J Neurotrauma 29, 162-167.

334. Diaz-Arrastia, R., Wang, K.K.W., Papa, L., Sorani, M.D., Yue, J.K., Puccio, A.M., McMahon, P.J., Inoue, T., Yuh, E.L., Lingsma, H.F., Maas, A.I.R., Valadka, A.B., Okonkwo, D.O., Manley, G.T., Casey, S.S., Cheong, M., Cooper, S.R., Dams-O'Connor, K., Gordon, W.A., Hricik, A.J., Menon, D.K., Mukherjee, P., Schnyer, D.M., Sinha, T.K. and Vassar, M.J. (2014). Acute biomarkers of traumatic brain injury: relationship between plasma levels of ubiquitin c-terminal hydolase-L1 and glial fibrillary acidic protein. J Neurotrauma 31, 19-25.

335. Hino, S.I., Tanji, C., Nakayama, K.I. and Kikuchi, A. (2005). Phosphorylation of β-catenin by cyclic AMP-dependent protein kinase stabilizes β-catenin through inhibition of its ubiquitination. Mol Cell Bio 25, 9063-9072.

336. Coghlan, V.M., Perrino, B.A., Howard, M., Langeberg, L.K., Hicks, J.B., Gallatin, W.M. and Scott, J.D. (1995). Association of protein kinase A and protein phosphatase 2B with a common anchoring protein. Science 267, 108-111.

337. Banke, T.G., Bowie, D., Lee, H.K., Huganir, R.L., Schousboe, A. and Traynelis, S.F. (2000). Control of GluR1 AMPA receptor function by cAMP-dependent protein kinase. J Neurosci 20, 89-102.

338. Tavalin, S.J., Colledge, M., Hell, J.W., Langeberg, L.K., Huganir, R.L. and Scott, J.D. (2002). Regulation of GluR1 by the A-kinase anchoring protein 79 (AKAP79) signaling complex shares properties with long-term depression. J Neurosci 22, 3044-3051.

339. Dell'Acqua, M.L., Dodge, K.L., Tavalin, S.J. and Scott, J.D. (2002). Mapping the protein phosphatase-2B anchoring site on AKAP79. J Biol Chem 277, 48796-48802.

340. Ehlers, M.D. (2000). Reinsertion or degradation of AMPA receptors determined by activity-dependent endocytic sorting. Neuron 28, 511-525.

341. Gomez, L.L., Alam, S., Smith, K.E., Horne, E. and Dell'Acqua, M.L. (2002). Regulation of A-kinase anchoring protein 79/150-cAMP-dependent protein kinase postsynaptic targeting by NMDA receptror activation of calcineurin and remodeling of dendritic actin. J Neurosci 22, 7027-7044.

342. Bales, J.W., Ma, X., Yan, H.Q., Jenkins, L.W. and Dixon, C.E. (2010). Regional calcineurin subunit B isoform expression in rat hippocampus following a traumatic brain injury. Brain Res 1358, 211-220.

343. Kurz, J.E., Hamm, R.J., Singleton, R.H., Povlishock, J.T. and Churn, S.B. (2005). A persistent change in subcellular distribution of calcineurin following fluid percussion injury in the rat. Brain Res 1048, 153-160.

344. Raman, I.M., Tong, G. and Jahr, C.E. (1996). β-adrenergic regulation of synaptic NMDA receptors by cAMP-dependent protein kinase. Neuron 16, 415-427.

345. Heinzelmann, M., Reddy, S.Y., French, L.M., Wang, D., Lee, H., Barr, T., Baxter, T., Mysliwiec, V. and Gill, J. (2014). Military personnel with chronic symptoms following blast traumatic brain injury have differential expression of neuronal recovery and epidermal growth factor receptor genes. Frontiers in Neurology 5, 1-9.

346. Thal, S.C., Schaible, E.V., Neuhaus, W., Scheffer, D., Brandsetter, M., Englehard, K., Wunder, C. and Forster, C.Y. (2013). Inhibition of proteasomal glucocorticoid receptor degradation restores dexamethasone-mediated stabilization of the blood-brain barrier after traumatic brain injury. Crit Care Med 41, 1305-1315.

347. Myeku, N., Wang, H. and Figueiredo-Pereira, M.E. (2012). cAMP stimulates the ubiquitin/proteasome pathway in rat spinal cord neurons. Neuroscience Letters 527, 126-131.

348. Hamakubo, T., Kannagi, R., Murachi, T. and Matus, A. (1986). Distribution of calpains I and II in rat brain. J Neurosci 6, 3103-3111.

349. Higuchi, M., Tomioka, M., Takano, J., Shirotani, K., Iwata, N., Masumoto, H., Maki, M., Itohara, S. and Saido, T.C. (2005). Distinct mechanistic roles of calpain and caspase activation in neurodegeneration as revealed in mice overexpressing their specific inhibitors. J Biol Chem 280, 15229-15237.

350. Jourdi, H., Lu, X., Yanagihara, T., Lauterborn, J.C., Bi, X., Gall, C.M. and Baudry, M. (2005). Prolonged positive modulation of α-amino-3-hydroxy-5-methyl-4-isoxazolepropionic Acid (AMPA) receptors induces calpain-mediated PSD-95/Dlg/ZO-1 protein degradation and AMPA receptor down-regulation in cultured hippocampal slices. J Pharmacol Exp Ther 314, 16-26.

351. Lu, X., Rong, Y. and Baudry, M. (2000). Calpain-mediated degradation of PSD-95 in developing and adult rat brain. Neuroscience Letters 286, 149-153.

352. Lu, X., Rong, Y., Bi, R. and Baudry, M. (2000). Calpain-mediated truncation of rat brain AMPA receptors increases their Triton X-100 solubility. Brain Res 863, 143-150.

353. Johnson, G.V.W., Litersky, J.M. and Jope, R.S. (1991). Degradation of microtubule-assocated protein 2 and brain spectrin by calpain: a comparative study. J Neurochem 56, 1630-1638.

354. Sedarous, M., Keramaris, E., O'Hare, M., Melloni, E., Slack, R.S., Elce, J.S., Greer, P.A. and Park, D.S. (2003). Calpains mediate p53 activation and neuronal death evoked by DNA damage. J Biol Chem 278, 26031-26038.

355. Logsdon, A.F., Turner, R.C., Lucke-Wold, B.P., Robson, M.J., Naser, Z.J., Smith, K.E., Matsumoto, R.R., Huber, J.D. and Rosen, C.L. (2014). Altering endoplasmic reticulum stress in a model of blast-induced traumatic brain injury controls cellular fate and ameliorates neuropsychiatric symptoms. Frontiers in Cellular Neuroscience 9, 1-14.

356. Posmantur, R., A. Kampfl, R. Siman, J. Liu, X. Zhao, G.L. Clifton, R.L. Hayes (1997). A calpain inhibitor attenuates cortical cytoskeletal protein loss after experimental traumatic brain injury in the rat. Neuroscience 77, 875-888.

357. Hall, E.D., Sullivan, P.G., Gibson, T.R., Pavel, K.M., Thompson, B.M. and Scheff, S.W. (2005). Spatial and temporal characteristics of neurodegeneration after controlled cortical impact in mice: more than a focal brain injury. J Neurotrauma 22, 252-265.

358. Saatman, K.E., H. Murai, R.T. Bartus, D.H. Smith, N.J. Hayward, B.R. Perri, T.K. McIntosh (1996). Calpain inhibitor AK295 attenuates motor and cognitive deficits following experimental brain injury in the rat. Proceedings of the National Academy of Science USA 93, 3428-3433.

359. Liang, Z., Liu, F., Grundke-Iqbal, I., Iqbal, K. and Gong, C.X. (2007). Down-regulation of cAMP-dependent protein kinase by over-activated calpain in Alzheimer disease brain. J Neurochem 103, 2462-2470.

360. Cuadrado-Tejedor, M., Hervias, I., Ricobaraza, A., Puerta, E., Perez-Roldan, J.M., Garcia-Barroso, C., Franco, R., Aguirre, N. and Garcia-Osta, A. (2011). Sildenafil restores cognitive function without affecting β-amyloid burden in an mouse model of Alzheimer's disease. British Journal of Pharmacology 164, 2029-2041.

361. Zhang, J. and Mahmood, G. (2016). Compositions and methods utilizing phosphodiesterase inhibitors to treat blast-induced tinnitus and/or hearing loss. USPTO (ed). Wayne State University: USA.

362. French, L., McCrea, M. and Baggett, M. (2003). The Military Acute Concussion Evaluation (MACE). Journal of Special Operations Medicine 8, 68-77.

363. McCrea, M., Iverson, G.L., Echemendia, R.J., Makdissi, M. and Raftery, M. (2013). Day of injury assessment of sport-related concussion. British Journal of Sports Medicine 47, 242-284.

364. Kelly, M.P., Coldren, R.L., Parish, R.V., Dretsch, M.N. and Russell, M.L. (2012). Assessment of acute concussion in the combat environment. Archives of Clinical Neuropsychology 27, 375-388.

365. Maruta, J., Suh, M., Niogi, S.N., Mukherjee, P. and Ghajar, J. (2010). Visual tracking synchronization as a metric for concussion screening. J Head Trauma Rehabil 25, 293-305.

366. Duckworth, J.L., Ling, G.S.F. and Rodgers, J. (2012). Blast gauge: quantifying exposure during an improvised explosive device attack. In: *Neurocritical Care Society 10th Annual Meeting*. Neurocrit Care: Denver, CO, pps. S84.

367. Guskiewicz, K.M., McCrea, M. and Marshall, S.W. (2003). Cumulative effects associated with recurrent concussion in collegiate football players: The NCAA concussion study. Journal of the American Medical Association 290, 2549-2555.

368. McCrea, M., Guskiewicz, K., Randolph, C., Barr, W.B., Hammeke, T.A., Marshall, S.W. and Kelly, J.P. (2009). Effects of a symptom-free waiting period on clinical outcome and risk of reinjury after sport-related concussion. Neurosurgery 65, 876-882.

369. Giza, C.C. and Hovda, D.A. (2001). The neurometabolic cascade of concussion. Journal of Athletic Training 36, 228-235.

370. Group, T.M.o.C.m.W. (2009). VA/DoD Clinical Practice Guideline for Management of Concussion/Mild Traumatic Brain Injury. Affairs, D.o.V., Defense, D.o. (eds): Washington D.C.

371. Vagnozzi, R., Signoretti, S., Tavazzi, B., Floris, R., Ludovici, A., Marziali, S., Tarascio, G., Amorini, A.M., Di Pietro, V., Delfini, R. and Lazzarino, G. (2008). Temporal window of metabolic brain vulnerability to concussion: a pilot ^{1}H-magnetic resonance spectroscopic study in concussed athletes - part III. Neurosurgery 62, 1286-1296.

372. Slobounov, S., Slobounov, E., Sebastianelli, W., Cao, C. and Newell, K. (2007). Differential rate of recovery in athletes after first and second concussion episodes. Neurosurgery 61, 338-344.

373. Prichep, L.S., McCrea, M., Barr, W., Powell, M. and Chabot, R.J. (2013). Time course of clinical electrophysiological recovery after sport-related concussion. J Head Trauma Rehabil 28, 266-273.

374. Reeves, T.M., Lyeth, B.G. and Povlishock, J.T. (1995). Long-term potentiation deficits and excitability changes following traumatic brain injury. Exp Brain Res 106, 248-256.

375. Flierl, M.A., Stahel, P.F., Beauchamp, K.M., Morgan, S.J., Smith, W.R. and Shohami, E. (2009). Mouse closed head injury model induced by a weight-drop device. Nature Protocols 4, 1328-1337.

376. Gawande, A. (2004). Casualties of war - military care for the wounded from Iraq and Afghanistan. The New England Journal of Medicine 352, 2471-2475.

377. Mabry, R.L., Holcomb, J.B., Baker, A.M., Cloonan, C.C., Uhorchak, J.M., Perkins, D.E., Canfield, A.J. and Hagmann, J.H. (2000). United States Army Rangers in Somalia: an analysis of combat casualties on an urban battlefield. J Trauma 49, 515-529.

378. Crye, C.C. and Fehlberg, E.O. (2004). Advanced combat helmet system. USPTO (ed). Lineweight Llc: United States.

379. Grujicic, M., Ramaswami, S., Snipes, J.S. and Dudt, P. (2016). Potential improvement in helmet blast-protection via the use of a polyurea external coating: combined experimental/computational analyses. J Materials: Design and Applications 0, 1-31.

380. Grujicic, M., Bell, W.C., Pandurangan, B. and Glomski, P.S. (2011). Fluid/structure interaction computational investigation of blast-wave mitigation efficacy of the advanced combat helmet. JMEPEG 20, 877-893.

381. Zhang, L., Makwana, R. and Sharma, S. (2013). Brain response to primary blast wave using validated finite element models of human head and advanced combat helmet. Frontiers in Neurology 4, 1-12.

382. Sarvghad-Moghaddam, H., Rezaei, A., Ziewjewski, M. and Karami, G. (2016). Evaluation of brain tissue responses because of the underwash overpressure of helmet and faceshield under blast loading. Int J Numer Meth Biomed Engng, 1-13.

383. Talsky, A., Pacione, L.R., Shaw, T., Wasserman, L., Lenny, A.M., Verma, A., Hurwitz, G., Waxman, R., Morgan, A. and Bhalerao, S. (2011). Pharmacological interventions for traumatic brain injury. BC Medical Journal 53, 26-31.

384. Kabadi, S.V. and Faden, A.I. (2014). Neuroprotective strategies for traumatic brain injury: improving clinical translation. Int J Mol Sci 15, 1216-1236.

385. Kochanek, P.M., Bramlett, H.M., Dixon, C.E., Shear, D.A., Dalton, D.W., Schmid, K.E., Mondello, S., Wang, K.K.W., Hayes, R.L., Povlishock, J.T. and Tortella, F.C. (2016). Approach to modeling, therapy evaluation, drug selection, and biomarker assessment for a multicenter pre-clinical drug screening consortium for acute therapies in severe traumatic brain injury: operation brain trauma therapy. J Neurotrauma 33, 513-522.

386. Center, M.U.M. (2013). Effects of Roflumilast on Cognition in Healthy Adults: a Behaviour-EEG Study. ClinicalTrials.gov (ed). National Library of Medicine (US): Bethesda (MD).

387. Corp., M.S.D. (2016). MK0952 in Patients With Mild-to-Moderate Alzheimer's Disease. ClinicalTrials.gov (ed). National Institutes of Health (US): Bethesda (MD).

388. Heckman, P.R.A., Wouters, C. and Prickaerts, J. (2015). Phosphodiesterase inhibitors as a target for cognitive enhancement in aging and Alzheimer's disease: a translational overview. Curr Pharm Des 21, 1-15.

389. Stoppini, L., Buchs, P.A. and Muller, D. (1991). A simiple method for organotypic cultures of nervous tissue. J Neurosci Methods 37, 173-182.

390. Duport, S., Robert, F., Muller, D., Grau, G., Parisi, L. and Stoppini, L. (1998). An *in vitro* blood-brain barrier model: Cocultures between endothelial cells and organotypic brain slice cultures. Proc Natl Acad Sci U S A 95, 1840-1845.

391. Sengupta, P. (2013). The laboratory rat: relating its age with human's. Int J Prev Med 4, 624-630.

392. Stuhmiller, J.H., Phillips III, Y.Y. and Richmond, D.R. (1991). The Physics and Mechanisms of Primary Blast Injury. In: *Conventional Warfare: Ballistics, Blast, and Burn Injuries*. Office of the Surgeon General: Department of the Army, pps. 241-270.

393. Miyamoto, E. (2006). Molecular mechanisms of neuronal plasticity: induction and maintenance of long-term potentiation in the hippocampus. J Pharmacol Sci 100, 433-442.

394. Lucke-Wold, B.P., Logsdon, A.F., Smith, K.E., Turner, R.C., Alkon, D.L., Tan, Z., Naser, Z.J., Knotts, C.M., Huber, J.D. and Rosen, C.L. (2015). Bryostatin-1 restores blood brain barrier integrity following blast-induced traumatic brain injury. Mol Neurobiol 52, 1119-1134.

395. de Lanerolle, N.C., Bandak, F., Kang, D., Li, A.Y., Du, F., Swauger, P.V., Parks, S., Ling, G. and Kim, J.H. (2011). Characteristics of an explosive blast-induced brain injury in an experimental model. J Neuropathol Exp Neurol 70, 1046-1057.

396. Leonardi, A.D.C., Keane, N.J., Hay, K., Ryan, A.G., Bir, C.A. and VandeVord, P.J. (2013). Methodology and evaluation of intracranial pressure response in rats exposed to complex shock waves. Annals of Biomedical Engineering 41, 2488-2500.

397. McAllister, T.W. (2011). Neurobiological consequences of traumatic brain injury. Dialogues Clin Neurosci 13, 287-300.

398. Ziemann, A.E., Allen, J.E., Dahdaleh, N.S., Drebot, I.I., Coryell, M.W., Wunsch, A.M., Lynch, C.M., Faraci, F.M., Howard III, M.A., Welsh, M.J. and Wemmie, J.A. (2009). The amygdala is a chemosensory that detects carbon dioxide and acidosis to elicit fear behavior. Cell 139, 1012-1021.

399. Gahwiler, B.H. (1984). Slice cultures of cerebellar, hippocampal, and hypothalamic tissue. Experientia 40, 235-308.

400. Lauer, L., Vogt, A., Yeung, C.K., Knoll, W. and Offenhausser, A. (2002). Electrophysiological recordings of patterned rat brain stem slice neurons. Biomaterials 23, 3123-3130.

401. Bourne, J.N. and Harris, K.M. (2008). Balancing structure and function at hippocampal dendritic spines. Annual review of neuroscience 31, 47-67.

402. Yuste, R. and Bonhoeffer, T. (2001). Morphological changes in dendritic spines associated with long-term synaptic plasticity. Annual review of neuroscience 24, 1071-1089.

403. Campbell, J.N., Register, D. and Churn, S.B. (2012). Traumatic brain injury causes an FK506-sensitive loss and an overgrowth of dendritic spines in rat forebrain. J Neurotrauma 29, 201-217.

404. Morris, R. (1984). Developments of a water-maze procedure for studying spatial learning in the rat. J Neurosci Methods 11, 47-60.

405. Olton, D.S., Collison, C. and Werz, M.A. (1977). Spatial memory and radial arm maze performance of rats. Learn. Mem. 8, 289-314.

406. Bevins, R.A. and Besheer, J. (2006). Object recognition in rats and mice: a one-trial non-matching-to-sample learning task to 'recognition memory'. Nature Protocols 1, 1306-1311.

Appendix: Publications

Peer-reviewed publications

Eight authored publications including five first-authored publications in print or submitted

1. **Vogel III, E.W.**, Panzer, M.B., Morales, F.N., Varghese, N., Meaney, D.F., Bass, C.R.D., Morrison, B., III (2017). Direct observation of low strain, high rate deformation of cultured brain tissue during primary blast and validation of finite element simulations, in preparation.

2. **Vogel III, E.W.**, Morales, F.N., Meaney, D.F., Bass, C.R.D., Morrison, B., III (2017). Phosphodiesterase-4 inhibition restored hippocampal long-term potentiation after primary blast, Exp. Neurol. In revisions.

3. **Vogel III, E.W.**, Rwema, S.H., Meaney, D.F., Bass, C.R.D., Morrison, B., III (2016). Primary blast injury depressed hippocampal long-term potentiation through disruption of synaptic proteins, J Neurotrauma. Available online.

4. Hue, C.D., Cho, F.S., Cao, S., Nicholls, R.E., **Vogel III, E.W.**, Sibindi, C., Arancio, O., Meaney, D.F., Bass, C.R.D, Morrison, B., III (2016). Time course and size of blood-brain barrier opening in a mouse model of blast-induced traumatic brain injury. J Neurotrauma, 33 (13), 1202-1211.

5. **Vogel III, E.W.**, Effgen, G.B., Patel, T.P., Meaney, D.F., Bass, C.R.D, Morrison, B., III (2016). Isolated primary blast inhibits long-term potentiation in organotypic hippocampal slice cultures. J Neurotrauma 33, 652-661.

6. Effgen, G.B., **Vogel III, E.W.**, Lynch, K.A., Lobel, A., **Hue, C.D.**, Meaney, D.F., Bass, C.R., Morrison, B., III. (2014). Isolated primary blast alters neuronal function with minimal cell death in organotypic hippocampal slice cultures. J Neurotrauma 31, 1202-1210.

7. Hue, C.D., Cao, S., Haider, S.F., Vo, K.V., Effgen, G.B.**, Vogel III, E.**, Panzer, M.B., Bass, C.R., Meaney, D.F., Morrison, B., III. (2013). Blood-brain barrier dysfunction after primary blast injury in vitro. J Neurotrauma 30, 1652-1663.
    - Cover feature: October 1, 2013 issue

8. Effgen, G.B.**,** Hue, C.D., **Vogel III, E.**, Panzer, M.B., Meaney, D.F., Bass, C.R., Morrison, B., III. (2012). A Multiscale Approach to Blast Neurotrauma Modeling: Part II: Methodology for Inducing Blast Injury to in vitro Models. Front. Neurol. 3, 23.

Book chapter

One first-authored review chapter in print

1. **Vogel III, E.W.**, Morrison, B., III., Evilsizor, M.N., Griffiths, D.R., Thomas, T.C., Lifshitz, J., Sutton, R.L., Long, J.B., Ritzel, D., Ling, G.S.F., Huh, J., Rahupathi, R.,

McIntosh, T.K. (2016). Experimental models of traumatic brain injury: clinical relevance and shortcomings. In C.S. Cox (Ed.) *Cellular Therapy for Neurological Injury*. (pp. 101-166). Boca Raton, FL: CRC Press.

Abstracts

Thirteen abstracts and conference proceedings including eight poster or oral presentations

1. **Vogel III, E.W.**, Bass, C.R., Meaney, D.F., Morrison III, B. (2016). Drug treatment prevents primary blast-induced deficit in long-term potentiation in rat brain slice cultures, IRCOBI Malaga, Spain.

2. **Vogel III, E.**, Bass, C.R., Meaney, D.F., Morrison III, B. (2016). Roflumilast treatment prevented primary blast-induced deficits in long-term potentiation, NNS Lexington, KY.

3. **Vogel III, E.W.**, Bass, C.R., Meaney, D.F., Morrison III, B. (2015). Delayed inhibition of long-term potentiation in rat brain slice cultures caused by primary blast exposure, IRCOBI Lyon, France.

4. **Vogel III, E.**, Bass, C.R., Meaney, D.F., Morrison III, B. (2015). Delayed primary blast-induced elimination of long-term potentiation in rat organotypic hippocampal slice cultures. NNS Santa Fe, NM.

5. **Vogel III, E.**, Effgen, G.B., Bass, C.R., Meaney, D.F., and Morrison III, B. (2014) Primary blast injury impairs learning in rat organotypic hippocampal slices. State-of-the-Science (SoS) Meeting on the Biomedical Basis for mTBI Environmental Sensor Threshold Values. McLean, VA.

6. **Vogel III, E.**, Villacorta, J., Bass, C.R., Meaney, D.F., and Morrison III, B. (2014) Primary blast injury erases long term potentiation in rat brain organotypic hippocampal slices, IRCOBI Berlin, Germany.

7. **Vogel III, E.**, Effgen, G.B., Bass, C.R., Meaney, D.F., Morrison III, B. (2014). Primary blast eliminated long-term potentiation in rat organotypic hippocampal slices, NNS San Francisco, CA.

8. Morrison III, B., Effgen, G.B., Hue, C.D., **Vogel, E.W.**, Bass, C.R., and Meaney, D.F. (2014). Studying blast traumatic brain injury with in vitro models, United States National Congress on Theoretical and Applied Mechanics. East Lansing, MI.

9. **Vogel E.,** Effgen G.B., Bass, C.R., Meaney D.F., and Morrison III, B. (2013). Primary blast injury initiates functional differences in rat organotypic hippocampal slices, IRCOBI Gothenburg, Sweden.

10. Effgen, G.B., **Vogel III, E.W.**, Lynch, K.A., Morrison III, B. (2013). In vitro primary

blast injury induced cell death in the hippocampus, IRCOBI Gothenburg, Sweden.

11. **Vogel III, E.**, Effgen G.B.**,** Bass, C.R., Meaney, D.F., and Morrison III, B. (2013). Primary blast injury induced electrophysiological changes in rat organotypic hippocampal slices, NNS Nashville, TN.

12. Effgen, G.B., **Vogel III, E.**, Lynch, K.A., Lobel, A., Hue, C.D., Bass, C.R., Meaney, D.F., Morrison III, B. (2013). Isolated primary blast-exposure induced cell death in the hippocampus, NNS Nashville, TN.

13. Hue, C .D., Vo, K.V., Effgen, G.B., **Vogel III, E.**, Panzer, M.B., Bass, C.R., Meaney, D.F., Morrison III, B. (2012). Integrity disruption of an in vitro blood-brain barrier model following exposure to blast overpressure. IRCOBI Dublin, Ireland.